To be published in "Physics Reports" Ref.TH.1388-CERN

RECENT DEVELOPMENTS IN THE COMPARISON BETWEEN THEORY AND EXPERIMENTS IN QUANTUM ELECTRODYNAMICS

B.E. Lautrup and A. Peterman
CERN - Geneva

and

E. de Rafael
Institut des Hautes Etudes Scientifiques
Bures-sur-Yvette

A B S T R A C T

This review is a survey of three main topics in quantum electrodynamics : fundamental bound systems ; anomalous magnetic moments and high energy experiments. The emphasis lies particularly in recent developments concerning the electron and muon anomalous magnetic moments.

Ref.TH.1388-CERN
10 August 1971

CONTENTS

INTRODUCTION

FUNDAMENTAL BOUND SYSTEMS

I. THE HYDROGEN ATOM

I.1 The Lamb Shift

I.2 The Fine Structure

I.3 The Hyperfine Structure

II. POSITRONIUM

II.1 The Fine-Structure Interval of the Ground State of Positronium

II.2 The Annihilation Rates of Orthopositronium and Parapositronium

III. MUONIUM

III.1 The Hyperfine-Splitting of the Muonium Ground State

THE ANOMALOUS MAGNETIC MOMENTS OF THE CHARGED LEPTONS

IV. THE ELECTRON ANOMALY

IV.1 The Second and Fourth order Contributions

IV.2 The Sixth order Contribution

IV.3 Measurements of the Electron Anomaly

V. THE QUANTUM ELECTRODYNAMICS CONTRIBUTION TO THE DIFFERENCE BETWEEN THE ANOMALOUS MAGNETIC MOMENTS OF MUON AND ELECTRON

V.1 The Fourth Order Contribution

V.2 The Sixth Order Contribution

VI. OTHER CONTRIBUTIONS TO THE MUON ANOMALY AND EXPERIMENTS

VI.1 The Hadronic Contributions

VI.2 The Weak Interaction Contribution

VI.3 Measurements of the Muon Anomaly

VII. "EXOTIC" CONTRIBUTIONS TO THE ELECTRON AND MUON ANOMALIES

VII.1 Generalities

VII.2 Modifications of Quantum Electrodynamics

VII.3 Suggested Couplings of Leptons to Exotic Particles

HIGH ENERGY EXPERIMENTS

VIII. SCATTERING EXPERIMENTS AT HIGH MOMENTUM TRANSFER

VIII.1 Colliding Beams Experiments

VIII.2 Bethe-Heitler Type Experiments

CONCLUSIONS.

REVIEW ARTICLES ON QUANTUM ELECTRODYNAMICS.

REFERENCES.

enough ($G_e = 0.00115 \pm 0.0004$) to confirm Schwinger's calculation(*) ($G_e = \alpha/2\pi$) . At present, the accuracy of the measurement of G_e is 3 p.p.m. ; and an adequate comparison with the theory requires the inclusion of the sixth order contributions to G_e (**) .

Does the muon have an anomalous magnetic moment as predicted by QED ? A positive answer to this important question, which bears upon one of the greatests puzzles in physics, i.e., the origin of the muon-electron mass difference, has been given by beautiful experiments performed at CERN. The accuracy of the first g-2 muon experiment[004] was 4×10^{-3} . The latest g_μ-2 experiment [007,008] has attained an accuracy of 28 parts in 10^5 and has clearly confirmed the vacuum polarization terms with virtual electron pairs predicted by QED (***) . The accuracy will very likely improve by a factor of 10 to 30 in the next generation of g_μ-2 experiments(†) .

(*) See Schwinger ref.003 ; reprinted in the compilation quoted in ref.R.15 ; paper No. 13.

(**) See the discussion in Section IV .

(***) The calculation of this contribution was first done by Peterman, ref.005 ; and by Suura and Wichmann, ref.006 . For further details see the discussion of section V.1 .

(†) Private communication from John Bailey, Francis Farley and Emilio Picasso .

The understanding of the $g_\mu - 2$ experimental result has been a challenge to theoreticians which has led to new developments in computational techniques. An early discrepancy between theory and experiment motivated the calculation of all the terms predicted by QED which, at sixth order, make the anomaly of the muon different from that of the electron. The result of these calculations has brought the theoretical prediction again within the errors of the experiment(*).

An important question about the precision tests of QED is the accuracy they can attain before they are also sensitive to the electromagnetic interactions of hadrons. The electron anomaly and systems like positronium and muonium are still far from being influenced by the electromagnetic interactions of hadrons. This makes them the more excellent candidates for future precision tests of QED. As we shall see the situation is different for the Lamb shift, the hyperfine structure in hydrogen, and for the muon anomaly. Here, an adequate comparison between theory and experiment requires the knowledge of contributions due to the electromagnetic interactions of hadrons. It is remarkable that in some cases, like the muon anomaly, the hadronic contributions can be related to empirical information already available from the high energy electron experiments. A very interesting link between high energy experiments and precision low energy experiments is thereby developing.

(*) This is discussed in detail in Section V .

The understanding of the g_μ-2 experimental result has be her point challenge to theoreticians which has led to new developments in c pton and tational techniques. An early discrepancy between theory and experi adequate motivated the calculation of all the terms predicted by QED which, with the sixth order, make the anomaly of the muon different from that of th electron. The result of these calculations has brought the theoreti prediction again within the errors of the experiment(*). s the the muon.

An important question about the precision tests of QED is parallel accuracy they can attain before they are also sensitive to the elec ts.IV & VII. magnetic interactions of hadrons. The electron anomaly and systems ld also positronium and muonium are still far from being influenced by the s been electromagnetic interactions of hadrons. This makes them the more t on low excellent candidates for future precision tests of QED. As we shall nd a the situation is different for the Lamb shift, the hyperfine structu on VIII. in hydrogen, and for the muon anomaly. Here, an adequate comparison ween theory and experiment requires the knowledge of contributions d which is to the electromagnetic interactions of hadrons. It is remarkable tha om the some cases, like the muon anomaly, the hadronic contributions can be exists related to empirical information already available from the high ene ave electron experiments. A very interesting link between high energy ex text we riments and precision low energy experiments is thereby developing. which

---

(*) This is discussed in detail in Section V .

The understanding of the g_μ-2 experimental result has been a challenge to theoreticians which has led to new developments in computational techniques. An early discrepancy between theory and experiment motivated the calculation of all the terms predicted by QED which, at sixth order, make the anomaly of the muon different from that of the electron. The result of these calculations has brought the theoretical prediction again within the errors of the experiment(*).

An important question about the precision tests of QED is the accuracy they can attain before they are also sensitive to the electromagnetic interactions of hadrons. The electron anomaly and systems like positronium and muonium are still far from being influenced by the electromagnetic interactions of hadrons. This makes them the more excellent candidates for future precision tests of QED. As we shall see the situation is different for the Lamb shift, the hyperfine structure in hydrogen, and for the muon anomaly. Here, an adequate comparison between theory and experiment requires the knowledge of contributions due to the electromagnetic interactions of hadrons. It is remarkable that in some cases, like the muon anomaly, the hadronic contributions can be related to empirical information already available from the high energy electron experiments. A very interesting link between high energy experiments and precision low energy experiments is thereby developing.

(*) This is discussed in detail in Section V .

The high energy experiments are also useful from another point of view. They can test the validity of the QED rules for the lepton and photon propagators in processes where the Born approximation is adequate yet the momentum transfers involved are large (of a few GeV/c with the present machines).

The main purpose in writing this review was to discuss the recent developments concerning the anomalous magnetic moment of the muon. This is done in Sections V, VI and VII. Clearly this requires a parallel discussion of the electron anomaly as well, which is made in Sects.IV & VII. We felt, however, that in order to keep some balance, there should also be a brief review of other fundamental QED topics where there has been some recent developments. We have therefore included a first part on low energy tests in fundamental systems : Sections I, II and III ; and a third part on electron and photon high energy experiments, Section VIII.

There is an important topic with implications for QED which is not discussed in this review ; i.e., the determination of α from the a.c. Josephson effect. The reason for this is that there already exists an extremely detailed exposition of the subject(*) to which we have nothing to add. Of course, in all the numerical estimates in the text we shall indicate the appropriate origin for the input value of α which is used.

(*) See Taylor, Langenberg and Parker, ref. R.16 .

We should finally like to point out that there are various excellent review articles on different aspects of QED in the literature[**]. In writing this review we have attempted more to complement the already existing literature rather than to write an encyclopaedic review of QED.

One comment about notations. We use the same metric and Dirac matrices as in J.D. Bjorken and S.D. Drell's textbooks, McGraw Hill, New-York .

(**) See the list of review articles at the end.

FUNDAMENTAL BOUND SYSTEMS

In this first part, we shall consider three fundamental bound systems : the hydrogen atom ; muonium ; and positronium (*) . We shall review the present status in the comparison between theory and experiment concerning : the Lamb-shift in atomic hydrogen ; the fine structure in hydrogen ; the hyperfine structure of the hydrogen ground state ; the fine-structure of the positronium ground state ; the annihilation rates of orthopositronium and parapositronium ; and the hyperfine-splitting of the muonium ground state.

(*) For a review of other hydrogen-like systems we recommend the reader the excellent review articles of Brodsky and Drell, ref.R.4 and of Wu and Wilets, ref.R.17 .

I. THE HYDROGEN ATOM

The basic features of the lower energy-level structure in the hydrogen atom are summarized in Fig.I.1 . In the Dirac theory, the degeneracy between the $n=2$ $P_{3/2}$ and $P_{1/2}$ levels is removed by the spin-orbit interaction. This leads to the fine structure $\Delta E\,(2P_{3/2} - 2P_{1/2})$, proportional[(*)] to $(Z\alpha)^4 m$, which corresponds to a level splitting of 10969.1 MHz . The interaction of the electron with the quantized electromagnetic field removes the degeneracy between the levels $n = 2$ $S_{\frac{1}{2}}$ and $P_{\frac{1}{2}}$. The corresponding level structure : $\Delta E\,(2S_{\frac{1}{2}} - 2P_{\frac{1}{2}}) = 1057.9$ MHz is the Lamb-shift. It is proportional to $\alpha m(Z\alpha)^4 \log(Z\alpha)$. Another cause of level splitting in the hydrogen-atom is the interaction of the magnetic moment of the orbital electron with the magnetic moment of the proton. In the ground state $n = 1$, this leads to a hyperfine structure between the triplet $F = 1$ and singlet $F = 0$ levels of 1420.4 MHz . The effect is proportional to $\frac{m}{M}(Z\alpha)^4 m$.

(*) Z is the atomic number, which for hydrogen is one. We shall, however, keep Z in our expressions as an indicative of the binding effects in contrast to the purely radiative effects.

I.1. The Lamb-Shift.

The two dominant contributions to the Lamb-shift can be qualitatively understood in the following way.

On the one hand the electron, in the presence of the electromagnetic field of the proton, can emit and reabsorb a photon (see Fig. I.2) . This leads to a physical spreading of the electron charge over a mean squared radius $< r^2 >$ which for a free electron is precisely

$$< r^2 > = \frac{6}{m^2} \frac{\alpha}{\pi} \left(\frac{1}{3} \log \frac{m}{\lambda} - \frac{1}{8} \right) \quad ,$$

where λ is an arbitrary small mass assigned to the photon. In the hydrogen atom, however, there is an effective lower limit (of the order of the hydrogen binding energy) to the energy of the photons which the bound electron can emit and reabsorb. Qualitatively one expects that a correct treatment of the binding effects will replace λ by the Rydberg which is the ionization energy of the ground state of the hydrogen atom

$$\lambda \sim \mathrm{Ry} = \tfrac{1}{2} m (Z\alpha)^2 = 13.6 \text{ eV} \quad ,$$

and

$$< r^2 > \sim \frac{1}{m^2} \frac{\alpha}{\pi} \log (Z\alpha)^{-1} \quad .$$

The potential corresponding to this charge density distribution diminishes the Coulomb binding $-\frac{Z\alpha}{r}$ and as a consequence the S levels are pushed higher by an amount

$$\mathcal{L} \sim \alpha(Z\alpha)^4 m \log (Z\alpha)^{-1} \sim 1000 \text{ MHz} \quad .$$

The detailed calculation[101-105] which also includes the contribution from the anomalous magnetic moment of the electron, leads to the result (see the first two entries in Table I.1 where the reduced mass correction has also been taken into account)

$$\mathcal{L}(\text{self-energy}) = 1077.63 \pm 0.02 \text{ MHz} \quad .$$

On the other hand, the effective potential seen by the electron is modified by the vacuum polarization due to virtual electron-positron pairs [107,108] (see Fig.I.3)

$$\frac{Z\alpha}{q^2} \to \frac{Z\alpha}{q^2} + \frac{Z\alpha}{q^2} \frac{1}{\pi} \int_{4m^2}^{\infty} \frac{dt}{t} \text{ Im } \Pi(t) \frac{q^2}{q^2-t} \quad ,$$

where $\frac{1}{\pi} \text{ Im } \Pi(t)$ is the vacuum polarization spectral function (which is positive definite)

$$\frac{1}{\pi} \text{ Im } \Pi(t) = \frac{\alpha}{\pi} \frac{1}{3} \left(1+\frac{2m^2}{t}\right)\sqrt{1-\frac{4m^2}{t}}\, \theta(t-4m^2) \quad .$$

The effective potential seen by the electron is more attractive than the Coulomb potential and as a consequense the S levels are lowered by an amount which turns out to be (without including the reduced mass correction)

$$\mathcal{L} \text{ (vac.pol.)} = \frac{\alpha}{\pi}(Z\alpha)^4 m \left(-\frac{1}{30}\right) = -27.13 \text{ MHz} \quad .$$

Experimentally, there are two accurate <u>direct</u> measurements of

the n = 2 Lamb-Shift in hydrogen.:

Triebwasser, Dayhoff and Lamb [109)*)] $\mathfrak{L}_{exp} = 1057.86 \pm 0.06$ MHz ;

Robiscoe, Shyn [110)] (revised) [160)] $\mathfrak{L}_{exp} = 1057.90 \pm 0.06$ MHz .

There are also three independent measurements of the interval $2P_{3/2}$-$2S_{1/2}$ in hydrogen, which combined with the theoretical value for the fine structure interval $\Delta E = 2P_{3/2}$-$2P_{1/2}$, give <u>indirect</u> determinations of the Lamb-shift :

Kaufman, Lamb, Lea and Leventhal [111)]

$(\Delta E - \mathfrak{L})_{exp} = 9911.38 \pm 0.03$; $\mathfrak{L} = 1057.65 \pm 0.05$;

Shyn, Williams, Robiscoe, and Rebane [112)]

$(\Delta E - \mathfrak{L})_{exp} = 9911.25 \pm 0.06$; $\mathfrak{L} = 1057.78 \pm 0.07$;

Vorburger and Cosens [113)]

$(\Delta E - \mathfrak{L})_{exp} = 9911.17 \pm 0.04$; $\mathfrak{L} = 1057.86 \pm 0.06$.

The accuracies of these determinations of the Lamb-shift range from 66 p.p.m. to 47 p.p.m. .

The terms which so far have been calculated are given in Table I.1 . A detailed analysis of the different contributions can be found in two ar-

*) Corrected by Robiscoe and Shyn [160)]

ticles(*) by Erickson and Yennie [114,115] . Of particular interest to us, because of recent changes in their evaluation, is the fourth order self-energy contributions which we discuss next.

The QED quantity which is involved in the calculation of the fourth order self-energy contribution to the Lamb-shift is the slope of the Dirac form factor of the electron to order α^2 . With the electron vertex definition

$$\bar{u}(p+q)\,\Gamma^{\mu}(p+q,p)\,u(p) =$$

$$\bar{u}(p+q)\left\{\gamma^{\mu}\,F_1(q^2) + \frac{i}{2m}\,\sigma^{\mu\nu}\,q_{\nu}\,F_2(q^2)\right\}u(p) \quad ,$$

we are interested in the evaluation of

$$\sigma^{(4)} = m^2 \left.\frac{dF_1^{(4)}(q^2)}{dq^2}\right|_{q^2=0} \quad .$$

There are seven Feynman diagrams contributing to $\sigma^{(4)}$. They are shown in Fig.I.4 and their contributions to the slope can be found in Table I.2 . The first attempt to this extremely intricate calculation was made by Weneser, Bersohn and Kroll [117] who gave analytic expressions for the contributions from the diagrams of Figs.I.4b,4e,4f,4g and bounds for the

---

(*) For a discussion of the nuclear recoil corrections see also Grotch and Yennie (Ref.116) .

others. Later on, Soto [118] made a complete analytic calculation of $\sigma^{(4)}$. Motivated by serious discrepancies between theory and experiment(*), Appelquist and Brodsky [119] undertook a numerical(**) reevaluation of $\sigma^{(4)}$. They found an overall-discrepancy in sign with the previous calculations and different absolute values for the non-infrared divergent terms of the cross (Fig.I.4a) and corner (Fig.I.4c,4d) graphs. Their results concerning the overall-discrepancy in sign and the evaluation of the corner graph were confirmed by another numerical calculation made by Lautrup, Peterman and de Rafael [120]; and an analytic calculation made by Barbieri, Mignaco and Remiddi [121]. Recently, Peterman [122] has undertaken a systematic investigation of the work by Soto [118] and given an analytic result for the cross graph (Fig.I.4a) in good agreement with the numerical result of Appelquist and Brodsky(***).

The new value of the fourth order self-energy contribution to the Lamb-shift,

$$\left(\frac{\alpha}{\pi}\right)^2 (Z\alpha)^4 \frac{m}{2} \left\{ -\frac{4819}{5184} - \frac{49}{432}\pi^2 + \frac{1}{2}\pi^2 \log 2 - \frac{3}{4}\zeta(3) = 0.46994 \right\}$$

(*) For a review of the comparison between theory and experiment, before Appelquist and Brodsky reevaluation of $\sigma^{(4)}$ see Brodsky Ref. R.3.

(**) For a description of the techniques used in their calculation see Section IV.2 .

(***) The recent analytic result of Barbieri, Mignaco and Remiddi [159] confirms the result of Peterman [122] and disagrees with ref. 124.

when added to the other contributions in Table I.1 leads to a theoretical value [123]

$$\mathcal{L}_{th} = 1057.911 \pm 0.012 \text{ MHz}.$$

This includes the recent result of Erickson [158]. The theoretical and experimental values for Lambshift in Hydrogen and Hydrogenic atoms is given in Table I.4.

I.2. The Fine Structure $\Delta E\,(2P_{3/2} - 2P_{1/2})$ in Hydrogen.

Let us denote ΔE_H, the $n=2$, $P_{3/2}$-$P_{1/2}$ level interval in atomic hydrogen (see Fig.I.1). The theoretical value of ΔE_H is well known

$$\Delta E_H = \frac{Ry(Z\alpha)^2}{16} \left\{ \left[1+\frac{5}{8}(Z\alpha)^2\right] \left(1+\frac{m}{M}\right)^{-1} \right.$$

$$\left. -\left(\frac{m}{M}\right)^2 \left(1+\frac{m}{M}\right)^{-3} + 2G_e \left(1+\frac{m}{M}\right)^{-2} + \frac{\alpha}{\pi}(Z\alpha)^2 \log Z\alpha \right\} .$$

The first term in the parenthesis : $1+\frac{5}{8}(Z\alpha)^2$, is the well known Dirac solution(*). The appearence of the reduced mass factor $(1+\frac{m}{M})^{-1}$ is explained in detail in Grotch and Yennie [116]. The $(\frac{m}{M})^2$ term, calculated by Barker and Glover [133], is the effect of the Dirac moments of the electron and the proton. The G_e term is the effect of the electron anomaly and is the first term of radiative origin. Its contribution is roughly

---

(*) See e.g., Bethe and Salpeter, ref. R.2 .

0.1 % , whereas the last term, which is also a radiative correction, contributes only about 1p.p.m. These radiative corrections have been calculated by the authors of refs. 127 and 128 . Bounds to the next uncalculated terms , $O\left[(\frac{\alpha}{\pi})(Z\alpha)^2\right]$, have been estimated by Erickson(*) . Since these terms are comparable to terms of order $O(\alpha^2 \frac{m}{M}$; $\alpha(\frac{m}{M})^2$; etc.) it seems more natural to expand the theoretical expression for ΔE_H in powers of $\frac{m}{M}$ and keep only the first power in this parameter. Thus we get

$$\Delta E_H = \frac{Ry(Z\alpha)^2}{16}\left\{\left[1+\frac{5}{8}(Z\alpha)^2\right]\left(1-\frac{m}{M}\right)+ 2G_e\left(1-2\frac{m}{M}\right)+ 2\frac{\alpha}{\pi}(Z\alpha)^2 \log Z\alpha\right\} .$$

From this equation, and using the "without quantum electrodynamics value" (WQED) $\alpha^{-1}= 137.03608(26)$ obtained from the a.c. Josephson effect(**), we get

$$\Delta E_H(\text{Th.}) = 10969.03 \text{ MHz} .$$

Combining the value of ΔE_H (Th.) with the theoretical value for the Lamb-shift (see Section I.1) we have that

$$(\Delta E_H - \mathcal{L}_H)_{\text{Th.}} = 2P_{3/2}-2S_{1/2} = 9911.13 \pm 0.03 \text{ MHz} .$$

(*) Quoted by Brodsky and Parsons, ref.134 .

(**) See Taylor, Parker and Langenberg, ref.R.16 .

As we pointed out in the precedent section, there are three independent measurements of the interval $2P_{3/2} - 2S_{1/2}$ in hydrogen [111,112,113]. We can combined these experiments with the theoretical prediction of $\Delta E_H - \mathcal{L}_H$ to obtain values for the fine structure constant α :

(i) the Vorburger-Cosens. measurement [113]

$$\Delta E_H - \mathcal{L}_H = 9911.17 \pm 0.04 \quad \text{MHz} \quad ,$$

combined with the theoretical prediction yields a 2.0 p.p.m. accurate value of α^{-1} ,

$$\alpha^{-1}_{(i)} = 137.03570(27) \quad ;$$

(ii) the weighted average of the values of refs. 111 and 112

$$\Delta E_H - \mathcal{L}_H = 9911.21 \pm 0.035 \quad \text{MHz} \quad ,$$

combined with $(\Delta E_H - \mathcal{L}_H)_{Th.}$ yields

$$\alpha^{-1}_{(ii)} = 137.03543(23) \qquad (2.25 \text{ p.p.m.})$$

The values $\alpha^{-1}_{(i)}$ and $\alpha^{-1}_{(ii)}$ are derived purely from radiation theory and experiment and they are in good agreement with the determination of α^{-1} from phase coherence effects in superconductors. At the present time, the accuracy on α^{-1} obtained with the new theoretical expression for the interval $2P_{3/2} - 2S_{1/2}$ is almost the same as that on the value of α^{-1} derived from the hydrogen hyperfine structure discussed in the next section.

In Table I.3 we have listed various determinations of α^{-1} obtained from different sources. This table clearly shows the consistency of QED in describing bound systems.

I.3. The Hyperfine Structure.

In Hydrogenic atoms, the interaction of the magnetic moment of the orbital electron with the magnetic moment of the nucleus leads to a splitting of a fine structure level with fixed orbital angular momentum ℓ and fixed total angular momentum j into hyperfine structure (h.f.s.) levels. To a first approximation, the energy separation between the two outermost levels is given by the Fermi formula [135]. For the ground state of the hydrogen atom (see Fig.I.1) this corresponds to a hyperfine frequency

$$\Delta \nu(\text{Fermi}) = \frac{16}{3} (Z\alpha)^2 \text{ Ry } \frac{\mu_p}{\mu_o^e} \simeq 1420 \text{ MHz}$$

where μ_p is the proton magnetic moment and μ_o^e the Bohr magneton

$$\mu_o^e = \frac{e\hbar}{2m_e c} \quad .$$

The measurement of the hyperfine-splitting of the hydrogen ground state is probably the most accurate number which is presently known in experimental physics [136]

$$\Delta\nu_{exp}(p\,e) = 1420.405\ 751\ 7864(17)\ \text{MHz} \quad .$$

It corresponds to an accuracy of 1.2 parts in 10^{12} ! More than a test of QED the h.f.s. has become a yardstick to measure our progress in theoretical physics. As we shall see below there is at present a gap of seven orders of magnitude between theory and experiment.

The framework for the formal treatment of the corrections to the Fermi formula is the Bethe-Salpeter equation. The dimensionless parameters which appear are :

$\frac{m}{M}$, electron to proton mass ratio ;

$\frac{R}{a_o}$, ratio of nuclear to atomic sizes ;

α , the fine structure constant ;

$Z\alpha$, the strength of the Coulomb potential.

A sequence of approximations in the corrections to $\Delta\nu(\text{Fermi})$ is established as follows(*). To first approximation, with

$$\Delta\nu_H(\text{h.f.s.}) = \Delta\nu(\text{Fermi})(1+\delta) \quad ,$$

the proton is taken as a fixed point Coulomb potential

(*) An excellent detailed exposition of the successive orders of approximation can be found in Brodsky and Erickson, ref.137 .

$$\frac{m}{M} \to 0 \quad \text{and} \quad \frac{R}{a_o} \to 0 \quad ;$$

radiative corrections are also neglected ; and only relativistic corrections are taken into account. This yields the Breit correction [138]

$$\delta_{Breit} = \frac{3}{2} (Z\alpha)^2 \quad .$$

At the next level, one still takes $\frac{m}{M} \to 0$ and $\frac{R}{a_o} \to 0$ but radiative corrections are taken into account as succesive powers of α ; the dependence on $(Z\alpha)$, which arises when binding is taken into account, is not however simply a power series in $(Z\alpha)$. Altogether, radiative plus binding corrections take the following form :

$$\delta_{Rad} + \delta_{Binding} = a_1 \frac{\alpha}{\pi} + c_{10}\alpha(Z\alpha) + a_2(\frac{\alpha}{\pi})^2 + \frac{\alpha}{\pi}(Z\alpha)^2[c_{22} \log^2(Z\alpha)^{-2} + c_{21} \log(Z\alpha)^{-2} + c_{20}] + a_3(\frac{\alpha}{\pi})^3 + c_{101} \alpha(\frac{\alpha}{\pi}) Z\alpha + \ldots$$

The coefficients a_1, a_2, a_3 are those which give the corresponding order contribution to the anomalous magnetic moment of the electron (*)

$$a_1 = \frac{1}{2}$$

$$a_2 = \frac{197}{144} + \frac{\pi^2}{12} - \frac{\pi^2}{2} \log 2 + \frac{3}{4} \xi(3) = - 0.3285$$

$$a_3 = 1.49 \pm 0.20 \ .$$

(*) See Section IV .

The coefficient c_{10} was first calculated by Kroll and Pollack [139] and Karplus, Klein and Schwinger [140]

$$c_{10} = \frac{5}{2} + \log 2 \quad .$$

The coefficients c_{22} and c_{21} have been calculated by Layzer [141] ; Zwanziger [142] ; and Brodsky and Erickson [137] . The latter authors have also calculated the dominant contribution to the coefficient c_{20} . The results are

$$c_{22} = -\frac{2}{3}$$

$$c_{21} = \frac{281}{360} - \frac{8}{3} \log 2$$

$$c_{20} = 18.4 \pm 5 \quad .$$

The higher order terms have not been calculated as yet. We recall that the coefficients c_{21} and c_{20} are state dependent(*). In fact, the values for the $n = 2$ S-level have also been calculated [141,142,137,143].

The next level of approximations takes into account the finite mass and structure of the proton. The corresponding corrections can be classified as follows

(i) reduced mass corrections ;

(ii) nonrelativistic size contributions δ_{NR} ;

(*) See e.g. Brodsky and Erickson [137] for a discussion.

(iii) additional recoil terms of order $\alpha\, m/M$ δ_{RC} ;

(iv) proton polarization corrections δ_p .

The reduced mass correction gives simply a factor

$$\left(\frac{M}{m+M}\right)^3$$

in the Fermi formula. Estimates of nonrelativistic size contributions were made by Brown and Arfken [144] ; and, more elaborated, by Zemach [145]. The calculation of Zemach, in which the nonrelativistic approximation to the wave function was used, has been analyzed in detail by Grotch and Yennie [116] within the framework of an effective potential model. It amounts to a correction

$$\delta_{NR} = -\, 2\, m\alpha\, R_p \quad ,$$

where

$$R_p = \int |\vec{u} - \vec{r}|\ \rho_M(\vec{u})\ \rho_E(\vec{r})\ d^3u\, d^3r$$

and $\rho_E(\vec{r})$, $\rho_M(\vec{r})$ denote the charge and magnetic distribution of the proton. Grotch and Yennie [116], using the expression

$$\rho_E(\vec{r}) = \rho_M(\vec{r}) = \Lambda^3/8\pi\ e^{-\Lambda r} \quad ,$$

with $\Lambda = 0.91\ M$, as suggested by the experimental determination of the proton form factors obtain

$$R_p = 1.02\ F \quad ,$$

which amounts to a correction

$$\delta_{NR} = - 38.2 \text{ p.p.m.}$$

to the Fermi formula. Additional recoil corrections of relative order $\alpha\, m/M$ have also been evaluated by Arnowitt [146] using the method of Karplus, Klein and Schwinger [147] and by Newcomb and Salpeter [148] using the Bethe-Salpeter equation. These corrections, which in the case of muonium can be calculated exactly(*), have been done for a point proton with an anomalous magnetic moment i.e., the vertex corresponding to the absorption of a virtual photon of energy-momentum q by the proton is put equal to

$$\Gamma^{\mu} = \gamma^{\mu} + \frac{\mu}{2M}\, i\, \sigma^{\mu\nu} q_{\nu} \quad .$$

The result is logarithmically divergent, due to the nonrenormalizability of the Pauli interaction. However, as was shown by the calculations of Iddings and Platzman [149], the divergence disappears when the form factors of the proton are taken into account. Iddings and Platzman calculate the corrections to $\Delta\nu$(Fermi) arising from two-photon-exchange (elastic-contribution). In fact, they calculate the contribution to the h.f.s. from the difference between a coupling with form factors and the point-like coupling vertex quoted above. This, when added to the result of the calculations of Arnowitt ; and Newcomb and Salpeter gives a finite correction of

$$\delta_p(\text{elastic}) = 3.6 \text{ p.p.m.} \quad .$$

(*) See Section III .

There are further corrections to this value arising from the polarizability of the proton, i.e. contributions to the h.f.s. from two-photon-exchange graphs with virtual hadronic states other than the proton itself. The possibility of calculating these corrections from experimental data on inelastic electron scattering from protons was first pointed out by Iddings [150]. The argument is analogous to Cottingham's formulation of the neutron-proton mass difference [151] in terms of the proton structure functions. However, in the case of the h.f.s. of hydrogen, what is needed are the spin dependent structure functions of the proton. These are accessible from experiments on inelastic scattering of polarized electrons from polarized protons(*). So far, the estimates of these corrections(**) give very small contributions

$$\delta_p(\text{inelastic}) \sim 1 - 2 \text{ p.p.m.}$$

From the comparison between the experimental result [136]

(*) For a discussion of the spin dependent of the nucleon structure functions where earlier references can be found see Doncel and de Rafael, ref.152 .

(**) The π-N S-waves contribution has been estimated by Guerin [153] to be 1 p.p.m. , and the π-N resonances to give a contribution smaller than 1 p.p.m. . The importance of hadronic continuum contributions has been particularly emphasized by Drell and Sullivan [154] ; and more recently by Chernak Struminski and Zinovjev [155], using a quasipotential method developed by Logunov and Tavkhelidze [156] and Faustov [157] .

$$\Delta\nu_{exp}(pe) = 1420.405\ 751\ 7864(17)\ \text{MHz} \quad ,$$

and the Fermi formula with all corrections discussed above incorporated, except the proton polarizability correction, and using the recommended value of α^{-1} (*) ,

$$\alpha^{-1} = 137.03608(26) \quad ,$$

one obtains

$$\frac{\Delta\nu_{exp} - \Delta\nu_{Th}}{\Delta\nu_{Th}} = 2.5 \pm 4.0\ \text{p.p.m.} - \delta_p(\text{inelastic}) \quad ,$$

consistent with the estimates of $\delta_p(\text{inelastic})$ [153-155] .

One can also use the theoretical expression of $\Delta\nu(\text{h.f.s.})$ to obtain the fine structure constant, via the comparison with the measured $\Delta\nu(\text{h.f.s.})$. The value one gets is

$$\alpha^{-1}(\text{h.f.s.}) = 137.03591(35) \quad ,$$

consistent with other determinations of α^{-1} (see Table I.3) .

(*) See Taylor, Parker and Langenberg, ref.R.16 .

II. POSITRONIUM

Positronium is the atom consisting of an electron and a positron. It was discovered(*) by Deutsch in 1951 . Positronium is clearly a fundamental system to test QED , in particular our understanding of the binding mechanism as described by the Bethe-Salpeter formalism [203,204].

At the present time, the only measurements performed in the positronium system are on the fine-structure splitting of the ground (n=1) state [205,208]; and on the decay rates of orthopositronium (the $^3S_1$ state)[209] and parapositronium (the ^1S_o state) . The first measurement of the decay rate of parapositronium Γ_p was obtained from a measurement value of Γ_p/Γ_o [210], where Γ_o denotes the decay rate of orthopositronium, and using the value of Γ_o quoted in ref. 209 (see also Ref.R.11). A direct measurement of Γ_p has only recently been reported [208]. A compilation of results is given in Table II.1 .

II.1 The Fine-Structure Interval of the Ground State of Positronium.

The qualitative features of the positronium energy levels, as predicted by the Schroedinger equation, are roughly $\frac{1}{2}$ those of hydrogen because of the reduced mass for positronium which is $m_e/2$. Hence the

---

(*) See ref.201 . For a review of the earlier experiments, see Martin Deutsch, ref.202 . For a more recent review, see ref.R.11.

ionization energy of the ground $n=1$ state of positronium which is 6.8 eV .

The fine-structure in positronium is of order $\alpha^2 Ry$ and the features here are very different from those of hydrogen. Besides the dipole interaction, as in the hydrogen h.f.s., there is an exchange interaction due to the virtual annihilation of the e^+e^- system in the triplet state into one γ [211-213]. In fact, the largest contribution comes from this virtual annihilation interaction which pushes the $^3S_1$ level upwards with respect to the ^1S_o level. The contributions to the triplet-singlet splitting of the positronium ground state have been recently calculated up to terms of relative order $\alpha^2 \log\alpha$ [214]. The result is

$$\Delta\nu = \alpha^2 Ry \left[\frac{7}{6} - \frac{\alpha}{\pi}\left(\frac{16}{9} + \log 2\right) - \frac{3}{4}\alpha^2 \log\alpha + O(\alpha^2)\right] \quad .$$

The contributions of relative order $\alpha^2 \log\alpha$ represent recoil corrections arising from low momentum components of the wave function associated with the Bethe-Salpeter equation for positronium. The techniques used in the calculation by Fulton, Owen and Repko [214] are those previously described by Karplus and Klein [213] and by Fulton and Martin [215]. The terms of relative order α^2 have not been calculated as yet. The theoretical prediction from the calculated terms is thus

$$\Delta\nu_{th.} = 2.03415 \times 10^5 \text{ MHz} \quad ,$$

to be compared with the most recent measurement [208]

$$\Delta\nu_{exp.} = (2.03403 \pm 0.00012) \times 10^5 \text{ MHz} \quad (60 \text{ ppm}) \quad .$$

II.2. The Annihilation Rates of Orthopositronium and Parapositronium.

The annihilation rate of orthopositronium (the $^3S_1$ e^+e^- state) has been measured to an accuracy of 0.2% [209] (see also Ref. R.11) :

$$\Gamma_o(\text{exp.}) = (0.7262 \pm 0.0015)\ 10^7 \text{ sec}^{-1} \quad .$$

The theoretical value for the 3γ ray annihilation, which includes only the lowest order contribution was calculated by Ore and Powell [216] :

$$\Gamma_o(\text{th.}) = \frac{\alpha^6}{\pi} m \frac{2}{9} (\pi^2 - 9) = (0.72112 \pm 0.00001)\ 10^7 \text{ sec}^{-1} \quad .$$

Recently, the correction term of relative order α due to the interference of the lowest order diagrams with the higher order diagrams involving photon-photon scattering has also been calculated [217], using numerical integration techniques. The effect is to lower the orthopositronium decay rate :

$$\Gamma_o(\text{th.}) = \frac{\alpha^6}{\pi} m \frac{2}{9} (\pi^2 - 9) \left[1 - \frac{\alpha}{\pi} (0.741 \pm 0.017) + \ldots\right] \quad .$$

It must be noted, however, that the photon-photon scattering correction is only a part of the complete correction of relative order α . The calculation of the other terms, is clearly necessary for an adequate

comparison with the experimental value.

The theoretical value for the 2γ annihilation rate of parapositronium (^1S_o) is known up to terms of relative order α. The lowest order term was first calculated by Dirac [218] and the corrections of relative order α by Harris and Brown [219]:

$$\Gamma_p(\text{th.}) = \frac{\alpha^5}{2} m \left[1 - \frac{\alpha}{\pi}(5 - \frac{\pi^2}{4})\right] = 0.798 \times 10^{10} \text{ sec}^{-1} .$$

Recently, the first direct measurement of the parapositronium annihilation rate has been made [208]. The experiment, which is set to measure the fine-structure interval of the ground state of positronium, involves the measurement of an induced Zeeman transition between magnetic substates of ground-state positronium. Detection of coincident 2γ ray annihilation rather than detection of the γ-ray energy spectrum, as done in previous experiments, was used. The natural line width of the Zeeman transition yields the value of Γ_p:

$$\Gamma_p(\text{exp.}) = (0.799 \pm 0.011)\ 10^{10} \text{ sec}^{-1} , \ (1.4\%)$$

where a one-standard-deviation error is given, in excellent agreement with the theoretical value.

III. MUONIUM

Muonium is the atom consisting of an electron and a positive muon. It was discovered by Hughes and collaborators [301] in 1960 . The muonium system provides an excellent ground to test our understanding of electromagnetic binding when two different masses are involved ; and eventually to detect a possible breakdown of electron-muon universality. Recently, precision measurements of the muonium ground state hyperfine structure and the magnetic moment of the muon have yielded a new determination of the fine-structure constant α , to an accuracy comparable with that reached in measurements of α using the Josephson effect.

III.1. The Hyperfine-Splitting of the Muonium Ground State.

The lowest order splitting of the singlet and triplet levels of muonium ground state is given by the Fermi formula [135]

$$\Delta\nu = \frac{16}{3}\,\alpha^2\,\mathrm{Ry}\,\frac{\mu_\mu}{\mu_o^e} \quad ,$$

where μ_μ is the muon magnetic moment and μ_o^e the Bohr magneton

$$\mu_o^e = \frac{e\hbar}{2m_e c}$$

and

$$\mu_\mu = \mu_o^\mu\,(1 + a_\mu)$$

where $\mu_o^{\mu} = \frac{e\hbar}{2m_{\mu}c}$ and a_{μ} is the celebrated anomalous magnetic moment of the muon.

Qualitatively $\Delta\nu(\mu e) \sim 3\Delta\nu(pe)$, as expected from the ratio of muon to proton magnetic moments. Corrections to the Fermi formula have been calculated up to terms of relative order $\alpha(Z\alpha)^2$ for the radiative and binding corrections [302] and up to terms of relative order $\frac{m_e}{m_{\mu}}\alpha^2 \log\alpha$ for the recoil corrections [303]. Altogether, the theoretical expression for the hyperfine-splitting of the muonium ground state $\Delta\nu(\mu e)$ can be written in the following way

$$\Delta\nu(\mu e) = \frac{16}{3}\alpha^2 \, Ry \, \frac{\mu_{\mu}}{\mu_o^e} \left(1+\frac{m_e}{m_{\mu}}\right)^{-3} \left\{ 1+a_e+(Z\alpha)^2\frac{3}{2} + \right.$$

$$+ \alpha(Z\alpha)\left(-\frac{5}{2}+\log 2\right) + \frac{\alpha}{\pi}(Z\alpha)^2\left[-\frac{2}{3}\log^2(Z\alpha)^{-2} + \right.$$

$$\left. \left. + \left(\frac{281}{360} - \frac{8}{3}\log 2\right)\log(Z\alpha)^{-2} + 18.4 \pm 5\right] + \delta_{\mu} \right\} .$$

The factor $\left(1+\frac{m_e}{m_{\mu}}\right)^{-3}$ is a reduced mass correction. The corrections in curly brackets, except for the δ_{μ} term, are the same as for the hyperfine splitting of the 1S level of the hydrogen atom (*). The term a_e is the anomalous magnetic moment of the eletron. The term δ_{μ} represents the relativistic recoil corrections which for muonium, unlike the case of the hydrogen atom, can be calculated exactly. The expression for δ_{μ} reads

---

(*) See section I.3 .

$$\delta_\mu = \frac{m_e}{m_\mu} \left\{ - 3 \frac{\alpha}{\pi} \left[1 - \left(\frac{m_e}{m_\mu} \right)^2 \right]^{-1} \log \frac{m_\mu}{m_e} \right.$$

$$\left. - \frac{9}{2} \alpha^2 \log\alpha \left(1 + \frac{m_e}{m_\mu} \right)^{-2} \right\} .$$

The leading term is well known. It has been calculated by various authors [304-306]. However, the correction term of relative order $\frac{m_e}{m_\mu} \alpha^2 \log\alpha$ which represents recoil effects arising from low-momentum components of the muonium Bethe-Salpeter equation is known only since recently. It has been calculated by Fulton, Owen and Repko [303].

The numerical estimate of $\Delta\nu(\mu e)$ requires two quantities as input which have to be taken from experiments : the fine structure constant α ; and the ratio μ_μ/μ_o^e . The latter can be obtained from measurements of the ratio of the magnetic moment of the muon to the magnetic moment of the proton μ_μ/μ_p which recently have been performed to an accuracy of a few p.p.m. by two groups [307-308]. It is thanks to these new precise measurements of μ_μ / μ_p that muonium has become a precision test of QED. The previous measurements [309-311] of μ_μ / μ_p had errors of 13-22 p.p.m., too large to profit fully from the more accurate determinations of $\Delta\nu(\mu e)$ [312-313-308].

(i) Precision Measurements of the Magnetic Moment of the Muon.

The value of the ratio μ_μ / μ_p reported by a University of Washington-Lawrence Radiation Laboratory collaboration [307] is

$$\frac{\mu_\mu}{\mu_p} = 3.183347(9) \quad (2.8 \text{ p.p.m.}) \ ,$$

to be compared with previously reported values (see Table III.1.). In terms of the muon mass, this determination of μ_μ / μ_p implies

$$\frac{m_\mu}{m_e} = 206.7683(9) \quad (2.9 \text{ p.p.m.}) \ .$$

The ratio μ_μ / μ_p measured by the authors of ref.307 was performed in three chemical environments showing no substantial differences. This is in contradiction with the suggestion by Ruderman [314] that a correction due to the effect of diamagnetic shielding on the muon moment should exist.

An independent determination of μ_μ / μ_p has been made by Telegdi and collaborators at the University of Chicago [308]. In this experiment, both the hyperfine splitting $\Delta\nu(\mu e)$ and the muon magnetic moment μ_μ are determined from measurements of the Zeeman (F,M_F) transitions : $(1,1) \leftrightarrow (1,0)$ and $(1,-1) \leftrightarrow (0,0)$ in the region of intermediate coupling. The external magnetic field is chosen at a "magic" value, for which the frequencies of the two Zeeman transitions become, to first order, field independent. The results are

$$\Delta\nu(\mu e) = 4463.3022(89) \text{ MHz}$$

and

$$\mu_\mu / \mu_p = 3.183373(13) \ .$$

The latter value has been obtained assuming that the bound-state g fac-

tors are not affected by collisions with the host gas atoms. If,on the contrary, as suggested by calculations by Herman(*), a pressure shift of -11 p.p.m. corresponding to the experimental conditions of ref.308 is assumed, then

$$\mu_\mu / \mu_p = 3.183337(13) \quad ;$$

in excellent agreement with the result obtained by the authors of ref.307 .

(ii) Comparison between theory and experiment(**).

The theoretical values for $\Delta\nu(\mu e)$ which are obtained using the recommended value of the fine structure constant

$$\alpha^{-1} = 137.03602(21) \quad ;$$

and the values of μ_μ / μ_p quoted above are

$$\Delta\nu^{Th}(\mu e)_{Chicago} = 4463.313(21) \text{ MHz}$$

$$\Delta\nu^{Th}(\mu e)_{Wash./LRL} = 4463.323(19) \text{ MHz} \quad .$$

The most precise experimental determinations of $\Delta\nu(\mu e)$ have been made by the Chicago group [308] and by the Yale group [315]

(*) See ref.308 , note (2) added in proof.

(**) We acknowledge a helpful discussion on this point with Professor Thomas Fulton.

Chicago , $\Delta\nu(\mu e) = 4463.3022(89)$; ref.308

Yale , $\Delta\nu(\mu e) = 4463.310(30)$; ref.315 .

Comparing these values to the theoretical predictions given above it can be seen that the Chicago and the later Yale experimental results are within one standard deviation of the theoretical values.

The remarkable accuracy of the $\Delta\nu(\mu e)$ measurement obtained by the Chicago group (2.0 p.p.m.) combined with the new determination of μ_μ / μ_p allows, from the theoretical expression of $\Delta\nu(\mu e)$ an independent determination of the fine structure constant α . The value thus obtained [308], is

$$\alpha^{-1} = 137.03617(30)$$

in excellent agreement with both the WQED value $\alpha^{-1} = 137.03608(26)$ and the recommended value (see Table I.3) .

THE ANOMALOUS MAGNETIC MOMENTS OF THE CHARGED LEPTONS

The anomalous magnetic moments (the "anomaly" $a = \frac{g-2}{2}$ of the charged leptons have for many years offered one of the most interesting and important challenges to both theoretical and experimental quantum electrodynamics. The CERN muon experiments are probably the most outstanding examples of high-precision experiments done with a high energy machine. The calculations of the sixth order QED contributions now in progress around the world (and in one case completed) are the highest order experimentally significant radiative corrections that have been evaluated, and are formidable challenges to algebraic manipulation and numerical integration techniques.

The best experimental value for the electron anomaly has been obtained recently by Rich and Wesley [401]

$$a_e^{exp} = (1\ 159\,657.7 \pm 3.5) \times 10^{-9} \quad .$$

The best experimental value for the muon anomaly is the CERN-storage ring value [007]

$$a_\mu^{exp} = (1\ 166\ 16\ \pm 31) \times 10^{-8} \quad .$$

The electron anomaly is a purely quantum electrodynamical quantity (see section VII). The theoretical value is

$$a_e^{th} = 0.5\ \frac{\alpha}{\pi} - 0.32848\ (\frac{\alpha}{\pi})^2 + (1.49 \pm 0.20)\ (\frac{\alpha}{\pi})^3 \quad ,$$

where the last term is the sixth order contribution with its theoretical uncertainty (see Section IV.2). With $\alpha^{-1} = 137.03608(26)$ we obtain

$$a_e^{th} = (1159655.4 \pm 3.3) \times 10^{-9} \quad .$$

The uncertainty has two parts, one from the fine structure constant (± 2.2) and one from theory (± 2.5) . Experiment and theory thus agree within one standard deviation(*) . It is interesting to note that a slight improvement in experiment and theory might lead to a value for the fine structure constant which is better than the Josephson value(**) .

The muon anomaly is <u>not</u> a pure QED quantity. The theoretical contribution from QED is (section V)

$$a_\mu^{QED} = 0.5 \frac{\alpha}{\pi} + 0.76578 \left(\frac{\alpha}{\pi}\right)^2 + (21.8 \pm 1.1) \left(\frac{\alpha}{\pi}\right)^3$$

which numerically becomes

$$a_\mu^{QED} = (1165814 \pm 14) \times 10^{-9} \quad .$$

To this we add the strong interaction contribution (section VI.1)

$$a_\mu^{Hadronic} = (65 \pm 5) \times 10^{-9}$$

(*) The Drell-Pagels-Parsons estimate [402-403] leads to $0.40(\frac{\alpha}{\pi})^3$ and thus it disagrees with the latest experiment, which corresponds to a sixth order term $(1.67 \pm 0.33) \left(\frac{\alpha}{\pi}\right)^3$.

(**) At present we obtain (disregarding the theoretical uncertainty)

$$\alpha_{g-2}^{-1} = 137.03582(41) \quad .$$

so that the full theoretical value is

$$G_{\mu}^{th} = (1165879 \pm 15) \times 10^{-9}$$

in reasonable agreement with experiment. In Table IV.1 the different contributions are exhibited.

IV. THE ELECTRON ANOMALY

The electron anomaly has been calculated completely up to and including the sixth order.

IV.1 The second and fourth order contributions.

In second order there is only one diagram (Fig.IV.1) which gives the famous Schwinger contribution [003]

$$a_e^{(2)} = \tfrac{1}{2}\frac{\alpha}{\pi} = (1161409.0 \pm 2.2) \times 10^{-9}$$

where we have used the value

$$\alpha^{-1} = 137.03608(26) \quad .$$

There are seven diagrams (Fig.I.4) which contribute to a_e at fourth order in e . The result is rather more complicated than the second order expression. Compared to the rational $\frac{1}{2}$, the transcendentals π^2 , $\pi^2 \log 2$ and $\zeta(3)$ now appear. These represent special values(*) of the dilog $Li_2(x)$ and the trilog $Li_3(x)$. More precisely [405-409]

$$a_e^{(4)} = \left(\frac{\alpha}{\pi}\right)^2 \left\{ \frac{197}{144} + \frac{\pi^2}{12} - \tfrac{1}{2}\pi^2 \log 2 + \frac{3}{4}\zeta(3) \right\} \quad .$$

This fundamental calculation by Karplus and Kroll [405] (later revised ; see Refs.406 and 407) was the first to demonstrate the consistency of the renormalization procedure in higher orders of perturbation theory.

(*) See e.g. Lewin, ref. 404 .

Numerically

$$a_e^{(4)} = -\,0.32848\,\left(\frac{\alpha}{\pi}\right)^2 = -\,1772.3 \times 10^{-9} \quad .$$

The electron anomaly should in fact be expressed as an expansion in the two parameters α and $\frac{m_e}{m_\mu}$. The leading term in $\frac{m_e}{m_\mu}$, coming from the diagram of Fig.IV.2, is however [410]

$$\left(\frac{\alpha}{\pi}\right)^2 \frac{1}{45} \left(\frac{m_e}{m_\mu}\right)^2 = 3 \cdot 10^{-12}$$

which, at the level of approximation needed, can be left out.

IV.2 The Sixth Order Contribution.

Considering the increase in difficulty between the second and fourth order it is not surprising that the evaluation of the sixth order anomaly is indeed hard. First of all the number of graphs is now 72 (Fig.IV.3) and the complexity of the graphs is such that an analytic evaluation in closed form is excluded with present day techniques for virtually all diagrams. Actually diagrams 19-22 (Fig.IV.3) have been evaluated in closed form [411]. In addition to the transcendentals encountered in $a_e^{(4)}$ there appear now special values of the polylogarithm $Li_4(x)$ [404]. As the diagrams lead in general to seven-fold integrals, one expects that the analytic results can involve special values of $Li_n(x)$ with n ranging from 1 to 7, apart from the possible appearance of elliptic integrals. Luckily, however, the diagrams are not more complicated than they allow for numerical evaluation.

Let us summarize the situation. The 72 diagrams contributing to $a_e^{(4)}$ fall into six different classes, the choice of which is mainly based on gauge invariance criteria.

Class I. Graphs 1-6, containing photon-photon scattering subgraphs

Class II. Graphs 7-18, containing second order (but not fourth order) vacuum polarization subgraphs.

Class III. Graphs 19-22, containing fourth order vacuum polarization subgraphs.

Class IV. Graphs 23-28, three-photon exchange.

Class V. Graphs 29-48, two-photon exchange.

Class VI. Graphs 49-72, one-photon exchange.

The first three classes contain fermion loops and coincide with the class division for the difference $a_\mu - a_e$. The last three classes contain no fermion loops and have been classified according to the number of photons crossing from one leg to another. This classification has the advantage of being gauge invariant. Inside some of the classes there are gauge invariant subclasses. We leave it to the reader to prove that the following sets of graphs yield a gauge invariant anomaly (after renormalization) : 1-6, 7-10, 11+12, 13+14+17+18, 15+16, 19, 20-22, 23-28, 29-48, 49-68, 69-72 . In Table IV.2 the history of the sixth order calculations is given. All six classes have been completely evaluated, although detailed results are not yet available for the last three.

The graphs of class III have been evaluated analytically by Mignaco and Remiddi [411] and checked numerically [414,416]. All the other diagrams have only been evaluated numerically. In Tables IV.3,4,5,6 the results of various calculations are presented. We have chosen to present the results as much as possible in the form and detail in which they were originally published. The analytic results for Class III [411] are given in Table IV. 3 . In Table IV. 4 a comparison is made between the results for Class II and III of Brodsky and Kinoshita [414] and Calmet and Perrottet [416]. The agreement is excellent(*). In Table IV.5 the results of De Rújula, Lautrup and Peterman [417] for the gauge invariant subset (69-72) of the Class VI graphs is presented. In Table IV. 6 the recent results of Calmet [418] are listed.

We give below the overall results :

Class I

$$G_{e,I}^{(6)} = 0.36(4)\ (\frac{\alpha}{\pi})^3 \qquad \text{Aldins et al } [412,413) .$$

Class II

$$G_{e,II}^{(6)} = \begin{cases} -0.153(5)\ (\frac{\alpha}{\pi})^3 & \text{Brodsky and Kinoshita } [414) \\ -0.151(3)\ (\frac{\alpha}{\pi})^3 & \text{Calmet and Perrottet } [416) . \end{cases}$$

(*) In Ref.416 graphs 13 and 14 should be interchanged with graphs 17 and 18 .

Class III

$$a_{e,III}^{(6)} = \begin{cases} 0.055429\ (\frac{\alpha}{\pi})^3 & \text{Mignaco and Remiddi } [411] \\ 0.05546(6)\ (\frac{\alpha}{\pi})^3 & \text{Brodsky and Kinoshita } [414] \\ 0.055(2)\ (\frac{\alpha}{\pi})^3 & \text{Calmet and Perrottet } [420] \end{cases}$$

Class IV, V and VI

$$a_{e,IV}^{(6)} + a_{e,V}^{(6)} + a_{e,VI}^{(6)} = 1.23(20)(\frac{\alpha}{\pi})^3 \quad \text{Levine and Wright } [419]$$

The uncertainty in this case is not obtained by statistical methods but it is rather an educated guess.

The overall result for the sixth order electron anomaly is then

$$a_e^{(6)} = (1.49 \pm 0.20)(\frac{\alpha}{\pi})^3 \quad ,$$

where we have used the analytic Class III result, and the weighted average of the Class II results. Details of the calculation by Levine and Wright [419] of the three classes IV, V, VI are as yet not available. It is therefore impossible to compare with the three partial calculations that have appeared previously [415,417,418] and that overlap with these classes (*).

All the 72 graphs have now been calculated. However, as "mirror graphs" give the same anomaly, only 41 of the 72 are independent.

(*) The results of Levine and Wright agree however with those of De Rújula et al (M.J. Levine, private communication).

In view of the complexity of the calculations the necessity for independent checks must be emphasized. So far such checks have only been carried out for class II and III, and in a few instances for graphs belonging to Classes IV, V and VI .

Technically the calculation of the Class I, II and III graphs is not different from the calculation of the corresponding graphs for $G_\mu - G_e$ (see Section V). For the remaining graphs some simplification can be obtained for those that contain self-energy and vertex insertions by using properly parametized forms of these insertions (*) . For those that do not contain such insertions (the irreducible ones) there is no way around a full-fledged parametrization of the three interlaced loops. The complexity of the sixth order graphs has necessitated extensive computer use for algebraic manipulations and numerical integrations. The γ-algebra and vector substitutions in the numerator of a graph can lead to hundreds and sometimes thousands of terms. So far four different algebraic programs have been used in connection with the calculations discussed here and in Sections I.1,II.2 and V.2 . The interpretative program SCHOONSCHIP written by Veltman [422] used in Refs. 411,417,421,217,123, and 5 , the language-oriented LISP-based program REDUCE written by A. Hearn [423], used in Refs.412,413,414 and 119 ; a LISP-program written by Calmet [420] used in refs.416 and 418 , and a program written by M.J. Levine [424] used in Refs. 415 and 419 .

The parametrizations of Feynman graphs generally have a singular (or alsmost singular) behaviour at some parts of the border of the integration region. Gaussian integration methods are very precise for

---

(*) See e.g., ref. 417 .

integrands with polynominal type behaviour, but lose rapidly in reliability for integrands with a steep rise towards the border. The singularities can, however, be removed by means of polynomial mappings, thereby smoothing out the function and allowing for Gaussian integration. This technique has been used by Levine and Wright [419] but has the disadvantage that it does not readily allow for an estimate of error. Straightforward Monte-Carlo methods do not work well for integrals that have their main contribution from some odd corner of the integration region, because the integrand is not preferentially sampled there. The following technique has proved adequate for many of the integrals met in QED : the integration region (the unit hypercube) is subdivided into a set of subvolumes by dividing the unit interval on each axis. In each subvolume the contribution to the integral and to its variance is estimated by random sampling of the integrand, (usually only in two points). Using the variances found one calculates an improved subdivision of the unit intervals and reiterates the above procedure. In this way the function is explored and the interval structure refined such that the interval density adjusts itself to the rate of variation of the integrand, thereby minimising the total variance. A program implementing this technique was originally devised by C.G. Sheppey [425] at CERN. It was first used by Aldins et al [412,413] in a QED context, but has since proved invaluable for many calculations.

IV.3. Measurements of the Electron Anomaly.

The best experimental value for the (negatively charged) electron anomaly has so far been obtained by Wesley and Rich [401]

$$a_{e^-}^{exp} = (1\ 159\ 657.7 \pm 3.5) \times 10^{-9} \quad .$$

This value represents an increase of 14×10^{-9} with respect to the preliminary measurement by the same authors [426]. The error has decreased by a factor of two.

The first indications that the electron possessed an anomalous magnetic moment were reported in 1947 [427-428-429] and Kusch and Foley's experimental value [002] turned out to agree with the calculation by Schwinger [003]. Over the years the precision on the measurements has steadily improved [430-433] in particular with the fundamental experiment of Wilkinson and Crane [434-435] in 1963. Their value agreed with the theoretical calculations until Rich [436] and others [437,438] reanalyzed the experiment and brought out a three standard deviation discrepancy. With the new experiments [426,401] this discrepancy has, however, again disappeared(*). Experiments along similar lines but with less precision have also been done by other groups(**).

(*) The original value of Wilkinson and Crane was
$a_e = 1\ 159622(27) \times 10^{-9}$ corrected by Rich to
$a_e = 1\ 159549(30) \times 10^{-9}$.

(**) See Table IV.7 .

The technique used by Wesley and Rich [426] is essentially the same as that used by Wilkinson and Crane [434] although the apparatus is completely new and the magnetic field is an order of magnitude stronger. Electrons with energy of around 100 keV are partially polarized by Mott scattering at 90° on a gold foil, and subsequently trapped in a magnetic bottle (~ 1000 G) for an accurately measured interval of time. After being ejected from the bottle the polarization of the electrons is analyzed by means of a second 90° Mott scattering. While trapped the average spin motion of the electrons can be described as a precession of their polarization relative to their velocity with a frequency

$$\omega_a = G.\omega_o$$

where G is the anomalous magnetic moment and $\omega_o = e\,B/m_o c$. (If the magnetic field is not homegoneous or not perpendicular to the velocity of the electrons, or if there are electric fields present this formula must be corrected appropriately). As a function of trapping time the polarization and thereby the counting rate will be modulated with this frequency. This permits determination of G . The magnetic field is measured by means of Nuclear Magnetic Resonance (NMR) probes determining the resonance frequency of protons in water. In fact

$$\omega_o = \omega_p(H_2O) \;/\; \left(\frac{\mu_p'}{\mu_B}\right)$$

where μ_p' is the magnetic moment of the proton in a water sample [439] and μ_B the Bohr magneton. The improvement of the accuracy on the anomaly is

essentially due to the larger magnetic field used by Wesley and Rich.

A very promising new experimental technique has been proposed[440] and a preliminary result obtained [441] by a Bonn group. They study polarized electrons circulating in a magnetic field at the cyclotron frequency ω_c. The spin can be flipped by applying a radio frequency (rf) field at the Larmor (spin flip) frequency $\omega_L = \omega_c(1+G)$ and the transition is maintained by the accompanying depolarization of the electrons. It is however also possible to observe the beat frequency $\omega_L - \omega_c = \omega_c G$ corresponding to a simultaneous spin flip and transition between two Landau levels (i.e. change of orbit). A measurement of both ω_L and $\omega_L - \omega_c$ leads to a determination of $\frac{G}{1+G} = \frac{\omega_L - \omega_c}{\omega_L}$. The advantage of this experiment over the previous ones is that the anomaly is measured rf spectroscopically, that the electrons are quite non-relativistic ($\sim$ few eV) and both ω_L and $\omega_L - \omega_c$ are determined by the same method in the same field. The preliminary value is

$$G_e = 1\ 159660(300) \times 10^{-9}$$

and is expected to improve considerably in the future.

The anomaly of the positron was originally measured by Rich and Crane [442] with a technique virtually identical with the one used by Wilkinson and Crane [434] (see the description above). They found the result

$$G_{e^+} = 0.001168(11) \quad .$$

More recently Gilleland and Rich [443] have improved the accuracy by increassing the length of time the positrons were trapped in the magnetic

bottle. The result was

$$a_{e^+} = 0.0011602(11) \quad .$$

The equality of anomalies for the electron and positron is a test of CPT invariance which implies

$$a_{e^-} = a_{e^+} \quad .$$

The experimental values for the electron anomaly have been tabulated in Table IV.7 .

V. THE QUANTUM ELECTRODYNAMICS CONTRIBUTION TO THE DIFFERENCE BETWEEN THE ANOMALOUS MAGNETIC MOMENTS OF MUON AND ELECTRON.

The graphs of the purely quantum electrodynamical contribution to the anomalous magnetic moment of a charged lepton, electron or muon, can be divided into two groups :

1. Graphs involving only one lepton
2. Graphs involving both leptons.

The anomaly for a lepton with mass m can therefore be written

$$G = G_1(m) + G_2(m,m') \quad ,$$

where m' is the mass of the other lepton. Since G is dimensionless, it follows that G_1 must be mass independent, and that G_2 can only depend on the mass ratio. We may then rewrite this equation as

$$G = G_1 + G_2(\frac{m}{m'}) \quad ,$$

which specialized to electron and muon becomes

$$G_e = G_1 + G_2(\frac{m_e}{m_\mu}) \quad ,$$

$$G_\mu = G_1 + G_2(\frac{m_\mu}{m_e}) \quad .$$

Due to the smallness of the ratio $\frac{m_e}{m_\mu}$ it is not necessary to evaluate $G_2(x)$ for all values of x , but only the asymptotic behaviour for small and large x . It follows from general arguments that $G_2(x)$ vanishes

as $x \to 0$. One may thus, in general, disregard the contribution $G_2(\frac{m_e}{m_\mu})$ to G_e . The difference

$$G_\mu - G_e = G_2(\frac{m_\mu}{m_e}) - G_2(\frac{m_e}{m_\mu})$$

only involves G_2 and the evaluation of $G_\mu - G_e$ is generally easier than the evaluation of the complete anomalies.

In the discussion below, we shall only include those graphs which give a non-vanishing contribution after renormalization. Thus we leave out all corrections to external lines. We also leave out all graphs representing renormalization counter-terms, assuming them to be implicitly included. The difference $G_\mu - G_e$ has so far been computed up to (and including) the sixth order. It vanishes at second order.

V.1 The fourth order contribution.

In fourth order there is only one graph that contributes to G_2 , namely the one obtained from the Schwinger graph by inserting a vacuum polarization loop in the photon line. Up to terms of the order of $(\frac{m_e}{m_\mu})^3$ we have the contribution to G_μ

$$G_2^{(4)}(\frac{m_\mu}{m_e}) = (\frac{\alpha}{\pi})^2 \left\{ \frac{1}{3} \log \frac{m_\mu}{m_e} - \frac{25}{36} \right.$$

$$\left. + \frac{\pi^2}{4} \frac{m_e}{m_\mu} - 4 (\frac{m_e}{m_\mu})^2 \log \frac{m_\mu}{m_e} + 3 (\frac{m_e}{m_\mu})^2 + O((\frac{m_e}{m_\mu})^3) \right\} .$$

The first two terms were evaluated by Suura and Wichmann [501] and by Peterman [502]. The remaining terms have been obtained by Elend [503] and by Erickson and Liu [504]. These authors have calculated the function $G_2^{(4)}(x)$ for all x. To the same accuracy, the contribution to G_e is [410]

$$G_2^{(4)}\left(\frac{m_e}{m_\mu}\right) = \left(\frac{\alpha}{\pi}\right)^2 \left\{ \frac{1}{45} \left(\frac{m_e}{m_\mu}\right)^2 + O\left(\left(\frac{m_e}{m_\mu}\right)^4\right) \right\} ,$$

which is vanishingly small, but has been included as a reminder of the fact that both G_e and G_μ depend on the mass ratio.

Hence the fourth order difference (Fig.IV.2) is

$$(G_\mu - G_e)^{(4)} = \left(\frac{\alpha}{\pi}\right)^2 \left\{ \frac{1}{3} \log \frac{m_\mu}{m_e} - \frac{25}{36} + \frac{\pi^2}{4} \frac{m_e}{m_\mu} - 4 \left(\frac{m_e}{m_\mu}\right)^2 \log \frac{m_\mu}{m_e} + \frac{134}{45} \left(\frac{m_e}{m_\mu}\right)^2 + O\left(\left(\frac{m_e}{m_\mu}\right)^3\right) \right\} .$$

Numerically we have

$$(G_\mu - G_e)^{(4)} = 1.09426 \left(\frac{\alpha}{\pi}\right)^2 = 5904.1 \times 10^{-9}$$

V.2 The sixth order contribution.

In sixth order there are 24 graphs(*) contributing to

(*) Here we disregard the contribution from $G_2\left(\frac{m_e}{m_\mu}\right)$.

$G_\mu - G_e$. They are shown in Fig.V.1 . These graphs are naturally divided into three classes

I Graphs 1-6 , containing photon-photon scattering subgraphs

II Graphs 7-20, containing second order (but not fourth order) electron vacuum polarization subgraphs

III Graphs 21-24, containing fourth order electron vacuum polarization subgraphs.

Not all of these graphs are independent. Some are related to each other by charge conjugation, thereby giving the same anomalous magnetic moment contribution. Two graphs give the same anomalous magnetic moment if they arise from each other by reversing the directions of the muon line. Thus there are 14 independent sets of graphs, the only unpaired graphs being 9, 10, 21, and 24.

From Table V.1 which gives the history of the calculations of these graphs, it is seen that all graphs except those of Class I have been evaluated twice (one-graph 21-even three times). The two independent results for graphs 7-24 have been tabulated in Table V.2 and Table V.3 allowing for a detailed comparison of the values obtained from each graph. The uncertainties arise from the numerical integrations(*) .

(*) See the discussion at the end of Section IV.2 .

The agreement is generally very good, although there is a slight difference between the two values for graphs 7+8 .

We can now quote the overall results for the three classes(*)

Class I [412,413) : $(G_\mu - G_e)^{(6)}_I = (18.4 \pm 1.1)(\frac{\alpha}{\pi})^3$

Class II [507,421,506,414) : $(G_\mu - G_e)^{(6)}_{II} = \begin{cases} (-2.30 \pm 0.02)(\frac{\alpha}{\pi})^3 & \text{Table V.2} \\ (-2.32 \pm 0.10)(\frac{\alpha}{\pi})^3 & \text{Table V.3} \end{cases}$

Class III [410,505,414) : $(G_\mu - G_e)^{(6)}_{III} = \begin{cases} 4.2414(\frac{\alpha}{\pi})^3 & \text{Table V.2} \\ 4.21 \pm 0.03)(\frac{\alpha}{\pi})^3 & \text{Table V.3} \end{cases}$

The overall agreement between the two independent calculations is excellent, the small differences having largely cancelled out in the sum. The final result is

$$(G_\mu - G_e)^{(6)} = (20.3 \pm 1.1)\ (\frac{\alpha}{\pi})^3$$
$$= (254 \pm 14) \times 10^{-9} \quad .$$

(*) We add the uncertainties quadratically because of the statistical nature of the errors obtained by the particular integration technique which has been used. This is in contrast to the attitude of the authors of ref.414, who add the errors linearly in which case one would have obtained

$$(-2.30 \pm 0.05)\ ,\ (-2.32 \pm 0.20)\ ,\ (4.21 \pm 0.04)$$

for the results of Class II and III .

In view of the fact that the Class I contribution is by far the most important one, being an order of magnitude greater than the rest, and at the same time the only part that has not been checked by an independent group, we must emphasize the need for a recalculation. It would also be desirable to lower the uncertainty because the planned experiments on the muon anomaly may reach the precision of $\sim 15 \times 10^{-9}$.

We shall now discuss some of the techniques used in obtaining the sixth order result. The amplitude for an arbitrary vertex graph can be written $-i e \Gamma_\mu(p_2,p_1)$ where p_1 and p_2 are the momenta of the incoming and ougoing lepton. The most general expression between two spinors is

$$\bar{u}_2 \Gamma_\mu(p_2,p_1) u_1 = \bar{u}_2 \left\{ (F_1 + F_2)\gamma_\mu - \frac{(p_1+p_2)_\mu}{2m} F_2 + \frac{(p_2-p_1)_\mu}{2m} F_3 \right\} u_1$$

$$= \bar{u}_2 \left\{ F_1\gamma_\mu - i \sigma_{\mu\nu} \frac{(p_2-p_1)^\nu}{2m} F_2 + \frac{(p_2-p_1)_\mu}{2m} F_3 \right\} u_1 ,$$

which defines the three form factors $F_i((p_2-p_1)^2)$. By definition, the contribution to the anomalous magnetic moment is

$$G = F_2(0) \quad .$$

A graph can be subjected to two kinds of gauge transformations, external and internal. A set of graphs is invariant under external gauge transformations when

$$(p_2 - p_1)^\mu \ \bar{u}_2 \Gamma_\mu (p_2,p_1) u_1 = 0 \quad ,$$

which implies that $F_3 = 0$. This condition (current conservation) is not in general satisfied for individual graphs. In Fig.V.1 the sets of graphs invariant under external gauge transformations are 1+3+5 , 2+4+6, 7+11+14 , 8+12+13 , 9+15+16 , 10+17+18 , 19, 20, 21, 22, 23 and 24 . The external gauge transformations are, however, not relevant for the purely intrinsic quantity G , which will only be influenced by internal gauge transformations, i.e. transformations of the photon propagator of the form

$$\frac{g_{\mu\nu}}{k^2} \rightarrow \frac{g_{\mu\nu}}{k^2} + k_\mu k_\nu f(k^2)$$

where f is an arbitrary function. We leave it for the reader to prove that the following sets of graphs yield gauge invariant total contributions to the anomaly (after renormalization) : 1+3+5 , 2+4+6 , 7+8+9+10 , 11, 12, 13+17 , 14+18 , 15, 16, 19, 20, 21 and 22+23+24 . It can be seen that the contributions from each set is infrared convergent.

It is an interesting coincidence that the most difficult graphs to evaluate, namely those of Class I , are also the graphs that give the largest contribution. These graphs were evaluated by the combined efforts of Aldins, Brodsky, Dufner and Kinoshita [412,413] . Calling the off-shell photon-photon-scattering amplitude $\Pi_{\mu_1\mu_2\mu_3\mu_4}(k_1k_2k_3k_4)$,,,, $(k_1+k_2+k_3+k_4 = 0)$ we can write the vertex functions from graphs 1-6 using the notation of Fig. V.2

$$\Gamma_\mu(p_2,p_1) = - e^2 \int \frac{dk_1,dk_2}{(2\pi)^8} \quad \frac{\Pi_{\mu\nu\rho\sigma}(q,k_1,k_3,k_2)}{k_1^2\, k_2^2\, k_3^2}$$

$$\cdot\, \gamma^\nu\, (\not{p}_2 + \not{k}_2 - m_\mu)^{-1} \gamma^\rho\, (\not{p}_1 - \not{k}_1 - m_\mu)^{-1} \gamma^\sigma$$

where $q = p_2 - p_1$ and $k_3 = -k_2 - k_1 - q$.

An ingenious use of gauge-invariance made the extraction of the anomalous magnetic moment much simpler, at the same time explicitly removing the spurious logarithmic ultra-violet divergence inherent to the photon-photon scattering amplitude. Current conservation or gauge invariance gives rise to the identity

$$q^\mu\, \Pi_{\mu\nu\rho\sigma}\, (q,k_1,k_3,k_2) = 0 \quad ,$$

from which one obtains by differentiation

$$\Pi_{\mu\nu\rho\sigma}\, (q,k_1,k_3,k_2) = -q^\lambda \frac{\partial}{\partial q^\mu}\, \Pi_{\lambda\nu\rho\sigma}\, (q,k_1,k_3,k_2) \quad .$$

Thereby one can write

$$\Gamma_\mu(p_2,p_1) = q^\lambda\, \Gamma_{\mu\lambda}(p_2,p_1)$$

with

$$\Gamma_{\mu\lambda}(p_2,p_1) = e^2 \int \frac{dk_1 dk_2}{(2\pi)^8} \quad \frac{\frac{\partial}{\partial q^\mu}\, \Pi_{\lambda\nu\rho\sigma}(q,k_1,k_3,k_2)}{k_1^2\, k_3^2\, k_2^2}$$

$$\cdot\, \gamma^\nu\, (\not{p}_2 + \not{k}_2 - m_\mu)^{-1}\, \gamma^\rho (\not{p}_1 - \not{k}_1 - m_\mu)^{-1}\, \gamma^\sigma \quad .$$

In $\Gamma_{\mu\lambda}$, p_2 can be put equal to p_1 because one power of q is already taken outside. Differentiation of a graph with respect to an external momentum acts like the insertion of zero momentum photons and decreases the degree of divergence by one, thereby removing the spurious logarithmic divergence. The remainder of the calculation is in principle straightforward although very complicated. Aldins et al, used two different techniques for obtaining the parametric form of the integral, one being the standard Landau method (*) the other based on a method developed by Nakanishi [510] and Kinoshita [511] (double parametric representation). Part of the reduction to parametric form was done by hand, and part was carried out by means of REDUCE, a programing language for algebraic manipulation developed by Hearn [423] . Finally the (7-dimensional) parametric integral was evaluated numerically by means of the special numerical integration program described at the end of Section IV.1 . It was found that the Class I diagrams contains a logarithmic divergence for $m_e \to 0$ contrary to expectations [505] . Writing

$$(a_\mu - a_e)_I^{(6)} = \left(\frac{\alpha}{\pi}\right)^3 \left\{ C_1 \log \frac{m_\mu}{m_e} + C_2 \right\} .$$

Aldins et al found that C_1 could be expressed as a 5-dimensional integral with the value

$$C_1 = 6.4 \pm 0.1 .$$

The remainder C_2 was not determined directly but could be inferred from the overall value quoted above

---

(*) See e.g. Bjorken and Drell, Ref.509, Sec.18.4 .

$$C_2 \simeq -16 \pm 1 \quad .$$

The numbers C_1 and C_2 are surprisingly large. In all other cases purely numerical coefficients turn out to be of the order of unity. This unexpected behaviour also stresses a need for a recalculation of the Class I diagrams.

The remaining diagrams are all much simpler to evaluate. All of the Class III diagrams are examples of the graph shown in Fig.V.3 where the insertion G is a fourth order vacuum polarization graph. The vertex function from this graph is

$$\Gamma_\mu^{(G)}(p_2,p_1) = e^2\int \frac{dk}{(2\pi)^4}\ \gamma^\rho\ (\not p_2 - \not k - m_\mu)^{-1}\gamma_\mu\ (p_1 - \not k - m_\mu)^{-1}\gamma^\sigma\ D_{\rho\sigma}^{(G)}(k) \quad ,$$

where $D_{\rho\sigma}^{(G)}$ is the contribution to the photon propagator form the graph G . This quantity can be expressed in terms of a single spectral function

$$D_{\rho\sigma}^{(G)} = i\left(g_{\rho\sigma} - \frac{k_\rho k_\sigma}{k^2}\right)\frac{\Pi^{(G)}(k^2)}{k^2} \quad ,$$

satisfying a once subtracted dispersion relation

$$\frac{\Pi^{(G)}(k^2)}{k^2} = \int_0^\infty \frac{dt}{t}\ \frac{\frac{1}{\pi}\,\mathrm{Im}\,\Pi^{(G)}(t)}{t-k^2} \quad .$$

The imaginary part is given by

$$\theta(k)\ \mathrm{Im}\ \Pi^{(G)}(k^2) = \frac{-1}{6k^2}\sum_{n\in G}(2\pi)^4\delta^{(4)}(k-k_n)$$
$$< 0|\ J_\mu(0)|\ n >< n|\ J^\mu(0)|0 >$$

where the sum goes over the possible intermediate states in G. Accordingly we can write

$$\Pi_\mu^{(G)}(p_2,p_1) = \int_0^\infty \frac{dt}{t}\,\frac{1}{\pi}\,\mathrm{Im}\,\Pi^{(G)}(t)\,\Gamma_\mu^{(2)}(p_2,p_1,t)$$

where $\Gamma_\mu^{(2)}(p_2,p_1,t)$ is obtained from the usual second order graph replacing the photon propagator $-i\,g_{\mu\nu}/k^2$ by $-i\left(g_{\mu\nu}-\frac{k_\mu k_\nu}{k^2}\right)\frac{1}{k^2-t}$.

The anomalous magnetic moment satisfies the same equation

$$G^{(G)} = \int_0^\infty \frac{dt}{t}\,\frac{1}{\pi}\,\mathrm{Im}\,\Pi^{(G)}(t)\,G^{(2)}(t)$$

where $G^{(2)}(t)$ is the anomalous magnetic moment obtained from the second order graph replacing the photon propagator by $-i\left(g_{\mu\nu}-\frac{k_\mu k_\nu}{k^2}\right)\Big/k^2-t$. The $k_\mu k_\nu$ terms can be disregarded as they only contribute to the renormalization constant Z_1 and $G^{(2)}(t)$ is given by the well-known expression(*)

$$G^{(2)}(t) = \frac{\alpha}{\pi}\,K(t)$$

$$K(t) = \int_0^1 dx\,\frac{x^2(1-x)}{x^2+(1-x)\frac{t}{m_\mu^2}}$$

These expressions are valid for any kind of insertion G, in particular for the hadronic vacuum polarization (see Section VI.1). In the case of

---

(*) $K(t)$ is bounded, and monotonically decreasing

$$\frac{t_o}{t}\,K(t_o) \le K(t) < \frac{1}{3}\,\frac{m_\mu^2}{t} \qquad \text{for} \quad 0 < t_o \le t < \infty$$

fourth order vacuum polarization insertions, the function $\mathrm{Im}\,\pi^{(G)}(t)$ was already known from the work of Källen and Sabry [512], and the whole calculation boiled down to a one-dimensional integral which could be evaluated analytically with the result shown in Table V.2 .

For the analytic evaluation of the double bubble graphs 19-21, an expression very well suited is [506]

$$G^{(G)} = \int_0^1 dx(1-x) \left[- \pi^{(G)} \left(- \frac{x^2}{1-x} m_\mu^2 \right) \right] ,$$

which is obtained interchanging the order of integrations in x and t in the general expression for $G^{(G)}$. Here, the $\Pi^{(G)}$-function is simply a product of two second-order Π-functions.

For the Class II diagrams it follows by the same arguments as above that the anomaly for a graph is given by

$$G = \int_{4m_e^2}^{\infty} \frac{dt}{t} \frac{1}{\pi} \mathrm{Im}\,\Pi^{(2)}(t)\, G(t)$$

where $\Pi^{(2)}(t)$ is the second order vacuum polarization by electrons, and $G(t)$ is the anomaly from the fourth order graph obtained from a sixth order graph by replacing the photon propagator containing the vacuum polarization insertion by a massive propagator

$$- i \left(g_{\mu\nu} - \frac{k_\mu k_\nu}{k^2} \right) \frac{1}{k^2 - t} \quad .$$

The $k_\mu k_\nu$ terms can be disregarded because they are essentially gauge terms that cancel within the following sets of graphs : 7+8+9+10 ,

11+15 , 12+16 , 13, 14, 17, 18, 19, 20 . Thus at the expense of one extra integration relative to the fourth order calculation one can evaluate the anomaly from the Class II graphs [507,421,414] . It is even possible to perform the t-integration analytically in the limit $\frac{m_e}{m_\mu} \to 0$. For a graph (or set of graphs) for which $G(0)$ exists(*) one has to order $\frac{m_e}{m_\mu}$

$$G = \frac{\alpha}{\pi}\left\{\left(\frac{2}{3}\log\frac{m_\mu}{m_e} - \frac{5}{9}\right)G(0) + \frac{1}{3}G' + O\left(\frac{m_e}{m_\mu}\right)\right\}$$

where

$$G' = \int_0^{4m_\mu^2}\frac{dt}{t}\{G(t) - G(0)\} + \int_{4m_\mu^2}^{\infty}\frac{dt}{t}G(t)$$

does not depend on the mass ratio. The quantity $G(t)$ is a multidimensional integral (up to 5-dimensions) of the form

$$G(t) = \int\int\ldots\int \sum_{n\geq 1}\frac{A_n}{(B+Ct)^n} \quad ,$$

which can be integrated analytically over t . For $t = 0$, $G(t)$ is the ordinary fourth order anomaly from the graph (or set of graphs) obtained by removing the vacuum polarization insertion(**) . These fourth order

---

(*) If $G(0)$ does not exist (as for graphs 9-18) it is always possible to separate $G(t)$ into a regular part for which the analysis can be carried out as shown, plus an irregular part which can be evaluated explicitly.

(**) If $G(0)$ exists. Otherwise see the previous footnote.

anomalies have been given by Peterman, so that it is trivial to obtain the analytic form of the coefficient of $\log \frac{m_\mu}{m_e}$ (see Table V.2) .

The final stage of the Class II calculations is a numerical integration of the parametric integral again using the Sheppey program described at the end of Section IV.2 . The reason for the difference in the quoted uncertainties of the two different calculations of the Class II diagrams is probably due to the fact that the analytic integration over t was carried out in refs.506 and 507 (Table V.2) but not in ref.414 (Table V.3) .

VI. OTHER CONTRIBUTIONS TO THE MUON ANOMALY

VI.1 The Hadronic Contributions.

The importance of hadronic vacuum polarization insertions in the second order muon vertex (see Fig. V.3) was first pointed out by Bouchiat and Michel [601]. They remarked that resonances in the π-π system can lead to an enhancement of the vacuum polarization corrections which could be observable in precision measurements of G_μ. The first estimates of this effect(*) gave G_μ (Hadrons) $\sim 10^{-7}$, i.e, far below the error in the measurement of G_μ at that time which was [004] $\pm 5 \times 10^{-6}$. Since then, a new precision measurement of G_μ has been made [007,008]; and, simultaneously, colliding beam experiments have been performed at Novosibirsk [605, 606] and Orsay [607 - 609] which yield precious information on the hadronic contributions to G_μ.

The hadronic spectral function which appears in the Källen-Lehmann representation of the photon propagator (see the discussion of Class III diagrams in Section V.2) can be directly obtained from measurements of the total e^+e^- annihilation cross-section into hadrons. To lowest order in α (see Fig.V.3) and $t \geq 4m_\pi^2$,

---

(*) Independent calculations were also made by Durand, Ref. 602 and later, using new information on vector mesons, by Kinoshita and Oakes (Ref. 603) ; and by Bowcock (Ref. 604) .

$$\sigma_{e^+e^-\to\text{hadrons}}(t) = \frac{4\pi^2\alpha}{t}\frac{1}{\pi}\,\text{Im}\,\Pi^{(H)}(t) \quad ,$$

were t is the total e^+e^- centre-of-mass energy squared. The hadronic contributions to G_μ, due to vacuum polarization insertions in the second order muon vertex, can thus be directly related to the annihilation cross-section measured in the colliding beams experiments. Assuming that the dispersion integral for the hadronic vacuum polarization only requires one subtraction (charge renormalization) we have

$$G_\mu(\text{Hadrons}) = \frac{1}{4\pi^3}\int_{4m_\pi^2}^{\infty} dt\ \sigma_{e^+e^-\to\text{hadrons}}(t)\ K_\mu(t) \ ,$$

where $K_\mu(t)$ is a purely QED function which results from the combination of the two fermion propagators and the propagator of a "photon" with squared mass t in the muon vertex of Fig.IV.1 ,

$$K_\mu(t) = \int_0^1 dx\ \frac{x^2(1-x)}{x^2 + (1-x)\frac{t}{m_\mu^2}} \quad .$$

The function $K_\mu(t)$ is positive definite in the integration region $4m_\pi^2 \le t \le \infty$ and therefore $G_\mu(\text{Hadrons})$ must be positive. Notice that, for large values of t, $K(t)$ decreases as t^{-1} ,

$$K_\mu(t) \underset{t\to\infty}{=} \frac{1}{3}\ \frac{m_\mu^2}{t} + O\left[\left(\frac{m_\mu^2}{t}\right)^2 \log\left(\frac{t}{m_\mu^2}\right)\right] \quad .$$

It appears thus that the high energy contributions to $G_\mu(\text{Hadrons})$ are

depressed by the factor $K_\mu(t)$ (*). The G_μ(Hadrons) integral is dominated by the low energy region and, in particular, by those values of t corresponding to the mass squared of resonances which have the quantum numbers of the photon.

A calculation of G_μ(Hadrons) using the results of the Orsay colliding beams experiments has been done by Gourdin and de Rafael [610]. The total contribution to G_μ(Hadrons) was separated into an isoscalar contribution $I = 0$ and an isovector contribution $I = 1$. The isoscalar part $G_\mu(I=0)$ was estimated using vector meson dominance, taking into account the contributions from the ω and φ mesons :

$$G_\mu(I=0) \simeq \sum_{V=\omega,\varphi} \frac{3}{\pi} K_\mu(M_V^2) \frac{\Gamma(V\to e^+e^-)}{M_V}$$

$$= (6.1 \pm 1.2 + 5.0 \pm 0.8) \times 10^{-9} \quad .$$

(*) In particular, this explains why hadronic vacuum polarization insertions in the second order <u>electron</u> vertex can be neglected. They give a contribution

$$G_e(\text{Hadrons}) \simeq \frac{1}{12\pi^3} m_e^2 \int_{4m_\pi^2}^{\infty} \frac{dt}{t} \sigma_{e^+e^-\to\text{hadrons}}(t) \quad .$$

In fact, using the inequality $\frac{t_o}{t} K_\mu(t_o) \le K_\mu(t) \le \frac{1}{3} \frac{m_\mu^2}{t}$ for $t_o \le t$, we get

$$G_e(\text{Hadrons}) \le \frac{1}{12} \left(\frac{m_e}{m_\pi}\right)^2 \frac{1}{K_\mu(4m_\pi^2)} G_\mu(\text{Hadrons}) =$$

$$= 3.7 \times 10^{-5} G_\mu(\text{Hadrons}) \quad .$$

The isovector part $G_\mu(I=1)$ was estimated assuming that the $I = 1$ hadronic system is dominated by the π-π P-wave. The evaluation of the integral was made using the expression proposed by Gounaris and Sakurai for the pion form factor [611]. This expression, which is based on a generalized effective-range formula for π-π scattering, takes into account finite width effects and fits well the Orsay data ranging from 644 MeV to 886 Mev with the following values for the mass and the width of the ρ-meson

$$M_\rho = (770 \pm 4) \text{ MeV} , \Gamma_\rho = (111 \pm 6) \text{ MeV} .$$

The result obtained is

$$G_\mu(I=1) = (54 \pm 3) \times 10^{-9} .$$

Altogether $G_\mu(\text{Hadrons})$ is estimated to be

$$G_\mu(\text{Hadrons}) = (65 \pm 5)\ 10^{-9} .$$

Notice that the error quoted above only reflects the uncertainty in the Orsay data used as input. The uncertainties due to the extrapolation of the Gounaris and Sakurai expression for the pion form factor below 644 MeV and above 886 MeV , as well as the uncertainty in neglecting other contributions to the isoscalar part than those coming from the ω and the φ resonances can certainly be larger than 5×10^{-9} Clearly, more experiments with colliding beams in the region just above the two pion threshold and at high energies will be extremely welcome to

reduce these uncertainties.

There have been some attempts to bound the hadronic vacuum polarization contributions to a_μ . An analysis by Bell and de Rafael[612] shows that a proposed theoretical bound [613], based on the hypothesis of current-field identity [614], does not add usefully to the strict vector meson dominance (V.M.D.) estimate of $a_\mu(\text{Hadrons})$(*) . In fact, the estimated bound depends again on a V.M.D. approximation, and this moreover to a quantity for which that approximation is less reliable than for $a_\mu(\text{Hadrons})$ itself. It is possible, however, to bound $a_\mu(\text{Hadrons})$ in a different way by a quantity which governs all sufficiently low energy vacuum polarization effects [612] . Indeed, the hadronic contribution to the photon propagator is

$$\Pi^H(q^2) = \int_{4m_\pi^2}^{\infty} \frac{dt}{t} \; \frac{\frac{1}{\pi}\,\mathrm{Im}\,\Pi(t)}{t-q^2}$$

and we have

$$a_\mu(\text{Hadrons}) \lesssim \frac{\alpha}{\pi}\,\frac{m_\mu^2}{3}\,\Pi^H(0) \lesssim \frac{\alpha}{\pi}\,\frac{1}{3}\,m_\mu^2\left(1 - \frac{q^2}{4m_\pi^2}\right)\Pi^H(q^2)$$

for all negative q^2 . Large momentum transfer electron-electron scatter-

---

(*) Using the experimental input quoted in Refs. 607 - 609 , the strict V.M.D. estimate of $a_\mu(\text{Hadrons})$ is $(6\,1 \pm 5)\,10^{-9}$; see Refs. 610 and 612 .

ing experiments can be used to set a limit on $P^H(q^2)$ for particular values of q^2 . Present experimental results lead to an upper bound

$$G_\mu(\text{Hadrons}) \leq 9 \times 10^{-6} \quad ;$$

this limit, however, could be lowered down with improved empirical knowledge on electron-electron scattering at large momentum transfer and electron-positron annihilation at all available energies.

VI.2 The Weak Interaction Contribution.

To give a definite prediction for the contribution from weak interactions is not possible because of the inherent theoretical difficulties with higher order weak corrections. Estimates can however be made.

If the weak interactions are of the local four-fermion V-A type the diagram in Fig VI.1 will give rise to an anomaly for the muon. The corresponding diagram for the electron is obtained by interchanging e and μ. Power counting indicates that the anomaly will be quadratic in the cut-off and by dimensionality arguments one would expect

$$a_\mu^F \simeq C\, G_F^2\, \Lambda^2\, m_\mu^2$$

where G_F is the Fermi coupling constant, Λ is a cut-off and C a numerical constant. This constant, surprisingly, turns out to be zero [615]; therefore, the dominant term to be expected from the four-fermion interaction is +)

$$a_\mu^F \simeq C\, G_F^2\, m_\mu^4\, \log \frac{\Lambda}{m_\mu} \simeq 10^{-12}$$

much too small to be of importance. If, however, the weak interactions are mediated by an intermediate charged boson, W, the weak anomaly will only be of first order in $G_F = \sqrt{2}\, g^2/m_W^2$. The corresponding diagram is shown in Fig. VI.2. The history of this diagram has been particularly controversial [615-622]. Only the last two calculations (Brodsky and Sullivan [621], Burnett and Levine [622]) agree on the expression *)

+) See, however, ref. 634.

*) The case $K_W = 0$ considered by Schaffer [620] also agrees with this expression.

$$a_\mu^W = \frac{G_F m_\mu^2}{8\pi^2\sqrt{2}} \left(2(1-K_W) \log \xi + 10/3 \right) \quad .$$

Here K_W is the anomalous magnetic moment of the W and ξ is the regularizer used in the ξ-limiting procedure [623] . The overall factor is

$$\frac{G_F m_\mu^2}{8\pi^2\sqrt{2}} \simeq 1.0 \times 10^{-9} \quad .$$

The other factor is in principle unknown. Brodsky and Sullivan take $\xi = \alpha$ (the fine structure constant) and $K_W = 0$, obtaining

$$a_\mu^W \simeq - 10 \times 10^{-9}$$

while Burnett and Levine get

$$a_\mu^W = - 20 \times 10^{-9}$$

using $\xi = (\frac{m_W}{\Lambda})^2 = \left(\frac{2 \text{ GeV}}{300 \text{ GeV}}\right)^2$ and also $K_W = 0$.

VI.3. Measurements of the Muon Anomaly.

The best experimental value for the muon anomaly has been obtained at CERN [007,008] and the value is(*)

$$a_\mu^{exp} = 0.00116616(31) \quad .$$

The first determination of the muon anomaly was the precision measurement by Garwin et al [624] of the magnetic moment of the muon. Combined with the measurement of the muon mass the anomaly could be calculated. The precision (see Table VI.1) was however not sufficient to see the effect of the fourth order term (section V.1) which differs from the corresponding term in the electron anomaly due to vacuum polarization by electrons. The subsequent CERN experiment[625,004,626,627] although much more precise, did still not allow any definite conclusion to be reached about the fourth order term. The second CERN experiment which gave the final number quoted above, however, established that the muon anomaly differed from the electron anomaly by the amount predicted by theory. It was even so precise that it was necessary to include the sixth order term in the theoretical value in order to obtain full agreement with experiment

---

(*) This value contains results for both μ^- and μ^+ , thus assuming CPT. Separating μ^+ and μ^- contributions one has $a_{\mu^-} - a_{\mu^+} = (50 \pm 75) \times 10^{-8}$ (see ref.R.1) as a test of CPT .

The CERN experiments measure the anomaly directly (as in the electrons anomaly experiments) from the precession of the spin of the muon relative to its momentum. In a uniform magnetic field B the precession rate (in the laboratory) is

$$\omega_a = a \frac{e}{m_\mu c} B$$

independent of the velocity of the muons. The spin (Larmor) precession frequency of muons at rest in vacuum is

$$\omega_\mu = (1+a) \frac{e}{m_\mu c} B$$

such that

$$\frac{a}{1+a} = \frac{\omega_a}{\omega_\mu} \quad .$$

The quantity ω_μ cannot be determined directly, but one can measure the precession frequency of protons in water ω'_p by means of a nuclear magnetic resonance (NMR) magnetometer in the same magnetic field. Combined with the measurements [629,630] of the ratio $\lambda = \omega'_\mu / \omega'_p$ of muon to proton precession frequencies in water we find

$$\frac{a}{1+a} = \frac{\omega_a}{\omega'_p} \cdot \frac{1}{\lambda} \frac{1}{1+\epsilon}$$

where we have put $\frac{\omega'_\mu}{\omega_\mu} = \frac{1}{1+\epsilon}$. The Ruderman [631] correction ϵ representing the diamagnetic shielding of the field of the muon in water has recently been experimentally shown to be negligible [629].

The frequency ω_a is measured by observing the decay of muons

in a storage ring with an almost uniform magnetic field ($\sim$17 kG) . The muons ($\sim$ 1.3 GeV) are obtained from the nearly forward decay of π's created when a proton beam ($\sim$ 10 GeV) hits a target inside the ring . The muons are on the average longitudinally polarized ($\sim$ 26%) when they become trapped, but while they are circulating before they decay the spin will turn relatively to the momentum with the frequency ω_G . The decay rate in the forward direction will be modulated with this frequency. The top end of the electron spectrum seen at the inside of the ring corresponds to near forward decays and will thus also be modulated with ω_G . For further details we refer the reader to for instance refs.007, 008 and R.1 .

A new g_μ-2 experiment [632,633,R.1] is being planned at CERN as a continuation to the previous experiments. Ingeneous new features lead to an expected overall improvement of the uncertainty by a factor of 20 .

Finally let us mention that Henry et al [628] have also measured G_μ with a technique resembling that of the measurements of the electron anomaly (section IV.3). The result deviates from theory by two standard deviations, but the precision is rather low (see Table VI.1) .

VII. "EXOTIC" CONTRIBUTIONS TO THE ELECTRON AND MUON ANOMALIES.

In this section we present a summary of the various speculative contributions to the anomalies. It is generally impossible to give definite predictions for such contributions due to the lack of knowledge of the coupling constants and masses of the hypothetical particles or fields involved. Instead we shall turn the argument around and use the agreement between theory and experiment to put limits on such parameters.

VII.1. Generalities.

If a theory gives a certain contribution Δa to the anomaly of a charged lepton, this quantity is restricted(*) by the inequality

$$|\Delta a + a^{th} - a^{exp}| \lesssim C \sqrt{(\sigma^{th})^2 + (\sigma^{exp})^2} \quad ,$$

where $a^{th} \pm \sigma^{th}$ and $a^{exp} \pm \sigma^{exp}$ are the theoretical and experimental lepton anomalies with associated one standard deviation uncertainties(**). The constant C is related to the confidence limit of the bound, We shall choose a 95% confidence limit with

$$C = 1.96 \quad .$$

(*) We assume that two or more exotic contributions do not conspire to cancel each other.

(**) We have added these uncertainties quadratically although this is not a unique choice.

We have (sections IV.3 and VI.2)

$$a_e^{exp} = (1159657.7 \pm 3.5) \times 10^{-9} \quad ; \quad a_e^{th} = (1159655.4 \pm 3.3) \times 10^{-9}$$

$$a_\mu^{exp} = (1166160 \pm 310) \times 10^{-9} \; ; \quad a_\mu^{th} = (1165879 \pm 15) \times 10^{-9}$$

such that the inequality above becomes

$$-7.1 \times 10^{-9} \lesssim \Delta a_e \lesssim 11.7 \times 10^{-9}$$

$$-325 \times 10^{-9} \lesssim \Delta a_\mu \lesssim 887 \times 10^{-9} \; .$$

Observe that the muon bound is dominated by the experimental uncertainty.

Many of the exotic contributions to be discussed below depend on a mass parameter Λ which can be simply a high mass cut-off or the mass of a hypothetical heavy particle. The exotic contributions vanish in general when $\Lambda \to \infty$ and in most cases we have a quadratic dependence on $1/\Lambda$ i.e. for $\Lambda \gg m$

$$\Delta a = A \cdot \left(\frac{m}{\Lambda}\right)^2 \quad ,$$

where m is the lepton mass and A is a quantity consisting of coupling constants, numerical constants and perhaps a slowly varying function of the masses. (Let us stress, however, that there are examples discussed

below that do not have this form.) The bounds on ΔG lead to lower limits on Λ . The super scripts + and - correspond to $\Delta G > 0$ or $\Delta G < 0$:

electron

$$\Lambda_e^+ \gtrsim 4.8 \text{ GeV } \sqrt{A_e}$$

$$\Lambda_e^- \gtrsim 5.9 \text{ GeV } \sqrt{-A_e} \quad .$$

muon

$$\Lambda_\mu^+ \gtrsim 113 \text{ GeV } \sqrt{A_\mu}$$

$$\Lambda_\mu^- \gtrsim 183 \text{ GeV } \sqrt{-A_\mu} \quad .$$

These limits are somewhat better for negative exotic contributions because they make worse the agreement between theory and experiment.

Although the electron experiment is about 90 times more precise than the muon experiment the latter in general puts more stringent limits on exotic contributions. This is mainly due to the large mass of the muon which allows it to probe much smaller distances than the electron .

A very interesting case arises when we assume(*)

$$\Lambda_e = \Lambda_\mu = \Lambda$$

$$A_e \approx A_\mu = A$$

(*) These equations could be called e-μ-universality but we shall refrain from doing so here because of the ambiguous meaning of this terminology.

in which case we obtain

$$\Lambda^{+} \gtrsim 113 \text{ GeV } \sqrt{A}$$

$$\Lambda^{-} \gtrsim 183 \text{ GeV } \sqrt{-A} \quad .$$

Since now

$$\Delta G_e = \left(\frac{m_e}{m_\mu}\right)^2 \Delta G_\mu \quad ,$$

we obtain an <u>induced</u> bound on the exotic <u>electron</u> contributions from the bound on the corresponding <u>muon</u> contribution

$$-8.10^{-12} \lesssim \Delta G_e \lesssim 21.\ 10^{-12} \quad .$$

We can conclude quite generally that for any exotic contribution satisfying $\Delta G = A(\frac{m}{\Lambda})^2$; $A_e = A_\mu$; $\Lambda_e = \Lambda_\mu$ the agreement between theory and experiment for the muon anomaly guarantees that the electron anomaly is not influenced by it. This is the meaning of the usual statement : the electron anomaly is a pure QED quantity.

VII.2. Modifications of Quantum Electrodynamics.

In order to measure the "goodness" of QED, modifications of a general nature not specifying special interactions or particles have been attempted. As shown by Kroll [701] such ad-hoc modifications are severely restricted by local current conservation giving rise to Ward-type identities. A modification of the lepton propagator must be accompanied by a change of the vertex function, and Kroll showed that these almost completely cancel each other out, the only exception being the propagators involved in closed Fermion loops. In the case of the anomaly, modifications of the lepton propagator can first show up in fourth order and may be of the form

$$\Delta G \simeq K\left(\frac{\alpha}{\pi}\right)^2\left(\frac{m}{\Lambda}\right)^2$$

where K is a numerical constant and Λ is a cut-off characterizing the modification. For $K = \pm 1$ we obtain

$$\Lambda_e^+ \gtrsim 11 \text{ MeV} \qquad \Lambda_e^- \gtrsim 14 \text{ MeV}$$

$$\Lambda_\mu^+ \gtrsim 260 \text{ MeV} \qquad \Lambda_\mu^- \gtrsim 425 \text{ MeV} \quad .$$

The anomalous magnetic moment is therefore not particularly sensitive to modifications of the charged lepton propagator(*) .

(*) Notice however, that the effect of a modification of the eletron propagator on the muon anomaly (via the diagram in Fig. IV.2) has not been investigated. One might expect an enhancement for $\Lambda_e < m_\mu$ such that the muon experiment could limit Λ_e better than the electron experiment.

Vertex modifications, not due to propagator modifications, will give rise (besides the obvious possibility of an intrinsic anomaly) to second order effects of the form

$$\Delta\, G = K \frac{\alpha}{\pi} \left(\frac{m}{\Lambda}\right)^2 .$$

For $K = \pm 1$ we obtain(*)

$$\Lambda_e^+ \gtrsim 230 \text{ MeV} \qquad \Lambda_e^- \gtrsim 280 \text{ MeV}$$

$$\Lambda_\mu^+ \gtrsim 5.4 \text{ GeV} \qquad \Lambda_\mu^- \gtrsim 8.8 \text{ GeV}$$

Every modification of the photon propagator corresponds to a modification of the spectral function of the photon and the influence on the anomaly is most easily expressed(**) by the formula (see Section V.2)

$$\Delta\, G = \frac{\alpha}{\pi} \int_0^\infty \frac{dt}{t} \frac{1}{\pi} \operatorname{Im} \Delta\Pi(t)\, K(t)$$

(*) A recently [713] suggested modification of the charge form factor of the muon to explain slight deviations from μ-e universality

$$F_\mu(q^2) = 1 - b + b/(1 - q^2/\Lambda_\mu^2)$$

with $b \simeq 0.04$ leads to

$$\Delta\, G_\mu = -\frac{\alpha}{\pi} \frac{2}{3} b \frac{m_\mu^2}{\Lambda_\mu^2}$$

and thereby

$$\Lambda_\mu \gtrsim 1.4 \text{ GeV} .$$

(**) See e.g. Feinberg and Lederman, Ref.R.7 .

where

$$K(t) = \int_0^1 dx \; \frac{x^2(1-x)}{x^2+(1-x)\frac{t}{m^2}} \simeq \frac{1}{3}\,\frac{m^2}{t} \qquad \text{for} \quad t \gg m^2 \quad .$$

Since most modifications involve large t values we can use the asymptotic form and write

$$\Delta G = \frac{1}{3}\,\frac{\alpha}{\pi}\,\left(\frac{m}{\Lambda}\right)^2 L$$

where $\frac{L}{\Lambda^2}$ is defined by

$$\frac{L}{\Lambda^2} = \int_0^\infty \frac{dt}{t^2}\,\frac{1}{\pi}\,\mathrm{Im}\,\Delta\Pi(t) \quad .$$

For $L = \pm 1$ we obtain

$$\Lambda^+ \gtrsim 3.1 \text{ GeV} \quad , \quad \Lambda^- \gtrsim 5.1 \text{ GeV} \quad .$$

Observe that photon propagator modifications obey $\Delta G_e \simeq \left(\frac{m_e}{m_\mu}\right)^2 \Delta G_\mu$ and therefore they cannot influence significantly the electron anomaly.

If the space of quantum mechanical states has a positive definite metric $\mathrm{Im}\,\Delta\Pi(t)$ (and thereby L) must itself be positive definite. The traditional photon propagator modification

$$\frac{g_{\mu\nu}}{k^2} \rightarrow \frac{g_{\mu\nu}}{k^2} - \frac{g_{\mu\nu}}{k^2-\Lambda^2}$$

does not satisfy this requirement (it leads to $L = -1$). Lee and Wick[805-809], however, have recently proposed a theory to handle the problems associated with an indefinite metric.

VII.3. Suggested Couplings of Leptons to Exotic Particles.

(i) The most often occurring case is that of a neutral boson coupled to the charged leptons [703-707]. If the mass of the external lepton is m, the mass of the internal lepton M (which may or may not be equal to m), the mass of the boson is Λ, and its coupling is f (see Fig. VII.1), we have for the case of scalar, pseudoscalar, vector and pseudovector coupling the following general expression

$$\Delta G = \frac{f^2}{4\pi^2} \frac{m^2}{\Lambda^2} L \quad ,$$

$$L = \int_0^1 dx \frac{Q(x)}{(1-x)(1-(\frac{m}{\Lambda})^2 x) + (\frac{\mu}{\Lambda})^2 x} \quad ,$$

where $Q(x)$ is a polynomium in x dependent on the type of coupling. We list it for the four standard cases :

1) scalar $Q_s(x) = \frac{1}{2} x^2(1+\epsilon-x)$

2) pseudoscalar $Q_{ps}(x) = \frac{1}{2} x^2(1-\epsilon-x)$

3) vector $Q_v(x) = x(1-x)(x-2(1-\epsilon)) + \frac{1}{2} x^2(1+\epsilon-x)\, \lambda^2(1-\epsilon)^2$

4) pseudovector $Q_{pv}(x) = x(1-x)(x-2(1+\epsilon)) + \frac{1}{2} x^2(1-\epsilon-x)\, \lambda^2(1+\epsilon)^2$

where $\epsilon = M/m$ and $\lambda = m/\Lambda$. In the limit of a heavy boson, i.e., m, $M \ll \Lambda$ we have(*) in the four cases

---

(*) Also assuming $(\frac{M}{\Lambda})^2 \ll \frac{m}{M}$.

$$L_s = \frac{M}{m}\left(\log\frac{\Lambda}{M} - \frac{3}{4}\right) + \frac{1}{6}$$

$$L_{ps} = -\frac{M}{m}\left(\log\frac{\Lambda}{M} - \frac{3}{4}\right) + \frac{1}{6}$$

$$L_v = \frac{M}{m} - \frac{2}{3}$$

$$L_{pv} = -\frac{M}{m} - \frac{2}{3} \quad .$$

These expressions are valid for all m , $M \ll \Lambda$ (*) . We specialize them to the following cases :

a) If a neutral boson exists coupled to only one charged lepton [703-706] we have $M = m = m_\mu$ or m_e and

$$L_s = \log\frac{\Lambda}{m} - \frac{7}{12}$$

$$L_{ps} = -\log\frac{\Lambda}{m} + \frac{11}{12}$$

$$L_v = \frac{1}{3}$$

$$L_{pv} = -\frac{5}{3} \quad .$$

As the logarithm is slowly varying, we can conclude that if the coupling f is the same to muon and electron, the electron anomaly is free of the influence of such bosons (see Section VII.1). No absolute limit, can, however, be put upon the mass because of the lack of knowledge of the

---

(*) Also assuming $\left(\frac{M}{\Lambda}\right)^2 \ll \frac{m}{M}$.

coupling constants.

For a neutral vector boson[708], W°, one finds by combining the v and pv case (the cross terms do not contribute)

$$\Delta G^{W_\circ} = -\frac{4}{3}\frac{f^2}{4\pi^2}\frac{m^2}{\Lambda^2} \quad .$$

If one writes $f^2/\Lambda^2 = K\ {}^{G_F}\!/\!_{\sqrt{2}}$ where K is a numerical constant one obtains

$$\Delta G_\mu^{W_\circ} = -3 \times 10^{-9}\ K$$

and one finds the rather uninteresting limit

$$K \lesssim 110 \quad .$$

b) If a neutral leptonic boson coupled to e and μ exists[707]

$$e^- \mu^+ \leftrightarrow z^o$$

then we have for electron and muon respectively the dominant terms

$$L_s^\mu \simeq \frac{1}{6} \qquad L_s^e \simeq \frac{m_\mu}{m_e}\left(\log\frac{\Lambda}{m_\mu} - \frac{3}{4}\right)$$

$$L_{ps}^\mu \simeq \frac{1}{6} \qquad L_{ps}^e \simeq -\frac{m_\mu}{m_e}\left(\log\frac{\Lambda}{m_\mu} - \frac{3}{4}\right)$$

$$L_v^\mu \simeq -\frac{2}{3} \qquad L_v^e \simeq \frac{m_\mu}{m_e}$$

$$L_{pv}^\mu \simeq -\frac{2}{3} \qquad L_{pv}^e \simeq -\frac{m_\mu}{m_e} \quad .$$

Observe that for the electron we have a strong enhancement. The induced limit on ΔG_e does not obey the inequality stated in Section VII.1 but rather the following less restrictive inequalities

$$\left.\begin{array}{l} -9.6 \times 10^{-9}\ F \\ -26\ .\ 10^{-9}\ F \\ -6.4 \times 10^{-9} \\ -2.4 \times 10^{-9} \end{array}\right\} \lesssim \Delta G_e \lesssim \left\{\begin{array}{ll} 26 \times 10^{-9}\ F & S \\ 9.6 \times 10^{-9}\ F & PS \\ 2.4 \times 10^{-9} & V \\ 6.4 \times 10^{-9} & PV \end{array}\right.$$

where $F = \log \frac{\Lambda}{m_\mu} - \frac{3}{4}$.

c) Neutral μ-p resonance.

If a neutral lepto-baryonic resonance of non-zero spin exists with a mass of about 1.9 GeV [710], the contribution can be estimated (disregarding strong interactions) from the general formulas given above by putting $M = m_\mu$, $M = m_p$. Assuming spin 1 and a coupling [711] $f(1+\lambda i\gamma_5)\ \gamma_\mu$, we obtain in the not quite justified approximation $\Lambda \gg 1$ GeV

$$\Delta G_\mu = \frac{f^2}{4\pi^2}\ \frac{m_\mu^2}{\Lambda^2}\left((1-\lambda^2)\ \frac{m_p}{m_\mu} - (1+\lambda^2)\ \frac{2}{3}\right) \quad .$$

In the experimentally favored case $\lambda = 1$ we obtain

$$\frac{f^2}{4\pi} \lesssim 3.\ 10^{-4}$$

which is far above the estimate of a lower limit (10^{-13}) obtained from the neutrino experiment [711].

ii) Neutral Leptonic Resonance.

If a neutral $\pi\mu$ ($\sim$ 430 MeV) resonance ν^*_μ exists [712]; and the spin is $\frac{1}{2}$, the dominating contribution in the not quite justified limit m_μ, $m_\pi \ll m_{\nu^*}$ is

$$\Delta G_\mu = \frac{f^2}{4\pi^2} \frac{m_\mu}{m_{\nu^*_\mu}} \left(\frac{1}{4}(1-\lambda^2) - \frac{1}{6} \frac{m_\mu}{m_{\nu^*_\mu}} (1+\lambda^2) \right)$$

for a coupling of the form $f(\gamma_5 + \lambda)$. For $\lambda = 0$ we obtain the limit on the coupling constant(*)

$$\frac{f^2}{4\pi} \lesssim 6.10^{-5}$$

iii) Magnetic monopoles.

If magnetic monopoles exist, one may expect they contribute to the anomaly of the leptons. However, because of their huge coupling, no trustworthy method exists for calculating their contribution. Perturbation theory is not valid, unless the effective coupling turns out to be $g\frac{m}{M}$ where g is the monopole coupling, m the lepton mass, and M the monopole mass. From general considerations, this seems to be the case if

---

(*) The lower limit is $1.6.10^{-11}$. Private communication from A. De Rújula.

the contribution arises via the vacuum polarisation. Taking(*) $L = \frac{g^2}{4\pi^2}\frac{1}{15}$ we obtain (with M the monopole mass)

$$\Delta G \simeq \frac{1}{45}\frac{\alpha}{\pi}\frac{g^2}{4\pi^2}\left(\frac{m}{M}\right)^2$$

which at best is unreliable. The bound on M is (taking $\frac{e^2}{4\pi}\frac{g^2}{4\pi} \approx 1$)

$$M \gtrsim 5.4 \text{ GeV} \quad .$$

No serious significance should however be attributed to this number.

(*) This is the value obtained for the vacuum polarization by heavy charged fermion pairs [407] .

HIGH ENERGY EXPERIMENTS

VIII. SCATTERING EXPERIMENTS AT HIGH MOMENTUM TRANSFER.

One of the aims of these experiments is to test the validity of QED at small interaction distances. High energy scattering experiments with very large momentum transfer q , say $q \gtrsim 2$ GeV/c , can probe interaction distances $R \sim \hbar/q \lesssim 10^{-14}$ cm . To obtain such large momentum transfers one has resorted to the colliding beams type of experiment and to the so-called Bethe-Heitler type of experiment.

VIII.1 Colliding Beams.

Four types of experiments have been carried out :

(i) Møller scattering $e^-e^- \rightarrow e^-e^-$, see Fig.VIII.1 ;

(ii) Bhabha scattering $e^+e^- \rightarrow e^+e^-$, see Fig.VIII.2 ;

(iii) Annihilation into muon pairs $e^+e^- \rightarrow \mu^+\mu^-$, see Fig.VIII.3 ;

(iv) Annihilation into photon pairs, $e^+e^- \rightarrow \gamma\gamma$, see Fig.VIII.4 .

(i) Møller scattering was done at the Princeton-Stanford storage ring at total energies of the colliding electrons

$E_{C.M.} = \sqrt{S} = 600$ MeV [801] and 1100 MeV [802]. The experiment measured the angular dependence of the cross section but not the absolute magnitude. The observed angular distribution was compared with the Møller formula [803] modified by radiative corrections [804]. A convenient way to make this comparison is to assume a modification factor for the photon propagator of the form(*)

$$\frac{1}{q^2} \rightarrow \left(\frac{1}{q^2} \pm \frac{1}{q^2 - \Lambda_{\pm}^2} \right) .$$

The maximum-likelihood value of Λ_-^2 from the 1100 MeV data is

$$\frac{1}{\Lambda_-^2} = -0.06 \pm 0.06 \ (\text{GeV}^{-2}) \ \text{(statistical error only)} .$$

The corresponding limits of $\Lambda_{\pm}$ are

$$\Lambda_- > 4 \text{ GeV} \quad \text{and} \quad \Lambda_+ > 2.4 \text{ GeV} ,$$

at a 95% confidence level.

(*) The modification with a minus sign has received much attention lately in connection with the problem of divergence difficulties in Physics. In a series of papers, Lee and Wick have reexamined the classical difficulties innherent to such a modification and have presented a new theory of quantum electrodynamics [805-809].

(ii) Large angle Bhabha scattering has been performed at the Orsay storage rings(*) at a total energy $\sqrt{S}$ = 1020 MeV . In this experiment the absolute Bhabha cross section $\sigma_{e^+e^-}$ was measured(**). The determination of $\sigma_{e^+e^-}$ implies a simultaneous measurement of the number of Bhabha scattering events $N_{e^+e^-}$ and the luminosity L of the storage ring, since

$$N_{e^+e^-} = L\,\sigma_{e^+e^-} \quad .$$

In order to determine the luminosity L , the double bremsstrahlung reaction $e^+e^- \rightarrow e^+e^- + 2\gamma$ of known cross-section $\sigma_{2\gamma}$ [813-816] was chosen. In the Orsay experiment, the two photons of double bremsstrahlung are emitted at very small angle (of a few mrad.). Therefore, a breakdown of QED at large momentum transfer cannot give an appreciable effect on $\sigma_{2\gamma}$. The simultaneous measurement of the two reactions leads to the determination of $\sigma_{e^+e^-}$,

$$\sigma_{e^+e^-} = \sigma_{2\gamma}\,\frac{N_{e^+e^-}}{N_{2\gamma}} \quad .$$

Experimentally, $\sigma_{e^+e^-}$ is obtained from the corrected number of Bhabha events and the value of the luminosity integrated over data taking time,

---

(*) For a technical description of the Orsay storage rings see e.g. J.E. Augustin, ref.810 .

(**) For a detailed description of this experiment see Ref. 811.The results were first reported at the Liverpool Conference ,see Ref.812.

$$\sigma_{exp} = [1.97] \pm 0.09 \text{ (statist.)} \pm 0.10 \text{ (system.)} \times 10^{-31} \text{ cm}^2 \quad .$$

The corresponding theoretical cross section [817] obtained from the calculation of the lowest order Feynman diagrams shown in Fig.VIII.2 and modified so as to take into account the radiative corrections(*) and the integration over accepted solid angle and average over the energy spectrum of incident electrons is found to be

$$\sigma_{th} = 2.13 \times 10^{-31} \text{ cm}^2 \quad .$$

When the comparison between theory and experiment is made by means of the cut-off parametrization indicated above, it is found that

$$\Lambda_- > 2.0 \text{ GeV} \quad \text{and} \quad \Lambda_+ > 3.8 \text{ GeV} \quad ,$$

at a 95% confidence level.

(*) The radiative corrections to $e^+e^- \rightarrow e^+e^-$ can be obtained from the calculations of Tsai, ref. 804 , for $e^-e^- \rightarrow e^-e^-$. The appropriate transcription, relevant to the Orsay experiment, has been made by Tavernier, ref. 818 . They lead to a decrease of the Born cross-section of 7.3% . Vacuum polarization corrections are negligible (< 0.1 %) . The radiative corrections to $e^+e^- \rightarrow e^+e^- + 2\gamma$ have been recently calculated by Baier (private communication from Dr.J. Buon). They are found to be small and do not alter the conclusions of the Orsay experiment. We wish to thank Dr. Buon for an informative discussion on this point.

Recently, electron-positron elastic scattering has also been performed at the Frascati storage ring, Adone(*) . The total energy $\sqrt{s}$ ranges from 1.4 GeV to 2.4 GeV . The published results [842] are based on an analysis of 3255 wide angle scattering events (WAS) . At these energies, the WAS events are suitable to test the validity of QED .

In the Frascati experiment, the reaction chosen as a monitor to determine the luminosity was Bhabha scattering at small angle scattering (SAS) . The SAS events involve small momentum transfers and therefore they are unaffected by a possible breakdown of QED at large momentum transfer. The comparison between theory and experiment made by means of the minus sign cut-off parametrization (see Table VIII.1) leads to the result

$$\Lambda_- > 6 \text{ GeV}$$

at a 95% confidence level.

(*) For a technical description of Adone, see e.g. F. Amman et al, ref. 841 .

(iii) The annihilation into a muon pair $e^+e^- \to \mu^+\mu^-$ has also been performed at Orsay(*) at the three total energies 580 MeV , 644MeV and 707 MeV . The muons were separated from the pions on the basis of their different range in the thick plate chambers. They obtained 62 events. This experiment tests the time-like propagator of the photon since only the annihilation graph shown in Fig.VIII.3 is present. From the analysis of the results in terms of a modification of the photon propagator it is found that

$$\Lambda_- > 1.3 \text{ GeV} \quad ,$$

at a 95% confidence level.

(iv) The annihilation into two photons $e^+e^- \to 2\gamma$ has been studied at the Novosibirsk storage rings [819]. The relative deviation of the experimental cross section for 2γ annihilation from the calculated one is

$$\frac{\Delta\sigma}{\sigma} = 0.1 \pm 0.2 \quad .$$

Notice that this experiment tests the electron propagator (see Fig.VIII.4). It is the electron which in this process is off-mass shell and carries a large four-momentum. When a cut-off for the fermion propagator is introduced in the same way as the (-) photon propagator modification, and no

---

(*) See Perez-y-Jorba, ref. 812 .

corresponding vertex correction(*)

$$\frac{1}{p^2-m^2} \rightarrow \frac{1}{p^2-m^2} - \frac{1}{p^2-m^2-\Lambda^2} \quad ,$$

it is found that

$$\Lambda \text{ (electron)} > 1.5 \text{ GeV}$$

at a 95% confidence level.

A summary of the results obtained from colliding beams experiments has been compiled in Table VIII.1 ,

---

(*) See the discussion in section VII.2 concerning the difficulties with this type of modification of a fermion propagator.

VIII.2 Bethe-Heitler Type Experiments.

Three types of experiments have been performed :

(i) Wide angle electron or muon pair photoproduction (see Fig. VIII.5);

(ii) Wide angle bremsstrahlung of electrons or muons (see Fig. VIII.6);

(iii) Trident production of leptons (see Fig. VIII.7) .

These processes have in common that, at lowest order of perturbation theory, the corresponding Feynman diagrams involve a fermion line which is off-shell and possible modifications to the corresponding propagator can be tested. Here, large off-shell fermion masses are attainable because the proton target, or the low Z nucleus target, can be used to fix the center of mass. The nuclear structure in the diagrams corresponding to Figs. VIII 5a, 6a and 7a can be factored out, and is known from measurements of the form factors in elastic electron scattering(*).

(i) Measurements of symmetric wide angle electron pair photoproduction have been done on carbon at DESY-MIT [821] and CEA [822], and on hydrogen at Daresbury [823]. In these experiments a symmetric detection system with respect to the incident photon beam direction is chosen so as

---

(*) For a recent review of the nucleon form factors, see e.g. Rutherglen, ref. 820 .

to eliminate the interference(*) of the Bethe-Heitler amplitudes (see Fig. VIII.5a) with the virtual Compton amplitude (see Fig. VIII.5b). Wide angle detection is used to minimize the effect of the virtual Compton-scattering cross-section(**) . In these experiments, the invariant mass of the lepton pair $m_{e^+e^-}$ goes up to 900 MeV/c^2 .

Measurements of symmetric wide angle muon pair photoproduction on carbon have also been reported [826-828] . The data corresponds to invariant masses of the muon pair $m_{\mu^+\mu^-}$ up to 1770 MeV/c^2 .

A traditional way to represent a breakdown of the lepton propagator has been to introduce a cut-off parameter Λ such as illustrated in Table VIII.1. Then, for values of p^2 small compared with Λ^2 and large compared with m^2 , the Bethe-Heitler cross-section σ_{BH} [830,831] has to be modified as follows [832]

$$\sigma = \sigma_{BH} \, (1+p^2/\Lambda^2) \quad .$$

(*) Notice that the e^+e^- pair produced by the virtual Compton amplitude and the e^+e^- pair of the Bethe-Heitler amplitudes are states which transform oppositely under charge conjugation. By a suitable choice of an asymmetric detection system, this interference term can be measured and the real part of the virtual Compton amplitude can thus be obtained.

(**) The Bethe-Heitler and Compton cross-sections differ in their angular dependence by a factor $\sim \theta^3$, where θ is the angle between the lepton and the incident photon direction.

Although there is certain arbitrariness in parametrizing the breakdown of QED, the modification suggested above has the serious inconvenience of violating the Ward-Takahashi identity. An analysis by Kroll [701] shows that a reasonable modification of the Bethe-Heitler type amplitude leads to a modification of the cross-section of the type

$$\sigma = \sigma_{BH} \left[1 \pm (Q_m^2/\Lambda_{\pm}^2)^n\right]$$

where $n = 2$ or a higher even number, and Q_m is the invariant mass of the final lepton system. Using this parametrization, with $n = 2$, the experiments mentioned above lead to the results shown in Table VIII.2 .

(ii) Experiments of wide angle bremsstrahlung of electrons on carbon have been done at Cornell [833], and on a hydrogen target at Frascati [834]. An experiment of bremsstrahlung of muons from 9 to 13 GeV/c on a carbon target has also been done by a Harvard-Case-McGill-SLAC collaboration [835]. Notice that in this type of processes the lowest order Feynman diagrams involve off-shell leptons which are both space-like (Fig.VIII.6b) and time-like (Fig.VIII.6a). The time-like lepton can be far off the mass shell if the final lepton and photon energies and angles are large. The results of these experiments, which have been summarized in Table III agree well with the predictions of QED (*)

(*) See ref.830, see also ref.839 .

(iii) Experiments on trident production (see Fig.VIII.7) are still on a preliminary stage to serve as precision tests of QED . There are, however, a number of very interesting features which have already been revealed by these experiments. Production of a muon pair by incident electrons at 4.9 GeV/c on a carbon target has been reported by a Northeastern-Austin collaboration [837]. Muon pairs were observed at invariant masses ranging from 0.4 GeV/c^2 to 0.9 GeV/c^2 ; the scattered electron was not observed. The data are consistent with predictions of a simple diffraction model for the virtual Compton amplitude (see Fig.VIII.7b) which interferes with the time-like QED amplitude (see Fig.VIII.7a). Within this model, a heavy photon of mass less than 400 MeV in the time-like propagator is excluded by the data.

Production of muon pairs by incident muons at 11 GeV/c on a lead target have been performed at Brookhaven by a Harvard-U.Mass.-McGill collaboration [838]. The angles and momenta of the incident muon and of all three final state muons were measured in optical spark chambers. Runs were made with positive and negative incident muons. The total number of events observed 75.2 ± 10.5 is in good agreement with the theoretical prediction 88.9 ± 2.6 which includes the interference term between the direct and exchange graphs(*). The theoretical prediction without

---

(*) Notice that in Fig.VIII.7a, in the case $\mu + A \rightarrow \mu + \mu^+ + \mu^- + A$, there are altogether eight Feynman diagrams : the 4 direct ones plus 4 obtained by exchange of the final fermion lines of equal charge. Theoretical discussions of trident experiments can be found in refs.839 and 840.

inclusion of the interference term would be 120.9 ± 2.6 events. In the experiment, the invariant mass spectrum of the two identical final particles clearly shows a depression at low invariant masses as predicted by the Pauli exclusion principle for fermions.

CONCLUSIONS

Quantum electrodynamics is in very good shape. No serious discrepancies exist between theory and experiment. The last year has seen improvements in several fields. In the high energy region cut-off masses are being pushed into the region of several GeV. In the low energy region, the precision on both experiment and theory is approaching one part per million.

The anomalous magnetic moment of the electron has been re-measured with a precision of 3 ppm. Simultaneously, the sixth order radiative correction has been calculated theoretically with the same precision. The two numbers agree beautifully.

By now, the theoretical value of the anomalous magnetic moment of the muon is known with a precision of 13 ppm. The crucial test of this number awaits the next CERN experiment.

The theoretical value for Lamb shift in hydrogen has been improved by analytic calculations of the fourth order slope of the Dirac form factor of the electron, and by a calculation of the $\alpha(Z\alpha)^6$ contribution. The theoretical uncertainty of 12 ppm is five times smaller than the experimental uncertainty, and the agreement between theory and experiment is excellent.

The increased precision of QED theory and experiment leads to accurate purely radiative values of the fine structure constant α. In one case (the $2S_{1/2} - 2P_{3/2}$ splitting in hydrogen) the precision is even comparable to that of the non-QED ac Josephson value.

ACKNOWLEDGEMENTS

The authors wish to thank the following persons for discussions, comments and criticism : J. Bailey, S. Brodsky, J. Buon, A. De Rujula, G.W. Erickson, T. Fulton, M.J. Levine, E. Picasso, A. Rich and V.L. Telegdi.

Table I.1 Compilation of contributions to the Lamb-shift : $2S_{\frac{1}{2}} - 2P_{\frac{1}{2}}$ in hydrogen *). ($\alpha^{-1} = 137.03608(26)$)

ORDER	DESCRIPTION AND REFERENCES	CORRECTION, UNITS $\frac{\alpha}{\pi}(Z\alpha)^4\frac{m}{6}$	NUMERICAL VALUE in MHz
$\alpha(Z\alpha)^4 m$	2nd order self-energy [101-106]	$(-2\log(Z\alpha)+\frac{m}{M}+\frac{11}{24}-\log\frac{K_o(2,0)}{K_o(2,1)})(1-3\frac{m}{M})$	1009.920
$\alpha(Z\alpha)^4 m$	2nd order magnetic moment [003]	$\frac{1}{2}(1-2.75\frac{m}{M})$	67.720
$\alpha(Z\alpha)^4 m$	2nd order vac. polarization [107, 108]	$-\frac{1}{5}(1-3\frac{m}{M})$	-27.084
$\alpha(Z\alpha)^5 m$	2nd order binding [125,126,115]	$(Z\alpha)(3\pi)(1+\frac{11}{128}-\frac{1}{2}\log 2+\frac{5}{192})$	7.140
			±0.00557
$\alpha(Z\alpha)^6 m$	4th order binding + higher orders [127-129,115,158]	$(Z\alpha^2)(a+b\log(Z\alpha)^2+c\log^2(Z\alpha)^2) + (Z\alpha)^3\pi.9.56$	-0.372 ±0.00491
	Higher orders Z and α uncertainty		±0.00568
$\alpha^2(Z\alpha)^4 m$	4th order self-energy [119]	$3\frac{\alpha}{\pi}$ 0.470	0.444
$\alpha^2(Z\alpha)^4 m$	4th order magnetic moment [403, 404]	$\frac{\alpha}{\pi}(-0.328)$	-0.102
$\alpha^2(Z\alpha)^4 m$	4th order vac. polarization [130, 512]	$\frac{\alpha}{\pi}(\frac{41}{54})$	-0.239
	Red.mass. uncertainty		±0.00341
$\alpha(Z\alpha)^4\frac{Zm}{M}m$	Recoil corrections [131,132,116]	$\frac{Zm}{M}(a_1+b_1\log(Z\alpha)^2)$	0.359
$\alpha(Z\alpha)^4(\frac{mR_p}{e})^2 m$	Proton size [114,116,158]	$\frac{\pi^2}{2}(\frac{mR_p}{e})^2$	0.125 ±0.00634
	Proton structure uncertainty		± ±0.00063
		TOTAL = 1057.911 ±0.012	

*) This table is an updated version of the compilation made by A. Peterman. The value of the Bethe logarithm $\log(K_o(2,1)/K_o(2,0))$ is that evaluated by Schwartz and Tiemann [106]. The constants a,b,c, a_1 and b_1 are the following : $a = -\frac{4\pi^2}{3}-4-4\log^2 2-0.28\pm0.5$; $b = \frac{55}{48}-4\log 2$; $c = -3/4$; $b_1 = -1/4$; $a_1 = 2\log\frac{K_o(2,1)}{K_o(2,0)}+\frac{97}{12}$.

TABLE I.2 Compilation of contributions to the slope of the Dirac form factor of the electron at fourth order(*). The graphs refer to those shown in Fig.I.4.

Graphs	Analytic Results	Numerical Results
cross (Fig.I.4a)	$-\frac{13}{36}\log\lambda^{-2}+\left(-\frac{1181}{1728}+\frac{\pi^2}{72}+\frac{7}{12}\pi^2\log 2-\frac{7}{8}\zeta(3)=2.3925\right)$ (Ref.123)	$-\frac{13}{36}\log\lambda^{-2}+2.37\pm0.02$ (Ref.119) $-\frac{13}{36}\log\lambda^{-2}+2.3924\pm0.0002$ (Ref.123)
ladder (Fig.I.4b)	$\frac{13}{36}\log\lambda^{-2}+\left(\frac{319}{864}-\frac{91}{432}\pi^2=-1.710\right)$ (Ref.118)	$\frac{13}{36}\log\lambda^{-2}-1.69\pm0.02$ (Ref.119)
corner (Fig.I.4c, I.4d)	$\frac{1}{12}\log^2\lambda^{-2}-\frac{1}{72}\log\lambda^{-2}+\left(\frac{1511}{1728}-\frac{209}{864}\pi^2-\frac{\pi^2}{12}\log 2+\frac{1}{8}\zeta(3)=-1.9328\right)$ (Ref.121)	$\frac{1}{12}\log^2\lambda^{-2}-\frac{1}{72}\log\lambda^{-2}-1.91\pm0.02$ (Ref.119) $\frac{1}{12}\log^2\lambda^{-2}-\frac{1}{72}\log\lambda^{-2}-1.95\pm0.05$ (Ref.120)
self-energy (Fig.I.4e, I.4f)	$-\frac{1}{12}\log^2\lambda^{-2}+\frac{1}{72}\log\lambda^{-2}+\left(-\frac{1109}{1728}+\frac{17}{72}\pi^2=1.688\right)$ (Refs.117,118, 121)	$-\frac{1}{12}\log^2\lambda^{-2}+\frac{1}{72}\log\lambda^{-2}+1.68\pm0.01$ (Ref.119)
vac.pol. (Fig.I.4g)	$\left(-\frac{1099}{1296}+\frac{77}{864}\pi^2=0.0316\right)$ (Refs.117,118,120)	0.0316 ± 0.0002 (Ref.119)

(*) All the diagrams have been evaluated in the Feynman gauge. For the analytic results of the vacuum polarization, self-energy and ladder diagrams we have corrected the overall sign error. All the results are given in units $(\alpha/\pi)^2$.

TABLE I.3. - Determinations of α^{-1} obtained from bound systems(*).

BOUND SYSTEM	DISCUSSION	VALUE OF α^{-1}
Hydrogen, ΔE_H	Section I.2	137.03545(59)
Hydrogen, $(\Delta E_H - \mathcal{L}_H)_{(i)}$	Section I.2	137.03570(27)
Hydrogen, $(\Delta E_H - \mathcal{L}_H)_{(ii)}$	Section I.2	137.03544(23)
Hydrogen, h.f.s.	Section I.3	137.03591(35)
Muonium , h.f.s.	Section III.1	137.03617(30)

(*) For reference, the value of α^{-1} obtained from the a.c. Josephson effect is $\alpha^{-1} = 137.03608(26)$.

TABLE I.4 Lamb shift in hydrogenic systems in MHz units.

System	Theory	Experiment	References
H (n = 2)	1057.911 ± 0.011	1057.90 ± 0.06	160
		1057.86 ± 0.06	109, 160
H (n = 3)	314.896 ± 0.003	315.11 ± 0.89	161
H (n = 4)	133.084 ± 0.001	133.18 ± 0.59	161
D (n = 2)	1059.271 ± 0.025	1059.28 ± 0.06	162 (revised)
He^+ (n = 2)	14044.765 ± 0.613	14045.4 ± 1.2	163
He^+ (n = 3)	4184.42 ± 0.18	4183.17 ± 0.54	164
He^+ (n = 4)	1769.088 ± 0.076	1776.0 ± 7.5	165
		1768.0 ± 5.0	166
		1769.4 ± 1.2	166 (revised)
Li^{++} (n = 2)	62763.41 ± 9.07	63031.0 ± 327.0	167
C^{5+} (n = 2)	$(783.678 \pm 0.251)10^3$	$(744.0 \pm 7)10^3$	168

These frequencies are essentially due to G.W. Erickson (Ref. 158 and private communication), but using $\alpha^{-1} = \alpha^{-1}_{wQED} = 137.03608$ instead of $\alpha^{-1} = 137.03602$. Lambshift for superheavy elements ($Z\alpha > 1$) can be found in Ref. 158.

TABLE II.1 . Compilation of results in positronium.

OBSERVABLE	EXPERIMENTS	THEORY
Fine-Structure of Ground State $^3S_1 - {}^1S_o$	$(2.03380 \pm 0.00040)\ 10^5$ MHz [206] $(2.03330 \pm 0.00040)\ 10^5$ MHz [207] $(2.03403 \pm 0.00012)\ 10^5$ MHz [208]	2.03427×10^5 MHz [211-214]
Decay-Rate Orthopositronium ($^3P_1$)	$(0.7262 \pm 0.0015)\ 10^7\ sec^{-1}$ [209, R.11]	$0.7211 \times 10^7\ sec^{-1}$ [216] (correction of ref.217 not included)
Decay-Rate Parapositronium (^1S_o)	$(0.799 \pm 0.011)\ 10^{10}\ sec^{-1}$ [208]	$0.798 \times 10^{10}\ sec^{-1}$ [218,219]

TABLE III.1 . Compilation of results in the determination of the muon magnetic moment.

OBSERVABLE	EXPERIMENTAL VALUE	REFERENCE
μ_μ / μ_p	3.183380(40)	Columbia, ref. 309
μ_μ / μ_p	3.183360(70)	Berkeley, ref. 310
μ_μ / μ_p	3.183330(44)	Princeton-Penn, ref. 311
μ_μ / μ_p	3.183347 (9)	Washington-LRL, ref. 307
μ_μ / μ_p		
(without pressure-shift correction)	3.183373(13)	Chicago, ref. 308
(-11 p.p.m. pressure-shift correction)	3.183337(13)	

TABLE III.2. Compilation of results on the hyperfine splitting of muonium ground state $\Delta\nu(\mu e)$. All numbers are in MHz .

EXPERIMENTS		THEORY(*)
Yale [317]	4463.15(6)	4463.313(21) (using μ_μ/μ_p = 3.183337(13))
Yale [318]	4463.302(27) (from Kr data)	
	4463.220(33) (from Ar data)	
Chicago [316]	4463.317(21)	
Yale [313]	4463.249(31)	
Chicago [308]	4463.3022(89)	
Yale [315]	4463.310(30)	4463.323(19) (using μ_μ/μ_p = 3.183347(9))

(*) The recent recoil correction of Fulton, Owen and Repko [303] has been included. The value of α^{-1} used is 137.03602(21) .

TABLE IV.1 . Contributions to the theoretical values for the lepton anomalies ($\alpha^{-1} = 137.03608(26)$) .

CONTRIBUTION	a_e^{th} ($\times 10^{-9}$)	a_μ^{th} ($\times 10^{-9}$)
QED 2.order	1161409.0 $\pm$ 2.2	1161409.0 $\pm$ 2.2
QED 4.order	- 1772.3	4131.8
QED 6.order	18.7 $\pm$ 2.5	273 $\pm$ 14
Hadronic	0 . 0	65 $\pm$ 5
TOTAL	1159655.4 $\pm$ 3.3	1165879 $\pm$ 15

TABLE IV.2 . History of the calculations of the sixth order contributions to the electron anomaly.

GRAPHS	AUTHORS	YEAR
19-22	Mignaco and Remiddi [411]	1969
1-6	Aldins et al [412,413]	1969
7-22	Brodsky and Kinoshita [414]	1970
7-22	Calmet and Perrottet [416]	1970
25+29+30	Levine and Wright [415]	1970
69-72	De Rújula et al [417]	1970
23-25,29,30,39,40	Calmet [418]	1971
23-72	Levine and Wright [419]	1971

TABLE IV.3 . Results of Mignaco and Remiddi [411] $G_4 = \sum_{n=1}^{\infty} \frac{1}{2^n n^4} = Li_4(\frac{1}{2}) = 0.51748$.

GRAPH	ANALYTIC FORM $x(\frac{\alpha}{\pi})^3$	NUMERIC VALUE OF NON- INFRARED TERMS $x(\frac{\alpha}{\pi})^3$
19	$-\frac{943}{324} - \frac{4}{135}\pi^2 + \frac{8}{3}\zeta(3)$	0.0025585
20 + 21	$\frac{1547}{432} - \frac{3}{2}\pi^2 + 2\pi^2\log 2 - 2\zeta(3) + \log(\frac{\lambda}{m_e})(\frac{119}{18} - \frac{2}{3}\pi^2)$	0.054675
22	$\frac{1145}{432} + \frac{161}{162}\pi^2 - \frac{22}{9}\pi^2\log 2 + \frac{49}{18}\zeta(3) - \frac{4}{9}\pi^2\log^2 2 + \frac{4}{9}\log^4 2$	
	$+ \frac{32}{3}G_4 + \log(\frac{\lambda}{m_e})(-\frac{119}{18} + \frac{2}{3}\pi^2) - \frac{7}{270}\pi^4$	- 0.001805

TABLE IV.4 . Comparison of results for Class II and III .

GRAPHS	BRODSKY and KINOSHITA [414]	CALMET and PERROTTET [416]
7 + 8	- 0.0032(3)	- 0.0031(10)
9 + 10	0.0532(4)	0.0522(10)
11 + 12	0.0273(3)	0.0274(5)
13 + 14	$-0.051(3) - 0.0314\log(\frac{\lambda}{m_e})$	- 0.0474(20) + infrared term
15 + 16	- 0.1161(14)	- 0.1151(9)
17 + 18	$-0.064(3) + 0.0314\ \log(\frac{\lambda}{m_e})$	$-0.0653(5) + 0.03160(52)\log(\frac{\lambda}{m_e})$
19	0.00255(2)	0.002559(15)
20 + 21 + 22	0.05291(6)	0.0522(21)

TABLE IV.5 . Results from De Rújula et al [417] .

GRAPHS	VALUE $(\frac{\alpha}{\pi})^3 x$
67	$-2.728(16) + (\frac{67}{24} - \frac{\pi^2}{18} - \frac{1}{3}\pi^2\log 2 + \frac{1}{2}\zeta(3))\log\lambda + \frac{1}{2}\log^2\lambda$
68 + 69	$6.538(12) + (-\frac{13}{4} + \frac{\pi^2}{9} + \frac{1}{3}\pi^2\log 2 - \frac{1}{2}\zeta(3))\log\lambda - \log^2\lambda$
70	$-3.332(11) + (\frac{11}{24} - \frac{\pi^2}{18})\log\lambda + \frac{1}{2}\log^2\lambda$

TABLE IV.6 . Results from Calmet [418].

GRAPHS	VALUE $x(\frac{\alpha}{\pi})^3$
23 + 24	1.206(65)
25	- 0.136(21)
29 + 30	- 1.431(91)
39 + 40	- 0.476(64)

TABLE IV.7. Experimental values for the electron anomaly.

Foley and Kusch (1947) [002]	0.00115(4)(*)
Koenig et al (1952) [430]	0.001146(12)(*)
Berniger and Heald (1954) [431]	0.001148(6) (*)
Franken and Liebes (1957) [432]	0.001165(11)(*)
Schupp et al (1961) [433]	0.0011609(24)
Wilkinson and Crane (1963) [434,435]	0.001159622(27)
Farago et al (1963) [444]	0.001153(23)
Rich (correction to ref.434) (1968) [436]	0.001159549(30)
Gräff et al (1969) [440]	0.00115966(30)
Wesley and Rich (preliminary value) (1970) [426]	0.001159644(7)
Wesley and Rich (1971) [401]	0.0011596577(35)

(*) These experiments actually measure $1+G_e$ and not G_e directly.

TABLE V.1. History of the calculations of the sixth order contributions to the difference of muon and electron anomalies.

GRAPHS (Fig.V.1)	AUTHORS and References	YEAR
21	Kinoshita [505]	1967
21 - 24	Lautrup, de Rafael [410]	1968
19 - 20	Lautrup, de Rafael [506]	1969
1 - 6	Aldins, Brodsky, Dufner, Kinoshita [412,413]	1969
11 - 18	Lautrup, Peterman, de Rafael [507]	1970
7 - 10	Lautrup [508]	1970
7 - 24	Brodsky, Kinoshita [414]	1970

TABLE V.2. Sixth order results from refs. 410,505,506,507 and 508.

Graphs and References	Semianalytical form $x(\frac{\alpha}{\pi})^3$	Numerical value $x(\frac{\alpha}{\pi})^3$
$7+8$ [508]	$\left(\frac{2}{9}+\frac{13}{27}\pi^2-\frac{10}{9}\pi^2\log 2+\frac{5}{3}\zeta(3)\right)\log\frac{m_\mu}{m_e}+2.09(2)$	$-1.23(2)$
9 [508]	$\left(\frac{1}{3}\log\frac{m_\mu}{m_e}-\frac{25}{36}\right)\log\frac{\lambda}{m_\mu}+\frac{1}{6}\log^2\frac{m_\mu}{m_e}+\left(-\frac{1}{8}+\frac{\pi^2}{27}\right)\log\frac{m_\mu}{m_e}-1.058(4)$	$4.962(4)$
10 [508]	$-\left(\frac{1}{3}\log\frac{m_\mu}{m_e}-\frac{25}{36}\right)\log\frac{\lambda}{m_\mu}-\frac{1}{6}\log^2\frac{m_\mu}{m_e}+\left(\frac{31}{72}+\frac{\pi^2}{27}\right)\log\frac{m_\mu}{m_e}-1.669(4)$	$-2.162(4)$
$11+12$ [507]	$\frac{1}{3}\log^2\frac{m_\mu}{m_e}+\left(-\frac{87}{36}+\frac{\pi^2}{27}+\frac{2}{9}\pi^2\log 2-\frac{1}{3}\zeta(3)\right)\log\frac{m_\mu}{m_e}+1.298(6)$	$5.807(6)$
$13+14$ [507]	$-2\left(\frac{1}{3}\log\frac{m_\mu}{m_e}-\frac{25}{36}\right)\log\frac{\lambda}{m_\mu}+\left(-\frac{67}{36}+\frac{\pi^2}{27}+\frac{2}{9}\pi^2\log 2-\frac{1}{3}\zeta(3)\right)\log\frac{m_\mu}{m_e}+0.618(6)$	$-1.387(6)$
$15+16$ [507]	$-\frac{1}{3}\log^2\frac{m_\mu}{m_e}+\left(\frac{31}{36}-\frac{\pi^2}{27}\right)\log\frac{m_\mu}{m_e}-0.884(4)$	$-7.717(4)$
$17+18$ [507]	$2\left(\frac{1}{3}\log\frac{m_\mu}{m_e}-\frac{25}{36}\right)\log\frac{\lambda}{m_\mu}+\left(\frac{11}{36}-\frac{\pi^2}{27}\right)\log\frac{m_\mu}{m_e}-0.356(2)$	$-0.676(2)$
$19+20$ [506]	$\left(\frac{119}{27}-\frac{4}{9}\pi^2\right)\log\frac{m_\mu}{m_e}-\frac{61}{162}+\frac{\pi^2}{27}$	0.1005
21 [410,505]	$\frac{2}{9}\log^2\frac{m_\mu}{m_e}-\frac{25}{27}\log\frac{m_\mu}{m_e}+\frac{317}{324}+\frac{\pi^2}{27}$	2.7241
$22+23+24$ [410]	$\frac{1}{4}\log\frac{m_\mu}{m_e}+\frac{1}{2}\zeta(3)-\frac{5}{12}$	1.5173

TABLE V.3. Sixth order results from ref. 414 .

$$f(\rho) = \frac{2}{3}\left(\log \frac{m_\mu}{m_e} - \frac{25}{12} + \frac{3\pi^2}{4}\,\frac{m_e}{m_\mu}\right)$$

Graphs	Semianalytical form $x(\frac{\alpha}{\pi})^3$	Numerical value $x(\frac{\alpha}{\pi})^3$
7 + 8	$2f(\rho)\,[-0.467] + 0.76(1)$	- 1.28(1)
9 + 10	$2f(\rho)\,[\ 0.778] - 0.53(6)$	2.88(6)
11 + 12 + 15 + 16	$f(\rho)\,[-0.654] - 0.53(7)$	- 1.96(7)
13 + 14	$f(\rho)\,[-0.564 - \log \frac{\lambda}{m_\mu}] - 0.18(3)$	- 1.41(3)
17 + 18	$f(\rho)\,[-0.090 + \log \frac{\lambda}{m_\mu}] - 0.45(3)$	- 0.65(3)
19 + 20		0.101(2)
21		2.72(2)
22 + 23 + 24		1.49(2)

TABLE VI.1 . Measurements of the Muon Anomaly.

AUTHORS	REFERENCES	ANOMALY
Garwin et al (1960)(*)	624	0.00113(14)
Charpak et al (1961)	625	0.001145(22)
Charpak et al (1962)	004, 626	0.001162(5)
Farley et al (1966)	627	0.001165(3)
Bailey et al (1968)	007,008,R.1	0.00116616(31)
Henry et al (1969),	628	0.001060(67)

(*) This experiment determined $g = 2(1+G)$ rather than G .

TABLE VIII.1. Limits on the breakdown of QED from colliding beams experiments.

Parametrization : $-\frac{1}{q^2} \rightarrow -\left(\frac{1}{q^2} \pm \frac{1}{q^2-\Lambda_{\pm}^2}\right)$ for the photon propagator and $\frac{1}{p^2-m^2} \rightarrow \frac{1}{p^2-m^2} - \frac{1}{p^2-m^2-\Lambda^2}$ for the fermion propagator.

EXPERIMENT	TESTS	REFERENCE	TOTAL C.M. ENERGY	CUT-OFF(95%c.l.)
$e^-e^- \rightarrow e^-e^-$	space-like photon	801 and 802	600 MeV and 1100 MeV	$\Lambda_- > 4$ GeV $\Lambda_+ > 2.4$ GeV
$e^+e^- \rightarrow e^+e^-$	space-like photon	811 and 812	1020 MeV	$\Lambda_- > 2.0$ GeV $\Lambda_+ > 3.8$ GeV
		842	1.4 GeV - 2.4 GeV	$\Lambda_- > 6$ GeV
$e^+e^- \rightarrow \mu^+\mu^-$	time-like photon	812	580 MeV , 644 MeV and 704 MeV	$\Lambda_- > 1.3$ GeV
$e^+e^- \rightarrow 2\gamma$	space-like electron	819	1028 MeV	Λ(electron)> 1.5 GeV

TABLE VIII.2. Limits on the breakdown of QED from measurements of symmetric wide angle lepton pair photoproduction(*).

Parametrization : $\sigma = \sigma_{BH} \left[1 \pm \left(\frac{Q^2}{\Lambda_\pm^2} \right)^2 \right]$ where Q is the invariant mass of the final lepton pair. For each experiment, the signature retained is the one which yields the lowest cut-off.

EXPERIMENT	REFERENCE	INVARIANT MASS OF LEPTON PAIR	CUT-OFF (95% c.l.)
$\gamma + C \rightarrow C + e^+e^-$	821	$Q \lesssim 900$ MeV/c^2	$\Lambda_+ > 1.6$ GeV/c^2
$\gamma + C \rightarrow C + e^+e^-$	822	$Q \lesssim 444$ MeV/c^2	$\Lambda_+ > 0.8$ GeV/c^2
$\gamma + p \rightarrow p + e^+e^-$	823	$Q \lesssim 490$ MeV/c^2	$\Lambda_+ > 0.7$ GeV/c^2
$\gamma + C \rightarrow C + \mu^+\mu^-$	827	$Q \lesssim 1225$ MeV/c^2	$\Lambda_- > 1.5$ GeV/c^2
$\gamma + C \rightarrow C + \mu^+\mu^-$	828	$Q \lesssim 2100$ MeV/c^2	$\Lambda_- > 2.3$ GeV/c^2
$\gamma + C \rightarrow C + \mu^+\mu^-$	829	$Q \lesssim 1770$ MeV/c^2	$\Lambda_- > 1.9$ GeV/c^2

(*) For earlier experiments on electron pair photoproduction, see Refs.824,825 . For an earlier experiment on muon pair photoproduction, see also Ref.826 .

TABLE VIII.3. Limits on the breakdown of QED from experiments of wide angle bremsstrahlung of leptons.

Parametrization : $\sigma = \sigma_{BH} \left[1 \pm \left(\frac{Q^2}{\Lambda_\pm^2}\right)^2\right]$ where Q is the invariant mass of the final lepton-photon system. For each experiment, the signature retained is the one which yields the lowest cut-off.(*)

EXPERIMENT	REFERENCE	INVARIANT MASS OF LEPTON-γ SYSTEM	CUT-OFF (95% c.l.)
$e^- + C \rightarrow e^- + C + \gamma$	833	$Q \lesssim 1030$ MeV/c^2	$\Lambda_+ > 1.5$ GeV/c^2
$\mu^\pm + C \rightarrow \mu^\pm + C + \gamma$	835	$Q \lesssim 650$ MeV/c^2	$\Lambda_- > 0.73$ GeV/c^2

(*) See also ref. 834 .

R.5 Eugene D. COMMINS, Application of Atomic Beams to Elementary-Particle and Nuclear Physics, Ann. Rev. Nuclear Science, 17 , 33 (1967).

R.6 F.J.M. FARLEY, The Status of Quantum Electrodynamics, Proceedings of the 1st meeting of the European Physical Society, Florence (1969).

R.7 Geral FEINBERG and Leon M. LEDERMAN, The Physics of Muons and Muon Neutrinos, Ann. Rev. Nuclear Science, 13 , 431 (1963).

R.8 Richard P. FEYNMAN, The Present Status of Quantum Electrodynamics, dans la Théorie Quantique des Champs, proceedings of the 12th Solvay meeting, Interscience publs. New-York ; R. Stoops, éditeur Bruxelles (1961).

R.9 R. GATTO, Analysis of Present Evidence on the Validity of Quantum Electrodynamics, in High Energy Physics, edited by E.H.S. Burhop, Vol.II , Academic Press (1968). There is a recent "addendum" to this review article.

R.10 Vernon W. HUGHES, Muonium , Ann. Rev. Nuclear Science, 16 , 445 (1966).

R.11 Vernon W. HUGHES, Muonium and Positronium, in Physics of the One-and-Two-Electron Atoms, pp.407-428 ; North-Holland (1969).

REVIEW ARTICLES ON QUANTUM ELECTRODYNAMICS

The following is a list of review articles on various aspects of quantum electrodynamics which we have found very useful to consult. No attempt at giving a complete list has been made. We apologize for omissions.

R.1 J. BAILEY and E. PICASSO, The Anomalous Magnetic Moment of the Muon and Related Topics, Progress in Nuclear Physics, Vol.12, part 1 , p.43 (1970).

R.2 Hans A. BETHE and Edwin E. SALPETER, Quantum Mechanics of One-and-Two-Electron Atoms, Springer-Verlag (1957).

R.3 Stanley J. BRODSKY, Status of Quantum Electrodynamics, Proceedings of the 4th International Symposium on Electron and Photon Interactions at High Energies, published by the Daresbury Nuclear Physics Laboratory, (1969).

R.4 Stanley J. BRODSKY and Sidney D. DRELL, The Present Status of Quantum Electrodynamics, Ann. Rev. Nuclear Science, 20 , 147 , (1970).

R.12 G. KÄLLÉN, Quantenelektrodynamik, Handbuch der Physik, Vol.V , Part 1 , pp.167-364 ; Springer-Verlag (1958).

R.13 A. PETERMANN, Atomic Energy Levels Shifts in Hydrogen-Like Atoms, Fortschr. Phys., 6 , 505 (1958).

R.14 E. PICASSO, Current Developments in the Study of Electromagnetic Properties of Muons, in High Energy Physics and Nuclear Structure edited by Samuel Devons, pp.615-635 , Plenum Press (1970).

R.15 Julian SCHWINGER, Selected Papers on Quantum Electrodynamics, Dover Publications, Inc., New-York (1958).

R.16 B.N. TAYLOR, W. PARKER and D.N. LANGENBERG, Determination of e/h , Using Macroscopic Quantum Phase Coherence in Superconductors : Implications for Quantum Electrodynamics and the Fundamental Physical Constants, Rev. Mod. Phys. 41 , 375 (1969).

R.17 C.S. WU and Lauwrence WILETS, Muonic Atoms and Nuclear Structure, Ann. Rev. Nuclear Science, 19 , 527 (1969).

REFERENCES

001. Willis E. LAMB, Jr. and Robert C. RETHERFORD, Phys. Rev. 72 , 241 (1947).

002. P KUSCH and H. FOLEY, Phys. Rev. 72, 1256(1947) ; 73, 412 (1948).

003. Julian SCHWINGER, Phys. Rev. 73 , 416 (1948).

004. G. CHARPAK, F.J.M. FARLEY, R.L. GARWIN, T. MULLER, J.C. SENS and A. ZICHICHI, Phys. Letters 1 , 16 (1962).

005. A. PETERMANN, Phys. Rev. 105 , 1931 (1957).

006. H. SUURA and E.H. WICHMANN, Phys. Rev. 105 , 1930 (1957).

007. J. BAILEY, W. BARTL, G. von BOCHMANN, R.C.A. BROWN, F.J.M. FARLEY, H. JÖSTLEIN, E. PICASSO and R.W. WILLIAMS, Phys. Letters 28B , 288 (1968).

008. J. BAILEY, W. BARTL, G. von BOCHMANN, R.C.A. BROWN, F.J.M. FARLEY, M. GLESCH, H. JÖSTLEIN, S. van der MEER, E. PICASSO and R.W. WILLIAMS, Precise Measurement of the Anomalous Magnetic Moment of the Muon, CERN Preprint (1971) .

101. H.A. BETHE, Phys. Rev., 72 , 339 (1947).

102. N.M. KROLL and W.E. LAMB, Phys. Rev. 75 , 388 (1949).

103. J.B. FRENCH and V.F. WEISSKOPF, Phys. Rev. 75 , 1240 (1949).

104. R.P. FEYNMAN, Phys. Rev. 74 , 1430 (1948) ; 76 , 769 (1949).

105. H. FUKUDA, Y. MIYAMOTO and S. TOMONAGA, Progr. Theor. Phys. 4 , 47 , 121 (1949).

106. C.L. SCHWARTZ and J.J. TIEMANN, Ann. Phys.(N.Y.), 6 , 178 (1958).

107. E.A. UEHLING, Phys. Rev. 48 , 55 (1935).

108. R. SERBER, Phys. Rev. 48 , 49 (1935).

109. S. TRIEBWASSER, E.S. DAYHOFF and W.E. LAMB Jr., Phys. Rev. 89 , 98 (1953).

110. R.T. ROBISCOE and T.W. SHYN, Phys. Rev. 168 , 4 (1968).

111. S.L. KAUFMAN, W.E. LAMB Jr., K.R. LEA and M. LEVENTHAL, Phys. Rev. Letters 22 , 507 (1969).

112. T.W. SHYN, W.L. WILLIAMS, R.T. ROBISCOE and T. REBANE, Phys. Rev. Letters 22 , 1273 (1969).

113. T.V. VORBURGER and B.L. COSENS, Phys. Rev. Letters 23 , 1273 (1969).

114. G.W. ERICKSON and D.R. YENNIE, Ann. Phys.(N.Y.) 35 , 271 (1965).

115. G.W. ERICKSON and D.R. YENNIE, Ann. Phys.(N.Y.) 35 , 447 (1965).

116. H. GROTCH and D.R. YENNIE, Rev. Mod. Physics 41 , 350 (1969).

117. J. WENESER, R. BERSOHN and N.M. KROLL, Phys. Rev. 91 , 1257 (1953)

118. M.F. SOTO Jr., Phys. Rev. Letters 17 , 1153 (1966) ; Phys. Rev. 2A , 734 (1970).

119. T. APPELQUIST and S.J. BRODSKY, Phys. Rev. Letters 24 , 562 (1970) ; Phys. Rev. A2 , 2293 (1970).

120. B.E. LAUTRUP, A. PETERMAN and E. de RAFAEL, Phys. Letters 31B , 577 (1970).

121. R. BARBIERI, J.A. MIGNACO and E. REMIDDI, Nuovo Cimento Letters, 3 , 588 (1970).

122. A. PETERMAN, Phys. Letters 35B, 325 (1971)

123. A. PETERMAN, CERN Preprint TH. 1354 (1971).(To be published in Phys.Letters)

124. J.A. FOX, CLNS-134 preprint (1970).

125. R. KARPLUS, A. KLEIN and J. SCHWINGER, Phys. Rev. 86 , 288 (1952).

126. M. BARANGER, H.A. BETHE and R.P. FEYNMAN, Phys. Rev. 92 , 482 (1953).

127. A.J. LAYZER, Phys. Rev. Letters 4 , 580 (1960).

128. H.M. FRIED and D.R. YENNIE, Phys. Rev. Letters 4 , 583 (1960).

129. A.J. LAYZER, J. Math. Phys. 2 , 292 , 308 (1961).

130. M. BARANGER, F.J. DYSON and E.E. SALPETER, Phys. Rev. 88 , 680 (1952).

131. E.E. SALPETER, Phys. Rev. 87 , 328 (1952).

132. T. FULTON and P.C. MARTIN, Phys. Rev. 95 , 811 (1954).

133. W.A. BARKER and F.N. GLOVER, Phys. Rev. 99 , 317 (1955) .

134. S. BRODSKY and R. PARSONS, Phys. Rev. 163 , 134 (1967).

135. E. FERMI, Z. Physik 60 , 320 (1930).

136. R. VESSOT, et al., IEEE Trans. Instr. Meas. IM-15, 165 (1966).

137. Stanley J. BRODSKY and Glen W. ERICKSON, Phys. Rev. 148 , 26 , (1966).

138. G. BREIT, Phys. Rev. 35 , 1447 (1930).

139. N. KROLL and F. POLLACK, Phys. Rev. 84 , 597 (1951) ; 86 , 876 (1952).

140. R. KARPLUS, A. KLEIN and J. SCHWINGER, Phys. Rev. 84 , 597 (1951).

141. A.J. LAYZER, Nuovo Cimento 33 , 1538 (1964).

142. D.E. ZWANZIGER, Nuovo Cimento 34 , 77 (1964).

143. D.E. ZWANZIGER, Phys. Rev. 121 , 1128 (1960).

144. G.E. BROWN and G.B. ARFKEN, Phys. Rev. 76 , 1305 (1949).

145. A.C. ZEMACH, Phys. Rev. 104 , 1771 (1956).

146. R. ARNOWITT, Phys. Rev. 92 , 1002 (1953).

147. R. KARPLUS, A. KLEIN and J. SCHWINGER, Phys. Rev. 86 , 288 (1952).

148. W.A. NEWCOMB and E.E. SALPETER, Phys. Rev. 97 , 1146 (1955).

149. C.K. IDDINGS and P.M. PLATZMAN, Phys. Rev. 113 , 192 (1959).

150. C.K. IDDINGS, Phys. Rev. 138 , B446 (1965).

151. W.N. COTTINGHAM, Ann. Phys. (N.Y.) 25 , 424 (1963).

152. M.G. DONCEL and E.de RAFAEL, IHES preprint (1971), (to be published in Il Nuovo Cimento).

153. F. GUERIN, Nuovo Cimento 50 , 211 (1967).

154. S.D. DRELL and J.D. SULLIVAN, Phys. Rev. 154 , 1477 (1967).

155. V.L. CHERNIAK, B.V. STRUMINSKI and G.M. ZINOVJEV, Dubna preprint E2 - 4740 (1969).

156. A.A. LOGUNOV and A.N. TAVKHELIDZE, Nuovo Cimento 29 , 380 (1963).

157. R.N. FAUSTOV, Nucl. Phys. 75 , 669 (1966).

158. Glen W. ERICKSON, Improved Lamb-Shift Calculation for all values of Z , University of Surrey, Preprint (1971).

159. R. BARBIERI, J. MIGNACO and E. REMIDDI, preprint S.N.S. 71/3, May 1971.

160. R. ROBISCOE, T. SHYN, Phys.Rev.Letters 24, 559 (1970).

161. C. FABJAN, F. PIPKIN, M. SILVERMAN, Phys.Rev.Letters 26, 347 (1971).

162. B. COSENS, Phys.Rev. 173, 49 (1968).

163. M. NARASHIMHAM, Thesis, University of Colorado (1969), unpublished.

164. O. MADER, M. LEVENTHAL, W.E. LAMB, jr., Phys.Rev. A3, 1832 (1971).

165. L. HATFIELD, R. HUGHES, Phys.Rev. 156, 102 (1967).

166. R. JACOBS, K. LEA, W.E. LAMB, jr., Bull.Am.Soc. 14, 525 (1969).

167. C. FAN, M. GARCIA-MUNOZ, I. SELLIN, Phys.Rev. 161, 6 (1967).

168. M. LEVENTHAL and D.E. MURNICK, Phys.Rev.Letters 25, 1237 (1970).

201. M. DEUTSCH, Phys. Rev. 82 , 455 (1951).

202. Martin DEUTSCH, Prog. Nucl. Phys. 3 , 131 (1953).

203. E.E. SALPETER and H.A. BETHE, Phys. Rev. 84 , 1232 (1951).

204. M. GELL-MANN and F. LOW, Phys. Rev. 84 , 350 (1951).

205. M. DEUTSCH and S.C. BROWN, Phys. Rev. 85 , 1047 (1952).

206. R. WEINSTEIN, M. DEUTSCH and S. BROWN, Phys. Rev. 94 , 758 (1954) ; "ibid". 98 , 223 (1955).

207. V.W. HUGHES, S. MARDER, and C.S. WU, Phys. Rev. 106 , 934 (1957).

208. E.D. THERIOT,Jr., R.H. BEERS, V.W. HUGHES, and K.O.H. ZIOCK, Phys. Rev. 2A , 707 (1970).

209. R.H. BEERS and V.W. HUGHES, Bull. Am. Phys. Soc. 13 , 633 (1968).

210. S. MARDER, V.W. HUGHES and C.S. WU, Phys. Rev. 98 , 1840 (1955).

211. J. PIRENNE, Arch. Sci. Phys. Mat. 28 , 233 (1946), and "ibid" 29 , 121, 207, 265 (1947).

212. R.A. FERRELL, Phys. Rev. 84 , 858 (1951).

213. R. KARPLUS and A. KLEIN, Phys. Rev. 87 , 848 (1952).

214. T. FULTON, D.A. OWEN and W.W. REPKO, Phys. Rev. Letters 24 , 1035 (1970) ; 25 , 782 (E) (1970) ; Phys. Rev. A (to be published).

215. T. FULTON and P.C. MARTIN, Phys. Rev. 93 , 903 (1954) ; "ibid" 95 , 811 (1954).

216. A. ORE and J.L. POWELL, Phys. Rev. 75, 1696 (1949).

217. P. PASCUAL and E. de RAFAEL, Nuovo Cimento Letters, 4 , 1144 (1970).

218. P.A.M. DIRAC, Proc. Cambridge Phil. Soc. 26 , 361 (1930).

219. I. HARRIS and L.M. BROWN, Phys. Rev. 105 , 1656 (1957).

301. V.W. HUGHES, D. McCOLM, K. ZIOCK and R. PREPOST, Phys. Rev. Letters 5 , 63 (1960).

302. Stanley J. BRODSKY and Glen W. ERICKSON, Phys. Rev. 148 , 26 (1966).

303. Thomas FULTON, David A. OWEN and Wayne W. REPKO, Phys. Rev. Letters.

304. R. ARNOWITT, Phys. Rev. 92 , 1002 (1963).

305. T. FULTON and P.C. MARTIN, Phys. Rev. 93 , 903 (1954) ; 95 , 811 (1954).

306. W.A. NEWCOMB and E.E. SALPETER, Phys. Rev. 97 , 1146 (1955).

307. J.F. HAGUE, J.E. ROTHBERG, A. SCHENCK, D.L. WILLIAMS, R.W. WILLIAMS, K.K. YOUNG and K.M. CROWE, Phys. Rev. Letters 25 , 628 (1970).

308. R. De VOE, P.M. Mc INTYRE, A. MAGNON, D.Y. STOWELL, R.A. SWANSON, and V.L. TELEGDI, Phys. Rev. Letters 25 , 1779 (1970) ; E

309. D.P. HUTCHINSON, J. MENES, G. SHAPIRO, and A.M. PATLACH, Phys. Rev. 131 , 1351 (1963).

310. G. McD. BINGHAM, Nuovo Cimento, 27 , 1352 (1963).

311. D.P. HUTCHINSON, F.L. LARSEN, N.C. SCHOEN, D.I. SOBER, and A.S. KANOFSKI, Phys. Rev. Letters 24 , 1254 (1970).

312. R.D. EHRLICH, H. HOJER, A. MAGNON, D. STOWELL, R.A. SWANSON, and V.L. TELEGDI, Phys. Rev. Letters 24 , 513 (1969).

313. P. CRANE, J.J. AMATO, V.W. HUGHES, D.M. LAZARUS, G. zu PUTLITZ, and P.A. THOMPSON, Bull. Am. Phys. Soc. 15 , 45 (1970).

314. M.A. RUDERMAN, Phys. Rev. Letters 17 , 794 (1966).

315. V.W. HUGHES et al , to be published.

316. R.D. EHRLICH, H. HOJER, A. MAGNON, D.Y. STOWELL, R.A. SWANSON, and V.L. TELEGDI, Phys. Rev. Letters 23 , 513 (1969).

317. W.E. CLELAND, J.M. BAILEY, M. ECKHAUSE, V.W. HUGHES, R.M. MOBLEY, R. PREPOST, and J.E. ROTHBERG, Phys. Rev. Letters 13 , 202 (1964).

318. P.A. THOMPSON, J.J. AMATO, P. CRANE, V.W. HUGHES, R. M. MOBLEY, G. Zu PUTLITZ, and J.E. ROTHBERG, Phys. Rev. Letters 22 , 163 (1969).

401. A. RICH, private communication.

402. S.D. DRELL and H.R. PAGELS, Phys. Rev. 140 , B397 (1965).

403. R.G. PARSONS, Phys. Rev. 168 , 1562 (1968).

404. L. LEWIN, Dilogarithms and associated functions, McDonald London (1958).

405. R. KARPLUS and N.M. KROLL, Phys. Rev. 77 , 536 (1950).

406. C.M. SOMMERFIELD, Phys. Rev. 107 , 328 (1957).

407. A. PETERMANN, Helv. Phys. Acta 30 , 407 (1957).

408. C.M. SOMMERFIELD, Ann. Phys. (N.Y.) 5 , 26 (1958).

409. M.V. TERENT'EV, Zh. Experim. i Teor. Fiz. 43 , 619 (1962) JETP 16 , 444 (1963) (English translation).

410. B.E. LAUTRUP and E. de RAFAEL, Phys. Rev. 174 , 1835 (1968).

411. J. MIGNACO and E. REMIDDI, Nuovo Cimento 60A , 519 (1969).

412. J. ALDINS, S. BRODSKY, A. DUFNER and T. KINOSHITA, Phys. Rev. Lett. 23 , 441 (1969).

413. J. ALDINS, S. BRODSKY, A. DUFNER and T. KINOSHITA, Phys. Rev. D1 , 2378 (1970).

414. S. BRODSKY and T. KINOSHITA, Phys. Rev.

415. M. LEVINE and J. WRIGHT, Carnegie-Mellon preprint (August 1970).

416. J. CALMET and M. PERROTTET, CNRS preprint 70/P339 (September 1970).

417. A. DE RÚJULA, B. LAUTRUP and A. PETERMAN, Phys. Lett. 33B , 605 (1970).

418. J. CALMET, University of Utah preprint (April 1971).

419. M. LEVINE and J. WRIGHT, Phys. Rev. Letters 26 , 1351 (1971).

420. J. CALMET, Thèse-Marseille 70/P. 336 (1970), Proceedings of the Colloquium on Computational Methods in Theoretical Physics, Marseille (CNRS) 1970 .

421. B.E. LAUTRUP, Phys. Letters 32B , 627 (1970).

422. M. VELTMAN, CERN preprint (1967).

423. A.C. HEARN, Stanford University Reprint No.ITP-247 (unpublished) A.C. HEARN, in Interactive Systems for Experimental Applied Mathematics, Edited by M. Klerer and J. Reinfelds (Academic Press, New-York, 1968) .

424. M. LEVINE, J. Comput. Phys. 1 , 454 (1967).

425. W. CZYZ, G.C. SHEPPEY and J.D. WALECHA, Nuovo Cimento 34 , 420 (1964).

426. J.C. WESLEY and A. RICH, Phys. Rev. Letters 24 , 1320 (1970).

427. J.E. NAFE et al, Phys. Rev. 71 , 914 (1947).

428. O.E. NAGDE et al, Phys. Rev. 72 , 971 (1947).

429. G. BREIT, Phys. Rev. 72 , 984 (1947).

430. S.H. KOENIG et al, Phys. Rev. 88 , 191 (1952).

431. R. BERINGER and M. HEALD, Phys. Rev. 95 , 1474 (1954).

432. P. FRANKEN and S. LIEBES, Phys. Rev. 104 , 1197 (1957).

433. A.A. SCHUPP et al, Phys. Rev. 121, 1 (1961).

434. D.T. WILKINSON and H.R. CRANE, Phys. Rev. 130 , 852 (1963).

435. D.T. WILKINSON, Ph.D. Thesis, University of Michigan 1962, (University Microfilms Inc., O.P. 63-478, Ann.Arbor, Michigan).

436. A. RICH, Phys. Rev. Letters 20 , 967 (1968) ; Phys. Rev. Letters 20 , 1221 (1968) Erratum ; Proceedings of the Third International Conference on Atomic Masses, R.C. Barker (Editor), University of Manitoba Press (Winnipeg).

437. G.R. HENRY and J.E. SILVER, Phys. Rev. 180 , 1262 (1969).

438. F.J.M. FARLEY, Cargese Lectures in Physics (ed. M.Levy), Vol.2 , (Gordon and Breach, N.Y.1968).

439. E. KLEIN, Z. Physik 208 , 28 (1968).

440. G. GRÄFF et al, Phys. Rev. Letters 21 , 340 (1968).

441. G. GRÄFF et al, Z. Physik 222 , 201 (1969).

442. A. RICH and H.R. CRANE, Phys. Rev. Letters 17 , 271 (1966).

443. J. GILLELAND and A. RICH, Phys. Rev. Letters 23 , 1130 (1969).

444. P.S. FARAGO et al, Proc.Phys.Soc.(London) 82 , 493 (1963).

445. I.A. GALBRAITH and R.B. GARDINER, J.Phys. A1 , 194 (1969).

501. H.SUURA and E. WICHMANN, Phys. Rev. 105 , 1930 (1957).

502. A. PETERMANN, Phys. Rev. 105 , 1931 (1957).

503. H.H. ELEND, Phys. Lett. 20 , 682 (1966) ; 21 , 720 (1966).

504. Glen W. ERICKSON and Henry H.T. LIU, UCD-CNL-81 report (1968).

505. T. KINOSHITA, Nuovo Cimento 51B , 140 (1967).

506. B.E. LAUTRUP and E. de RAFAEL, Nuovo Cimento 64A , 322 (1969).

507. B.E. LAUTRUP, A. PETERMAN and E. de RAFAEL, Nuovo Cimento 1A , 238 (1971).

509. J.D. BJORKEN and S.D. DRELL, Relastivistic Quantum Fields, McGraw-Hill, New-York, 1965.

510. N. NAKANISHI, Prog. Theor. Physics (Kyoto) 17 , 401 (1954).

511. T. KINOSHITA, J. Math. Phys. 3 , 650 (1962).

512. G. KÄLLÉN and A. SABRY, Kgl. Danske Vidensk. Selsk. Mat. Fys. Medd., n°17 (1955).

601. C. BOUCHIAT and L. MICHEL, J. Phys. Radium 22 , 121 (1961).

602. LOYAL DURAND III , Phys. Rev. 128 , 441 (1962).

603. T. KINOSHITA and R. J. OAKES, Phys. Letters 25B , 143 (1967).

604. J.E. BOWCOCK, Z. Phys. 211 , 400 (1968).

605. V.L. AUSLANDER, G.I. BUDKER, Ju.N. PESTOV, V.A. SIDOROV, A.N. SKRINSKY and A.G. KHABAKHPASHEV, Phys. Letters 25B , 433 (1967).

606. V.L. AUSLANDER, G.I. BUDKER, E.V. PAKHTUSOVA, Ju.N. PESTOV, V.A. SIDOROV, A.N. SKRINSKY and A.G. KHABAKHPASHEV, Sov. J. Nucl. Phys. 9 , 144 (1969).

607. J.E. AUGUSTIN, J.C. BIZOT, J. BUON, J. HAISSINSKI, D. LALANNE, P. MARIN, N. NGUYEN NGOC, J. PEREZ-Y-JORBA, F. RUMPF, E. SILVA and S. TAVERNIER, Phys. Letters 28B , 508 (1969).

608. J.E. AUGUSTIN, D. BENAKSAS, J. BUON, V. GRACCO, J. HAISSINSKI, D. LALANNE, F. LAPLANCHE, J. LEFRANCOIS, P. LEHMANN, P. MARIN, F. RUMPF and E. SILVA, Phys. Letters 28B , 513 (1969).

609. J.E. AUGUSTIN, J.C. BIZOT, J. BUON, B. DELCOURT, J. HAISSINSKI, J. JEANJEAN, D. LALANNE, P.C. MARIN, N. NGUYEN NGOC, J. PEREZ-Y-JORBA, F. RICHARD, F. RUMPF and D. TREILLE, Phys. Letters 28B , 517 (1969).

610. M. GOURDIN and E. de RAFAEL, Nucl. Phys. B10 , 667 (1969).

611. G.J. GOUNARIS and J.J. SAKURAI, Phys. Rev. Letters 21 , 244 (1968).

701. N.M. KROLL, Nuovo Cimento 45 , 65 (1966).

703. I.Yu. KOBZAREV and L.B. OKUN, Soviet Phys. JETP 14 , 859 (1962).

704. R. SUGANO, Prog. Theor. Phys. 28 , 508 (1962).

705. S.J. BRODSKY and E. de RAFAEL, Phys. Rev. 168 , 1620 (1968).

706. K.M. CASE, Phys. Rev. 76 , 1(1949).

707. S. NAKAMURA, H. MATSUMOTO, N. NAKAZAWA and H. UGAI Suppl.Progr.Theor.Phys. extra number (1968), 422.

708. M.L. GOOD, L. MICHEL and E. de RAFAEL, Phys. Rev. 151 , 1194 (1966).

710. I. BUDAGOV et al., Nuovo Cimento Letters 2, 689 (1969).

711. A. De RUJULA and R.K.P. ZIA, Nuclear Phys. B19 , 224 (1970).

712. C.A. RAMM, Nature 217, 913(1968) ; 227 , 1323 (1970).

713. W.T. TONER et al., SLAC-PUB-868 (1971).

801. W.C. BARBER, B. GITTELMAN, G.K. O'NEILL, B. RICHTER, Phys. Rev. Letters 16 , 1127 (1966).

802. W.C. BARBER, B. GITTELMAN, G.K. O'NEILL, B. RICHTER, Proc. of 14th Int. Conf. on High-Energy Physics, Vienna (1968).

803. C. MØLLER, Ann. Physik 14 , 531 (1932).

804. Y.S. TSAI, Phys. Rev. 120 , 269 (1960).

805. T.D. LEE and G.C. WICK, Nucl. Phys. B9 , 209 (1969) ; and B10 , 1 , (1969).

806. T.D. LEE, "A Relativistic Complex Pole Model with Indefinite Metric", in Quanta (University of Chicago Press, 1970), p.260.

807. T.D. LEE, Topical Conference on Weak Interactions (CERN, 1969), p.427.

809. T.D. LEE, "Feynman diagrams in a Finite Theory of Quantum Electrodynamics" , lectures at the Ettore Majorana International School of Physics, July 1970 .

810. J.E. AUGUSTIN, Thèse de Doctorat d'Etat, LAL 1212, Orsay (1969).

811. D. LALANDE, Thèse de Doctorat d'Etat, LAL 1235, Orsay (1970).

812. J. PEREZ-Y-JORBA, Proc. of 4th Int. Symp. on Electron and Photon Interactions at High Energies, edited by Daresbury Nuclear Physics Laboratory, p.213 (1969).

813. V.N. BAIER, V.M. GALITSKI, JETP Letters 2 , 165 (1965).

814. V.N. BAIER, V.S. FADIN, V.A. KHOZE, Soviet Physics JETP 23 , 1073 (1966).

815. P. DI VECCHIA, M. GRECO, Nuovo Cimento 50A , 319 (1967).

816. M. HONTEBEYRIE, Thèse de 3ème Cycle, N.668 , Fac. des Sciences, Bordeaux, (1969).

817. H.J. BHABHA, Proc. Roy. Soc. 154A , 195 (1935).

818. S. TAVERNIER, Thèse de 3ème Cycle, LAL , RI 68/7 (1968).

819. V. SIDOROV, Proc.of 4th Int. Symp. on Electron and Photon Interactions at High Energies, edited by Daresbury Nuclear Physics Laboratory, p.227 , (1969).

820. J.G. RUTHERGLEN, Proc. of 4th Int. Symp. on Electron and Photon Interactions at High Energies, edited by Daresbury Nuclear Physics Laboratory, p.163 (1969).

821. H. ALVENSLEBEN, U. BECKER, W.K. BERTRAM, M. BINKLEY, K. COHEN, C.L. JORDAN, T.M. KNASEL, R. MARSHALL, D.J. QUINN, R. RHODE, G.H. SANDERS and S.C.G. TING, Phys. Rev. Letters 21 , 15o1 , (1968).

822. J. TENNENBAUM, A. EISNER, G. FELDMAN, W. LOCKERETZ, F.M. LIPKIN and J.K. RANDOLPH, Proc. of 4th Int. Symp. on Electron and Photon Interactions at High Energies, edited by Daresbury Nuclear Physics Laboratory, Abstract n°145 (1969).

823. P.J. BIGGS, D.W. BRABEN, R.W. CLIFFT, E. GABATHULER, P. KITCHING and R.E. RAND, Phys. Rev. Letters 23 , 927 (1969).

824. E. EISENHANDLER, J. FEIGENBAUM, N. MISTRY, P. MOSTEK, D. RUST, A. SILVERMAN, C. SINCLAIR, and R. TALMAN, Phys. Rev. Letters 18 , 425 (1967).

825. K.J. COHEN, S. HOMMA, D. LUCKEY and L.S. OSBORNE, Phys. Rev. 173 1339 (1968).

826. J.K. de PAGTER, J.I. FRIEDMAN, G. GLASS, R.C. CHASE, M. GETTNER, E. von GOELER, ROY WEINSTEIN, and A.M. BOYARSKI, Phys. Rev. Letters 17 , 767 (1966).

827. S. HAYES, R. IMLAY, P.M. JOSEPH, A.S. KEIZER, J. KNOWLES and P.C. STEIN, Phys. Rev. Letters 22 , 1134 (1969).

828. S. HAYES, R. IMLAY, P.M. JOSEPH, A.S. KEIZER, J. KNOWLES and P.C. STEIN, Phys. Rev. Letters 24 , 1369 (1970).

829. D.R. EARLES, W.L. FAISSLER, M. GETTNER, G. LUTZ, K.M. MOY, Y.W. TANG, H. VON BRIESEN, Jr, E. von GOELER, and Roy WEINSTEIN, Phys. Rev. Letters 25 , 1312 (1970).

830. H.A. BETHE and W. HEITLER, Proc. Roy. Soc. (London) A146 , 83 , (1934).

831. J.D. BJORKEN, S.D. DRELL and S.C. FRAUTSCHI, Phys. Rev. 112 , 1409 (1958).

832. J.A. McCLURE and S.D. DRELL, Nuovo Cimento 57 , 1638 (1965).

833. R.H. SIEMANN, W.W. ASH, K. BERKELMAN, D.L. HARTILL, C.A. LICHTENSTEIN and R.M. LITTAUER, Phys. Rev. Letters 22 , 421 (1969).

834. C. BERNARDINI, F. FELICETTI, R. QUERZOLI, V. SILVESTRINI, C. VIGNOLA, L. MENEGHETTI VITALE, S. VITALE, G. PENSO, Proc. of

14th Int.Conf. on High Energy Physics, Vienna (1968), Abstract 707.

835. A.D. LIBERMAN, C.M. HOFFMAN, E. ENGELS Jr., D.C. IMRIE, P.G. INNOCENTI, Richard WILSON, C. ZAJDE, W.A. BLANPIED, D.G. STAIRS, and D.J. DRICKEY, Phys. Rev. Letters 22 , 663 (1969).

836. S.D. DRELL and J.D. WALECKA, Ann. Phys. (N.Y.) 28 , 18 (1964).

837. D. EARLES, H. von BRIESEN Jr., R. CHASE, W. FAISSLER, M. GETTNER, G. GLASS, E. von GOELER, G. LUTZ, R.PARSONS, P. ROTHWELL and R. WEINSTEIN, Proc. of 4th Int. Symp. on Electron and Photon Interactions at High Energies, edited by Daresbury Nuclear Physics Laboratory, Abstract n° 65 , (1969).

838. J.J. RUSSELL, R.C. SAH, M.J. TANNENBAUM, W.E. CLELAND, D.G. RYAN and D.G. STAIRS, Phys. Rev. Letters 26 , 46 (1971).

839. S.J. BRODSKY and S.C.C. TING, Phys. Rev. 145 , 1018 (1966).

840. D.C. EHN and G.R. HENRY, Phys. Rev. 162 , 1722 (1967).

841. F. AMMAN et al., Nuovo Cimento Letters 1 , 729 (1969).

842. B. BORGIA, F. CERADINI, M. CONVERSI, L. PAOLUZI, W. SCANDALE, G. BARBIELLINI, M. GRILLI, P. SPILLANTINI, R. VISENTIN, and A. MULACHIE, Phys. Letters, 35B , 340 (1971).

FIGURE CAPTIONS

Fig. I.1 Lower energy-level structure in the hydrogen atom.

Fig. I.2 Lowest order electron vertex contribution to the Lamb-shift.

Fig. I.3 Lowest order vacuum polarization contribution to the Lamb-shift.

Fig. I.4 Feynman diagrams contributing to the 4th order electron vertex. These are the diagrams which contribute to the slope of the Dirac form factor of the electron (see Section I.1) and to the anomalous magnetic moment of the electron (see Section IV.1).

FIGURE CAPTIONS

Fig.IV.1 Second order contribution to the lepton vertex.

Fig.IV.2 Mass dependent fourth order contribution to the lepton vertex.

Fig.IV.3 Mass independent sixth order contributions to the lepton vertex.

FIGURE CAPTIONS

Fig.V.1 Mass dependent sixth order contribution to the lepton vertex.

Fig.V.2 The light by light contribution to $G_\mu - G_e$

Fig.V.3 Vacuum polarization correction to g-2 .

FIGURE CAPTIONS

Fig. VI.1 The four-fermion V-A contribution to the anomalous magnetic moment of the muon.

Fig. VI.2 Weak contribution of the muon anomaly via the intermediate vector-boson W .

FIGURE CAPTIONS

Fig. VII.1 Neutral boson exchange.

FIGURE CAPTIONS

Fig.VIII.1 Lowest order Feynman diagrams contributing to Møller scattering.

Fig.VIII.2 Lowest order Feynman diagrams contributing to Bhabha scattering.

Fig.VIII.3 The lowest order annihilation graph for $e^+e^- \rightarrow \mu^+\mu^-$.

Fig.VIII.4 The annihilation graphs corresponding to $e^+e^- \rightarrow 2\gamma$.

Fig.VIII.5 Lowest order Feynman diagrams contributing to lepton pair photoproduction. In Fig.VIII.5a there are two diagrams obtained by attaching the exchanged photon to each lepton line.

Fig.VIII.6 Lowest order Feynman diagrams contributing to bremsstrahlung of leptons. The off-shell fermion in the diagram of Fig.VIII.6a is time-like, while in the diagram of Fig.VIII 6b is space-like.

Fig.VIII.7 Lowest order Feynman diagrams contributing to trident production.

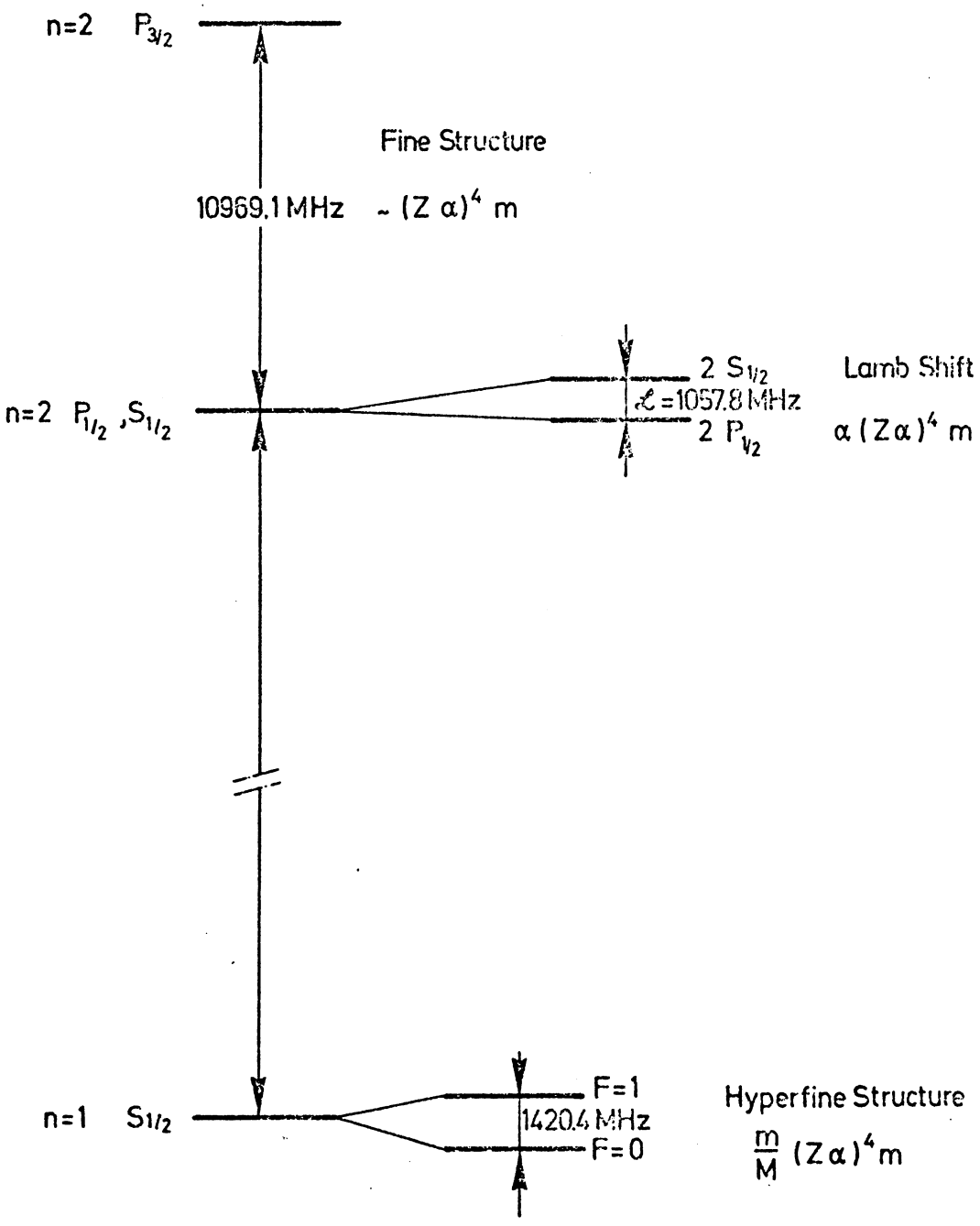
n=2 P3/2
Fine Structure
10969.1 MHz ~ (Z α)⁴ m
2 S1/2
Lamb Shift
ℒ = 1057.8 MHz
n=2 P1/2 , S1/2
2 P1/2
α (Zα)⁴ m
F=1
1420.4 MHz
n=1 S1/2
F=0
Hyperfine Structure
m/M (Zα)⁴m

FIG. I.1

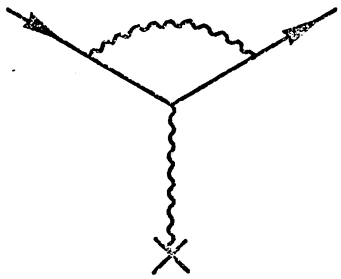

FIG. I. 2

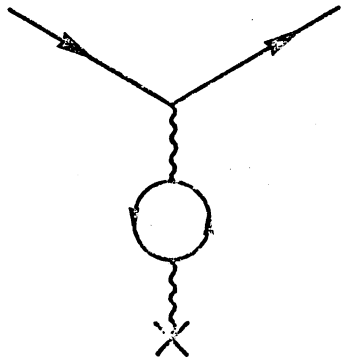

FIG. I. 3

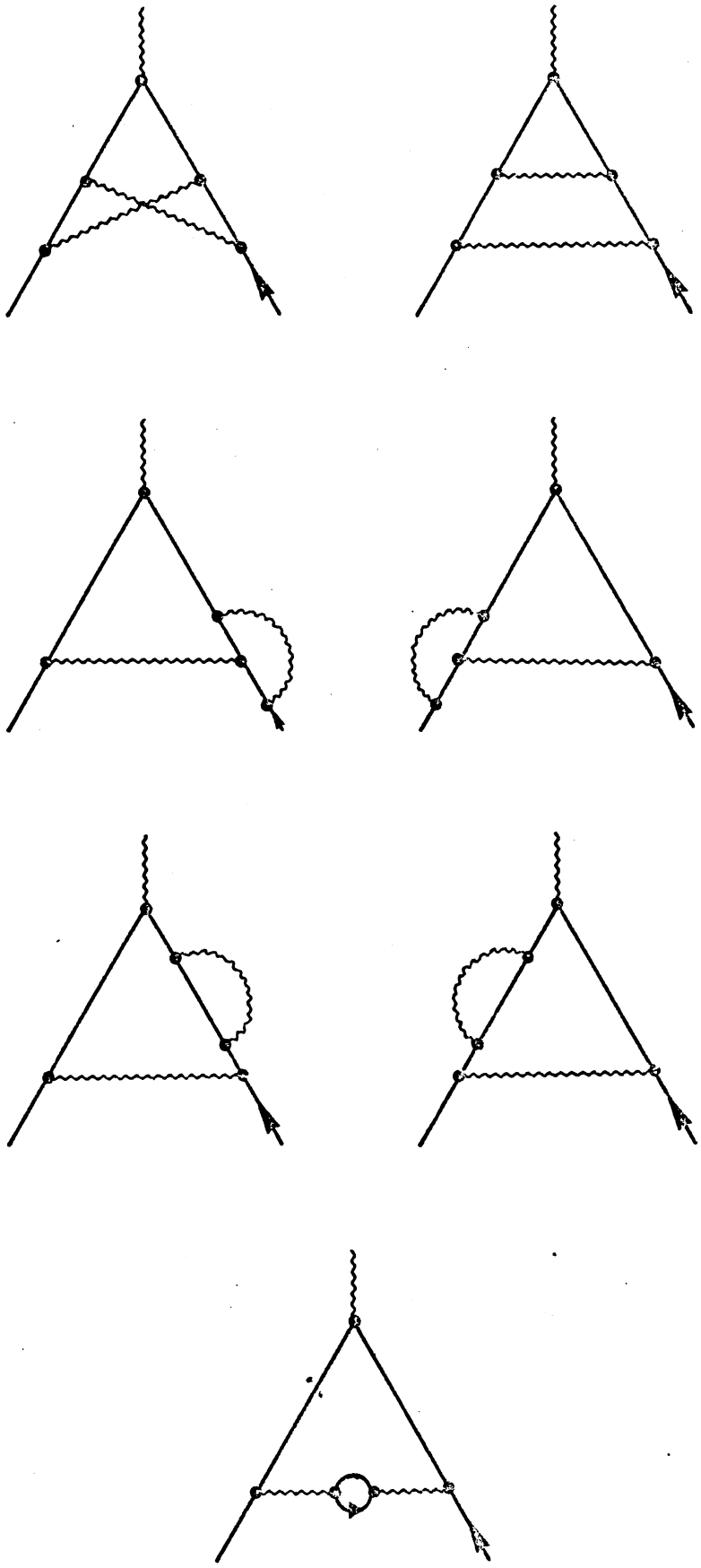

FIG.I.4

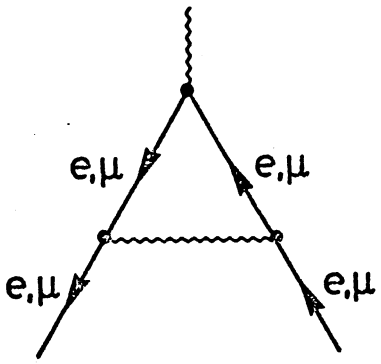

FIG. IV.1

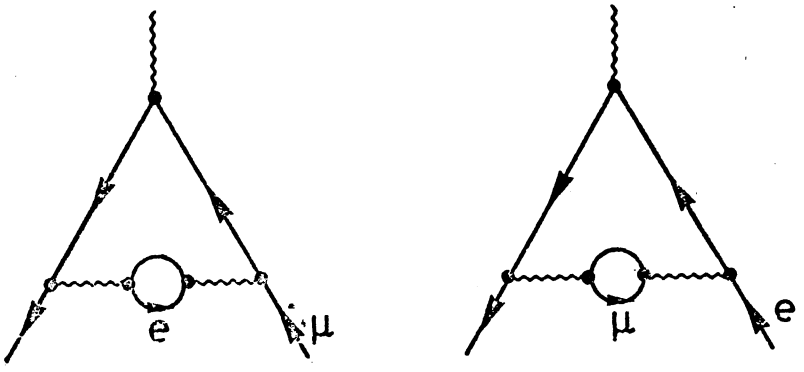

FIG. IV. 2

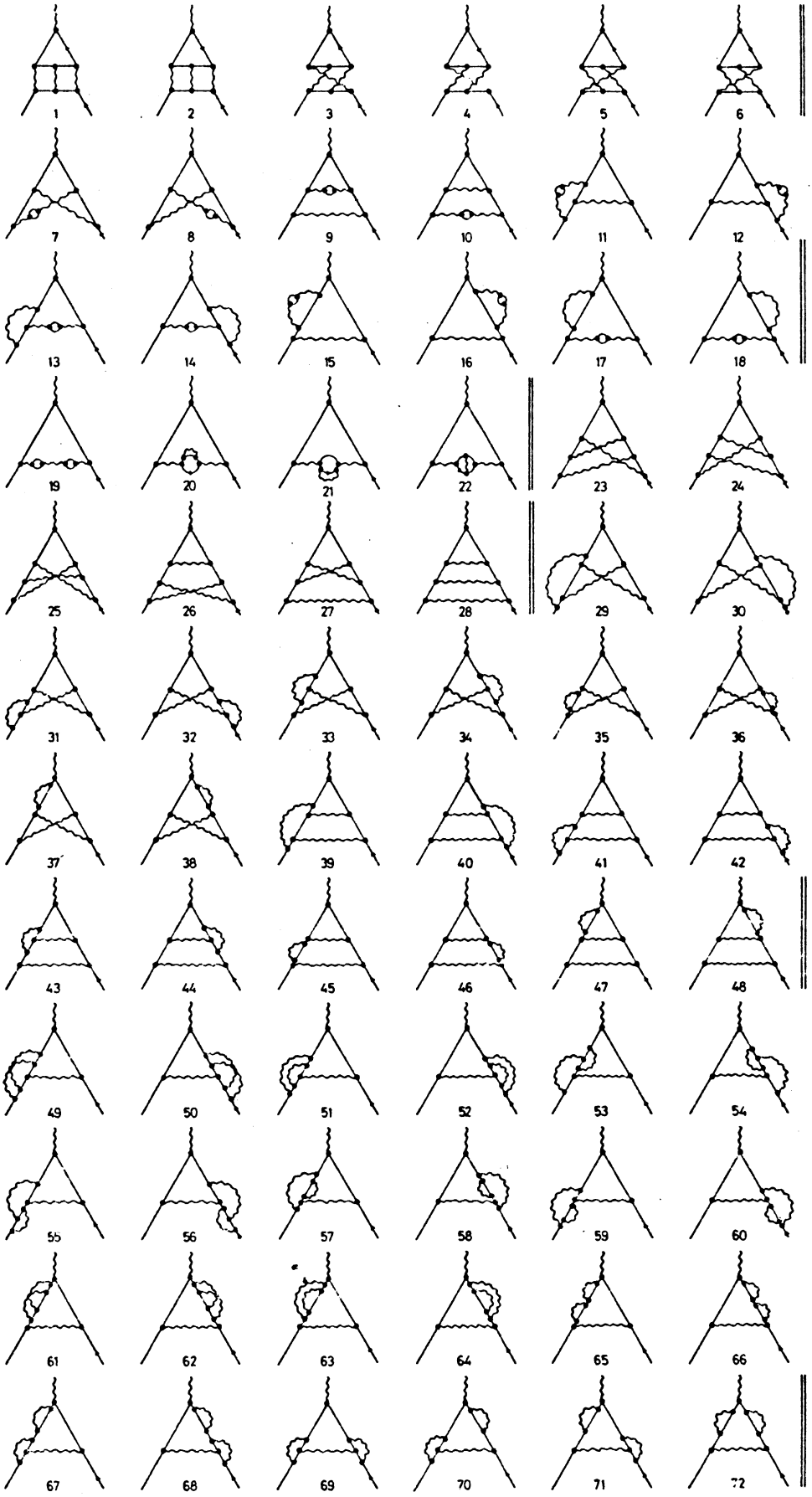
1
2
3
4
5
6
7
8
9
10
11
12
13
14
15
16
17
18
19
20
21
22
23
24
25
26
27
28
29
30
31
32
33
34
35
36
37
38
39
40
41
42
43
44
45
46
47
48
49
50
51
52
53
54
55
56
57
58
59
60
61
62
63
64
65
66
67
68
69
70
71
72

FIG. IV.3

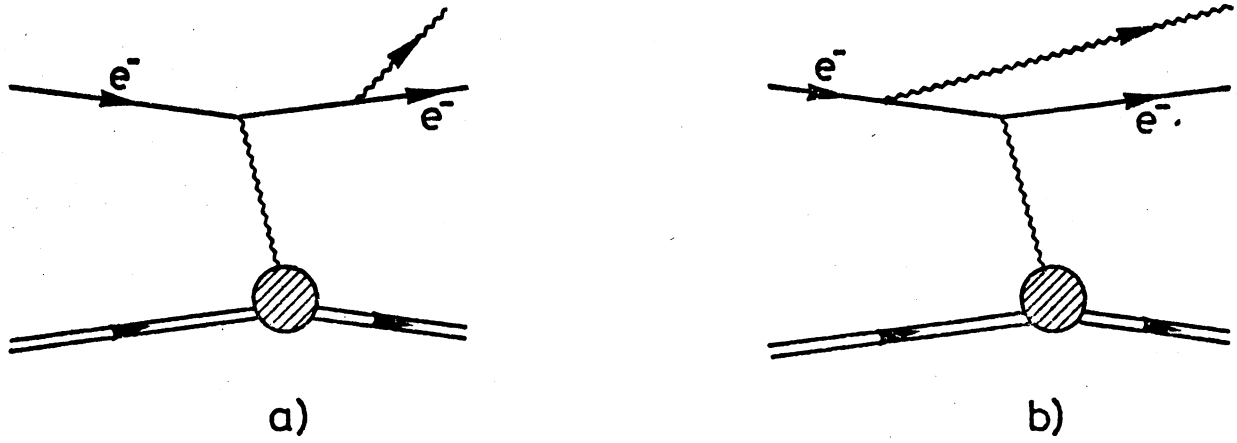

a) b)

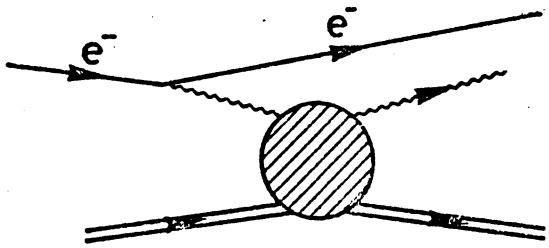

c)

FIG. VIII. 6

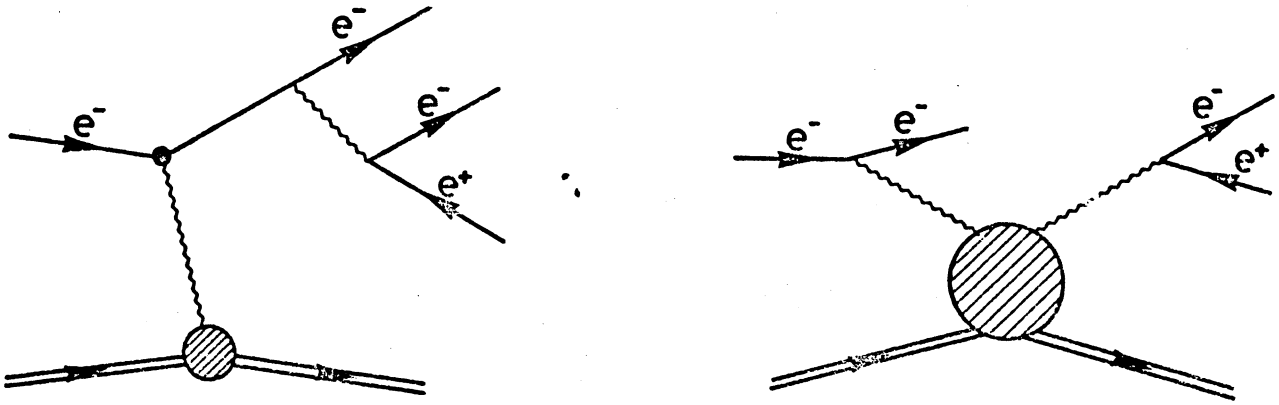

a) b)

FIG. VIII. 7